

DTIC FILE COPY



UNCLASSIFIED
SECURITY CLASSIFICATION OF THIS PAGE

REPORT DOCUMENTATION PAGE

Form Approved
OMB No. 0704-0188

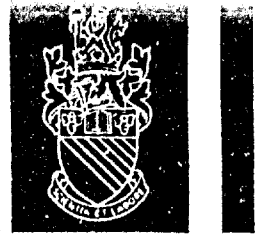
AD-A227 073

| | | | |
|--|---|--|--------------------------------|
| 1a. REPORT SECURITY CLASSIFICATION UNCLASSIFIED | | 1b. RESTRICTIVE MARKINGS | |
| 2a. SECURITY CLASSIFICATION AUTHORITY | | 3. DISTRIBUTION / AVAILABILITY OF REPORT Approved for public release, distribution is unlimited | |
| b. DECLASSIFICATION / DOWNGRADING SCHEDULE | | 5. MONITORING ORGANIZATION REPORT NUMBER(S) AEOSR-TR- 90 0941 | |
| PERFORMING ORGANIZATION REPORT NUMBER(S) | | 7a. NAME OF MONITORING ORGANIZATION AFOSR/NC | |
| 4a. NAME OF PERFORMING ORGANIZATION DEPARTMENT OF PHYSICS UMIST | 6b. OFFICE SYMBOL (if applicable) UMIST | 7b. ADDRESS (City, State, and ZIP Code) Bolling AFB, DC 20332-6448 | |
| 1. ADDRESS (City, State, and ZIP Code) Sackville Street, Manchester M60 1QD | | 9. PROCUREMENT INSTRUMENT IDENTIFICATION NUMBER AFOSR-88-0121 | |
| 1. NAME OF FUNDING / SPONSORING ORGANIZATION AFOSR | 8b. OFFICE SYMBOL (if applicable) NC | 10. SOURCE OF FUNDING NUMBERS | |
| 8c. ADDRESS (City, State, and ZIP Code) Bolling AFB, DC 20332-6448 | | PROGRAM ELEMENT NO. 61102F | PROJECT NO. 2310 |
| | | TASK NO. 2310/A | WORK UNIT ACCESSION NO. |
| 11. TITLE (Include Security Classification) POLARIZATION RADAR STUDIES OF PRECIPITATION: IMPLEMENTATION OF THE TECHNIQUE AND DATA INTERPRETATION | | | |
| 12. PERSONAL AUTHOR(S) ILLINGWORTH, ANTHONY JOHN | | | |
| 13a. TYPE OF REPORT FINAL | 13b. TIME COVERED FROM Feb 88 TO Feb 90 | 14. DATE OF REPORT (Year, Month, Day) 1990 July 25 | 15. PAGE COUNT |
| 16. SUPPLEMENTARY NOTATION | | | |
| 17. COSATI CODES | | 18. SUBJECT TERMS (Continue on reverse if necessary and identify by block number) | |
| FIELD | GROUP | POLARIZATION RADAR, ICE, HAIL, RAINDROPS, BRIGHT BAND, LIGHTNING. | |
| | | | |
| 19. ABSTRACT (Continue on reverse if necessary and identify by block number) | | | |
| <p>Polarization radar observations provide information on characteristics of precipitation particles not available with conventional weather radar. We report observations of four parameters made with the 25m Chilbolton dish; the largest steerable meteorological radar in the world. These are the first S-band measurements of the linear depolarisation ratio and the most accurate co-copolar correlations yet reported. Ten publications describe the work in more detail.</p> <p>This report demonstrates how the new parameters can be used to: differentiate ice from water, differentiate the different forms of ice (snow, hail pellets), locate areas where large hail is forming, and identify clouds posing a threat of triggered lightning before natural lightning or breakdown has occurred.</p> | | | |
| 20. DISTRIBUTION / AVAILABILITY OF ABSTRACT <input type="checkbox"/> UNCLASSIFIED/UNLIMITED <input type="checkbox"/> SAME AS RPT. <input type="checkbox"/> DTIC USERS | | 21. ABSTRACT SECURITY CLASSIFICATION UNCLASSIFIED | |
| 22a. NAME OF RESPONSIBLE INDIVIDUAL Lt Col James G. Stobie | | 22b. TELEPHONE (Include Area Code) (202) 767-4960 | 22c. OFFICE SYMBOL AFOSR/NC |

DTIC FILED
SEP 27 1990

The University of Manchester Institute of Science and Technology

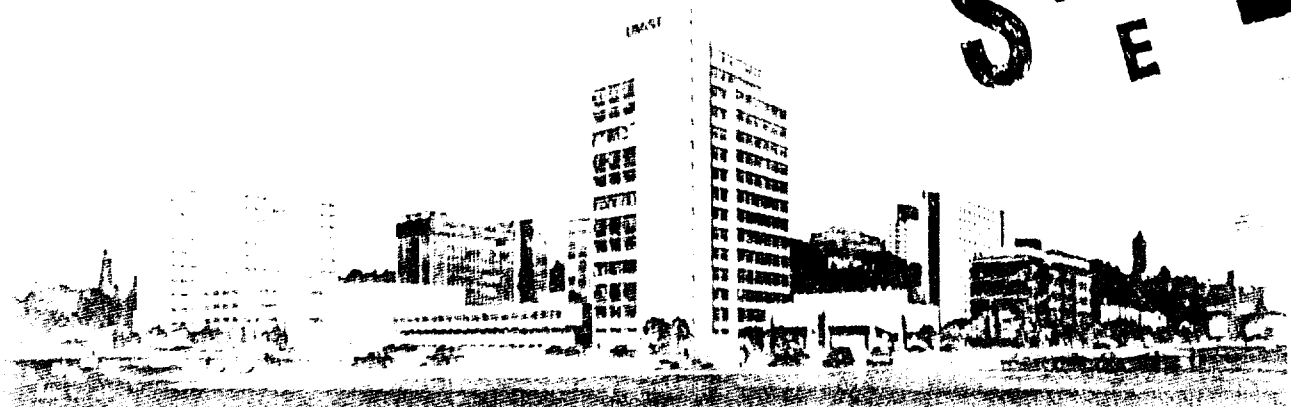
PO Box 88, Manchester M60 1OD. Telephone 061-236 3311. Telex 666094



"Original contains color.
plates: All DTIC reproduces
text will be in black and
white"

DISTRIBUTION STATEMENT A
Approved for public release;
Distribution Unlimited

DTIC
ELECTE
SEP 27 1990
S E D



AFOSR-TR- 90 0941

POLARISATION RADAR STUDIES OF PRECIPITATION:
IMPLEMENTATION OF THE TECHNIQUE AND
DATA INTERPRETATION

Contract No AFOSR 88-0121

FINAL SCIENTIFIC REPORT
15 Feb 1988 - 14 Feb 1990



Anthony J Illingworth

Department of Pure and Applied Physics

UMIST
P O Box 88
Manchester M60 1QD, UK

July 1990

Original contains color
plates. All other reproductions
will be in black and
white.

| | |
|--------------------|---------|
| A-1 | |
| Availability Codes | |
| Dist | Special |

Prepared for:

EUROPEAN OFFICE OF AEROSPACE RESEARCH AND DEVELOPMENT
LONDON, ENGLAND

Approved for public release;
distribution unlimited.

1. INTRODUCTION

This final report describes work performed with the Chilbolton dual polarisation radar under contract number AFOSR-88-0121 during 1988 and 1989. This work constitutes an extension to the radar work completed on grant AFOSR-86-0193 covering the years 1986 and 1987 (see final report dated 20 Jan 1988).

The Chilbolton dual polarization radar is the largest steerable meteorological radar in the world. It can transmit (and receive) pulses alternately polarised in the horizontal and vertical directions. The radar is fully operational and can currently record four independent polarization parameters containing information which enables, for the first time, the precipitation particles to be identified. The radar operates at S-band (10cm) so that propagation effects, which can be troublesome at C-band and X-band, are virtually absent.

We now summarise the polarization parameters:

- (a) Conventional Radar Reflectivity, Z.
Transmit and receive horizontal polarisation and measure ZH, the reflectivity expressed in dBZ relative to the return power for one mm raindrop per cubic meter. From Z alone we cannot distinguish ice from rain.
- (b) Differential Reflectivity, ZDR
The ratio of ZH to ZV, the reflectivities measured at horizontal and vertical polarisations. ZDR is a measure of particle shape.
- (c) The linear depolarisation ratio, LDR.
Transmit vertical and receive the horizontally polarised component, that is, the depolarised signal ZVH, and compare with ZH. ZVH is finite only for oblate tumbling particles. LDR senses fall mode and is an excellent detector of wet ice.
- (d) The copolar correlation $p(H,V)$.
The correlation between the time series of ZH and ZV for successive radar pulses. this parameter measures, amongst other things, the variety of shapes present.

The Chilbolton radar has made the first S-band observations of LDR and the most accurate measurements of $p(H,V)$ yet reported. This report shows how these new parameters may be used:

- (i) To distinguish between different types of ice, and specifically, to differentiate between areas where snow is forming and those where soft hail (graupel) is present.
- (ii) To identify and correct for errors in rainfall estimates caused by the enhanced return from melting snow (the bright band).
- (iii) To identify where damaging hail may be forming.
- (iv) To locate those clouds posing a threat of lightning, even before any natural lightning has occurred.

The colour plate overleaf shows how the radar can be used to detect clouds which are likely to produce a flash of lightning, even though no natural lightning or breakdown may have occurred.

FRONTISPIECE

RADAR OBSERVATIONS OF A TRIGGERED LIGHTNING EVENT

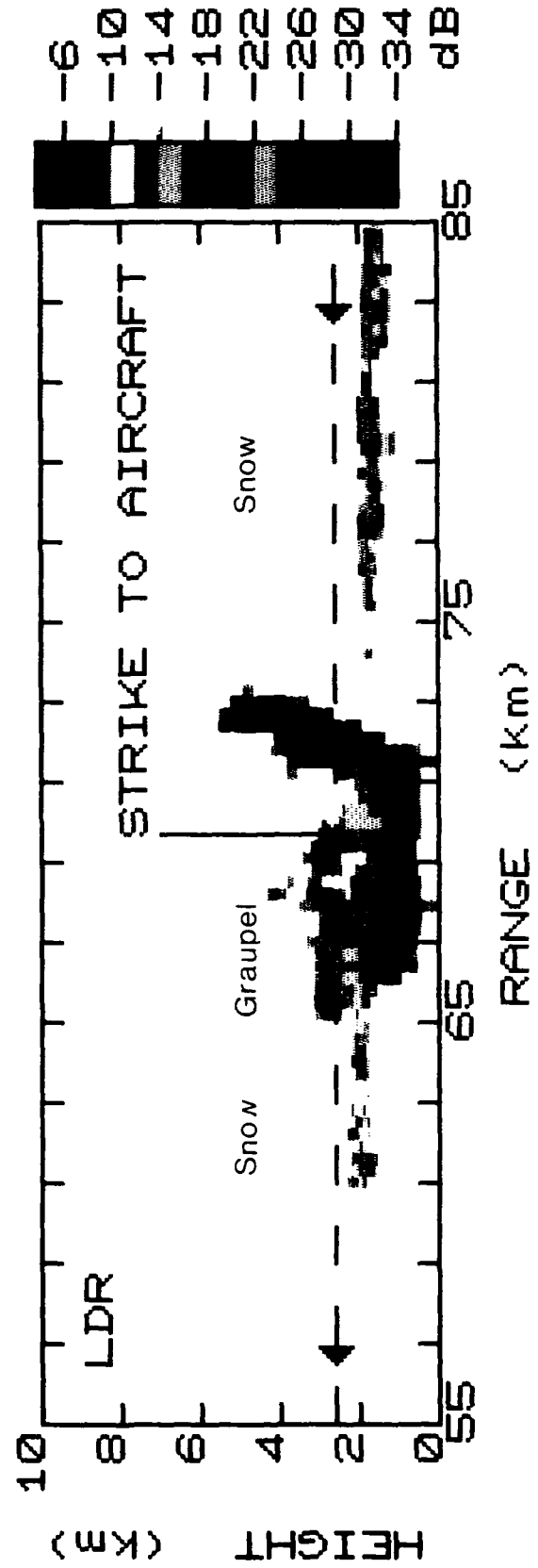
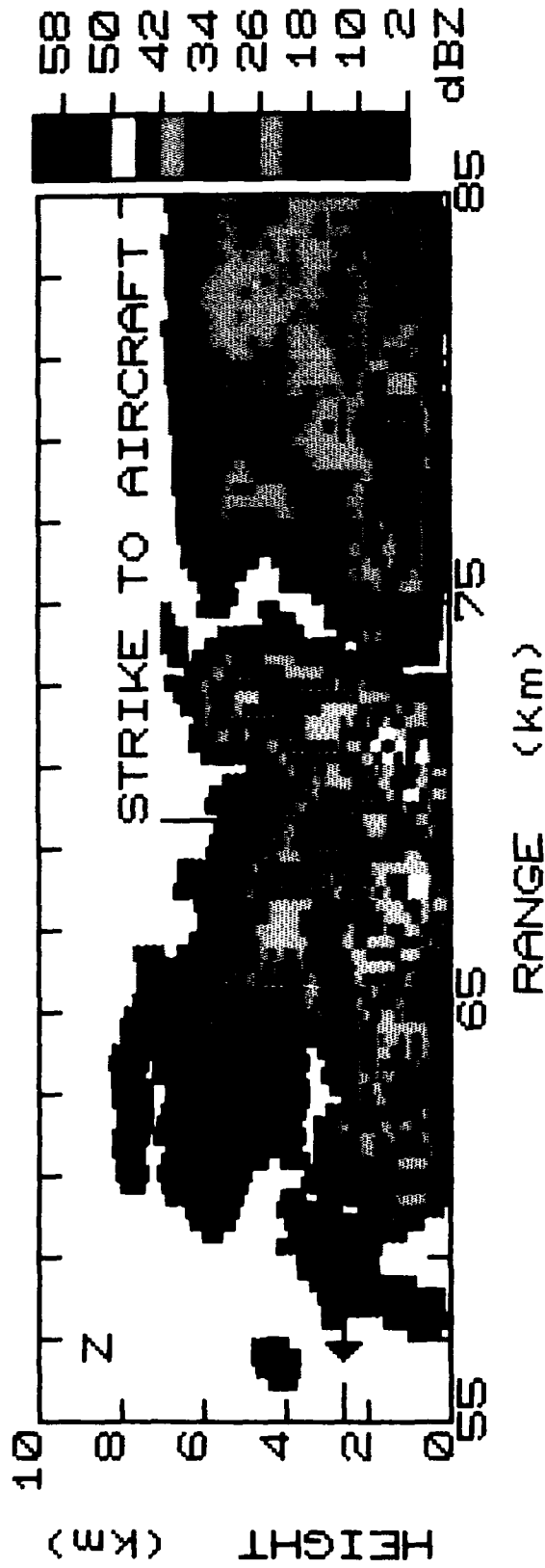
The upper half of the plot is a vertical section through a cloud of the conventional radar reflectivity, Z. The track of the penetrating aircraft at a height of 2.3km is also shown. Although values of Z at this height were only modest (40dBZ) the aircraft triggered a lightning strike as it penetrated the cloud. On this day no natural lightning had been observed before this time.

The lower half of the plot displays one of the new radar parameters, LDR, the linear depolarisation ratio, which we believe can identify those parts of the cloud posing a risk of triggered lightning.

The different types of ice in the cloud can be identified by the values of LDR when they melt. Values of LDR near -15dB (red in the figure) are indicative of oblate melting snow flakes. Such regions of the cloud should not pose a lightning risk. In contrast to this, a small region from 65 to 73km range has much lower values of LDR, near -26dB (green in the figure), where there are more spherical melting ice particles in the form of hail pellets (graupel). The 2-D probe on the penetrating aircraft confirmed the existence of snow and hail pellets in these two regions.

The triggered lightning event occurred when the aircraft traversed a region where the radar inferred the presence of small hail pellets. We believe that the LDR parameter has the potential to identify such a region of potential lightning risk.

RHI SCAN ON 13/07/88 AT 130501 UT
 TAPE 5130 RASTER 28 SCAN 2 AZ 270.00deg



2. OBSERVATION PROGRAM in 1988 and 1999

During 1988 and 1989 the Chilbolton radar reported the first LDR measurements at S-band, and also made measurements of $p(H,V)$ of unrivalled accuracy.

(a) Measurements have been made on numerous days at Chilbolton in stratiform and convective precipitation. The first coincident sets of data for the four parameters (Z, ZDR, LDR and $p(H,V)$) have been collected for several different rainfall types.

(b) On three days coincident flights with the Met Office C-130 aircraft have been carried out. Excellent data sets of 2-D probe observations of precipitation particle type with simultaneous radar coverage were obtained in ice and in the melting layer. Aircraft co-ordination worked well, with the quarter degree beam radar hitting the aircraft during most cloud penetrations; this represents a navigation accuracy of about 300m.

(c) On 13 July 1988 the aircraft triggered a lightning flash while passing through a cloud which was being scanned by the radar.

(d) From November 1988 to January 1989 the group from ETH (Zurich, Switzerland) located their mobile vertically pointing Doppler radar 10km upwind of Chilbolton for a co-ordinated study of the bright band. Vertical profiles with 50m resolution of the velocity and polarization parameters were obtained through bright bands in warm fronts, cold fronts and warm sector rainbands.

3. PUBLICATIONS

In our final report on contract no AFOSR 86-0192 we referred to three completed publications:

- (i) 'Detection of hail by dual polarisation radar'
Nature 320, 431-433, 1986.
- (ii) 'Polarization radar studies of precipitation development in convective storms'
Q J Roy Met Soc, 113, 469-489, 1987.
- (iii) 'Radar observations and modelling of warm rain initiation'
Q J Roy Met Soc 113, 1171-1191, 1987.

A further ten publications have been completed in the two years of the current grant. Copies of these ten publications are included in this report as they best summarise the work completed. A large amount of data is still being analysed.

1. A J Illingworth and I J Caylor
'Radar observations and modelling of warm rain initiation'
1988 10th Int Conf on Cloud Physics, Bad Homburg, Germany.
2. A J Illingworth
'The formation of rain in convective clouds'
1988 Nature, 336, No 6201, 754-756.
3. A J Illingworth and I J Caylor
'Polarization radar estimates of raindrop size spectra and rainfall rates'
1989 J Oceanic and Atmos Tech, 6, 939-949.
4. A J Illingworth and I J Caylor
'Identification of precipitation particles using dual polarization radar'
1988 10th Int Conf on Cloud Physics, Bad Homburg, Germany.
5. I J Caylor and A J Illingworth
'Dual linear polarisation time series as an aid to hydrometeor identification'
1988 IGARSS '88 Symp. Edinburgh, Sept. REF ESA SP-284.
6. I J Caylor and A J Illingworth
'Identification of the bright band and hydrometeors using co-polar dual polarization radar'
1989 24th Conf on Radar Meteorology, Tallahassee, Florida.
7. A J Illingworth and I J Caylor
'Cross polar observations of the bright band'.
1989 24th Conf on Radar Meteorology, Tallahassee, Florida.
8. S E Hopper, A J Illingworth and I J Caylor
'Bright band errors in rainfall measurement: identification and correction using linearly polarised radar returns'
Int Symp on Hydrol Appl of Weather Radar, Salford, UK 1989.
9. I J Caylor, J W F Goddard, S E Hopper and A J Illingworth
'Bright band errors in radar estimates of rainfall: identification and correction using polarization diversity'
1989 COST-73 Int Semin on Weather Radar Networking, Brussels.
10. I Frost, A J Illingworth and I J Caylor
'Aircraft and polarization radar measurements of a triggered lightning event'
1989 Int Conf on Lightning and Static Electricity, Bath, UK.

The topics covered by these papers can be considered in seven groups. We list these groups below, and then in Section 4 consider the findings in more detail:

(a) DEVELOPMENT OF WARM RAIN (Papers 1 and 2)

Polarisation radar observations show that rain (in the absence of ice) first develops as a very low concentration (less than one per cubic meter) of large drops (above 4mm diameter). Rain normally has several thousand drops per cubic meter. Modelling of USA and UK data suggests that these first raindrops are formed on giant nuclei. This is of relevance for theories of rainfall development and implications for attempted weather modification. Such unexpectedly large raindrops in weak echoes could pose an erosion threat to returning space vehicles.

(b) RAINDROP SIZE DISTRIBUTIONS (Papers 3)

This paper presents new data on the shape of large raindrops, and uses these to derive raindrop size and concentrations from observations of Z and ZDR. A statistical study of the variability of naturally occurring raindrop spectra is also given.

(c) POLARISATION PROPERTIES OF FLARE ECHOES (Papers 4 and 6)

Flare echoes are artefacts which result from triple scattering via the ground and occur in low reflectivity regions where Z is low. Triple scattering only occurs in the horizontal polarisation and so flare echoes are accompanied by very high positive values of ZDR.

(d) INTERPRETATION OF CO-POLAR CORRELATION (Papers 4, 5, and 6)

In these papers we report the most accurate measurements yet obtained of the co-polar correlation. They show that it may be used to measure the breadth of the raindrop size spectra, to differentiate between snow and graupel, and how it promises to provide a means of identifying where hail is growing within a cloud.

(e) INTERPRETATION OF LINEAR DEPOLARISATION RATIO, LDR (Paper 7)

This paper presents the first measurements of LDR at S-band, and shows how it can be used to measure the canting angle of raindrops, to identify the bright band, and to distinguish between snow and hail pellets. A colour plot in the paper shows the very different values of LDR for the different types of ice.

(f) USE OF LDR TO CORRECT FOR BRIGHT BAND ERRORS (Papers 8 and 9)

The bright band is region of enhanced radar reflectivity caused by melting snowflakes. Values of Z are about 10dB higher than in the rain, and these high values of Z can lead to overestimates in inferred rainfall rates by up to a factor of ten. These two papers show how the new LDR parameter can be used to identify these errors and also suggests methods of correcting them.

(g) RADAR OBSERVATIONS OF TRIGGERED LIGHTNING (Paper 10)

The findings of this paper are summarised in the frontispiece, the triggered lightning event confirms that the radar is able to identify those regions of the cloud posing a lightning risk.

4. DETAILED ANALYSIS OF THE SIX TOPICS

(A) WARM RAIN DEVELOPMENT (Papers 1 and 2).

The precise mechanism by which rain is formed in clouds in which ice is not present has been the cause of much discussion. The cloud drops formed by condensation are usually so small that they do not possess enough momentum to collide with one another to grow to raindrops. In our earlier report (AFOSR 86-0193) we discussed some UK measurements which indicated that early echoes of warm convective clouds, although having quite modest values of Z of only 20dBZ, already had large positive values of ZDR; these findings indicate the presence of raindrops of 3 or 4mm diameter, but because of the low value of the total reflectivity, these first raindrops must be present in concentrations of much less than one for every ten cubic meters. In mature clouds raindrops are present in concentrations of thousands per cubic meter.

In these papers we present data on the evolution of raindrop spectra. We show that such echoes are common in the USA when warm rain processes are operating. The USA data come from the CP2 radar operating in Alabama. It appears that initially such a low concentration of large drops is stable with very little collision-induced drop rupture; when a critical size is reached, the drops do break up, the concentration increases, more collisions occur and the distributions rapidly moves towards that normally observed in mature clouds.

Such warm rain processes should be common in Florida. The existence of such large drops early in the life of a cloud is quite unexpected. Aircraft sampling these clouds with conventional probes would not sense them, but they could cause erosion to returning space vehicles.

(B) RAINDROP SIZE DISTRIBUTIONS (Paper 3)

The differential reflectivity (ZDR) measures the mean shape of hydrometeors and provides an estimate of the mean size of raindrops. Observations of ZDR for rain may be combined with the conventional radar reflectivity factor (Z) and fitted to any two-parameter raindrop size distribution and this information used to derive more accurate rainfall rates. In such work the precise shape of raindrops is a critical parameter. Recently available data suggest that large raindrops are more oblate than previously believed. These new shapes support the idea that ZDR values above 3.5dB can be attributed to rain. Average values of ZDR as a function of Z obtained in heavy rain by the Chilbolton radar agree very closely with those predicted using the new shapes. Statistics are presented of the natural variability of raindrop spectra in heavy rain. Analytic expressions are proposed for computing rainfall rates from Z and ZDR.

(C) POLARIZATION PROPERTIES OF FLARE ECHOES (Papers 4 and 6)

Flare echoes are caused by triple scattering from a high Z region at a height h, down to the ground, then back to the radar via the precipitation, thus forming a spurious echo a distance h being the intense core. It has already been established that the Doppler velocities in flare echoes are in error. We report that flare echoes are invariably accompanied by very large values of positive ZDR. These ZDR values do not reflect the properties of the hydrometeors, but are an artefact of the triple scattering. They arise because induced vertical dipoles do not radiate along their axes down to the ground, and, as a consequence, all the triple scattered power is in the horizontal, and large positive ZDR results.

Analysis of the triple scattering echoes at X and S-band confirms that for a given value of Z the flare echo is proportional to $(\text{wavelength})^{-4}$, and is 19dB more intense at X-band. For some large storms there is so much attenuation at X-band that the Z values on the far side are so reduced that the flare can be absent. Observations of the Doppler velocities of flares using ZH and ZV reveal that only the velocity derived from ZH are in error. Doppler measurements are usually made using the ZH channel but our findings suggest that Doppler problems would be reduced if the ZV channel was used.

(D) INTERPRETATION OF THE CO-POLAR CORRELATION (Papers 4,5 and 6)

This new variable is defined as the correlation between the time series of successive estimates of ZH and ZV. For the Chilbolton radar 64 pulse pairs are transmitted alternately polarised in the horizontal and the vertical. To compute ZDR the mean values of these ZH and ZV estimates are used. We have constructed a system for recording these individual estimates at 64 different gates. This system streams on to magnetic tape at 40kBytes per second.

As precipitation particles reshuffle in space, then the received signal fluctuates. If the particles are all the same shape then both ZH and ZV fluctuate in the same way and the correlation is unity. If there is a variety of different shapes present, then the correlation falls.

It appears that Chilbolton radar is able to make these correlation measurements with unrivalled accuracy. Values in light rain are over 0.995, and fall to 0.98 in heavier rain when larger oblate raindrops coexist with the smaller spherical ones. There are only a very few reports in the literature of values of $p(H,V)$; observations with CP2 and at NSSL (both in the USA) seem to reach a maximum value of 0.95. The reason for the higher values possible at Chilbolton may be as a result of the extreme purity of the antenna beam pattern, and the low level of any ground clutter. Such high correlations do agree with theoretical values computations for rain, and because of the accuracy available it seems possible to estimate the breadth of the raindrop size distribution. If the raindrop size distribution is represented as a gamma function with an index m, then the value of m reflects the breadth of the size spectra and can be estimated from $p(H,V)$.

Very low values of $p(H,V)$ for precipitation are confined to the bright band where snow is melting, and large oblate particles flutter and rock from side to side as they fall. Indeed the low values of $p(H,V)$ can be used to identify the bright band.

Our computations show that extremely low values of $p(H,V)$ should occur when particles become large enough that Mie scattering occurs. This could be the basis of detecting hail large enough to cause damage. Other methods of hail detection suffer from ambiguities due to wet or dry growth, but this method relies only on Mie scattering and so triggers at a certain hail size for a given wavelength.

Ground clutter also has low correlations. We expect returns due to anomalous propagation also to have low values, and suggest that correlation values could be used to detect and reject spurious echoes due to anaprop.

Some advantages of the correlation technique are:

- (i) It is unaffected by differential attenuation and so, in contrast to ZDR, should be applicable at shorter wavelengths.
- (ii) $p(H,V)$ can be estimated using a short time series, thus overcoming the long dwell times sometimes needed to measure ZDR.
- (iii) The correlation is unaffected by differential phase shifts.

(E) INTERPRETATION OF THE LINEAR DEPOLARISATION RATIO, LDR
(Paper 7)

These are the first measurements of LDR made at S-band. At this wavelength the values of LDR are unaffected by depolarisation of the incident beam, an effect which makes interpretation of LDR difficult at 5cm and almost impossible at 3cm.

The colour figure in this paper shows LDR measurements made in two showers, one containing graupel and a second with snow. From this and many other observations we conclude:

(i) LDR values in the rain are very low, and are usually restricted by the antenna isolation to -32dB. In heavier rain LDR values are slightly higher and are consistent with a mean canting angle of raindrops of about 5 degrees.

(ii) LDR values in dry ice are usually near to the antenna limit, this is because at microwave frequencies the ice particles generally appear spherical. However, in stratiform rain some high ZDR regions, usually accompanied by moderate Z, can have detectable values of LDR. Such regions are thought to have single crystals of ice, and because of their higher dielectric constant and oblate shape they can give a small but finite cross polar return. Similarly, areas of graupel in convective clouds can have a value of LDR slightly above -32dB, again this results from the more dense but slightly oblate ice.

(iii) By far the highest values of LDR are associated with melting wet ice. Melting snow is associated with values which are higher than -20dB, and can be interpreted as being due to wet particles with an axial ratio of about 0.55. Melting graupel gives LDR values of about -26dB, consistent with an axial ratio of about 0.85. Aircraft flights have confirmed these particle inferences. We suggest that LDR is an excellent method of differentiating between snow and graupel.

(iv) Ground clutter has values of LDR above -3dB. Thus LDR has a potential use in identifying and rejecting echoes due to anaprop.

Technologically the advantages of LDR is that no fast switch is required, instead two receive channels are needed. One problem is that the low power in the cross-polar channel may be susceptible to contamination by ground clutter if the antenna has poor sidelobe performance. Clearly the sensitivity of LDR is also limited by the cross-polar performance of the antenna.

(F) USE OF LDR TO CORRECT FOR BRIGHT BAND ERRORS (Papers 8 and 9)

Papers 8 and 9 analyse the increased values of reflectivity in the bright band which result from melting snow. Rainfall values derived from Z can as a consequence lead to overestimates of rain rate by up to a factor of ten. These papers show that values of LDR above -20dB are an excellent detector of the bright band. A simple algorithm can then be used to correct the value of Z and improve the rain rate estimates. A statistical study of the Z and LDR data suggests that rainfall estimates are improved if 8dB is subtracted from the measured Z when the accompanying value of LDR is above -20dB.

(G) POLARIZATION RADAR MEASUREMENTS OF A TRIGGERED LIGHTING FLASH.
(Paper 9)

The passage of an aircraft through clouds can trigger lightning which would not occur naturally. On 13 July 1988 a triggered event occurred in a cloud which was simultaneously being scanned by the Chilbolton radar. The triggered lightning occurred when the aircraft was penetrating an area of the cloud where LDR indicated the presence of graupel. Direct measurements made by the aircraft confirm the presence of graupel in this region. The frontispiece to this report displays the precise values of Z and LDR when the triggered event occurred. It is interesting to note that this cloud has only modest values of Z and a low echo top and is not an obvious candidate for electrical activity.

This finding has important practical implications. It suggests that, for the first time, it is possible to identify a cloud which is likely to trigger lightning before any natural lightning or breakdown as occurred. We are currently engaged in further work for EOARD to examine this hypothesis further. During the summer of 1989 we are comparing lightning location data with polarisation radar observations to check that lightning is only observed in clouds where the radar indicates the presence of graupel.

ACKNOWLEDGEMENTS

The implementation of the differential reflectivity and linear depolarisation ratio measurement was pioneered by J W F Goddard of the Rutherford Appleton Laboratory. We acknowledge very many helpful discussions with J W F Goddard and J Eastment (both of RAL) concerning both the technical aspects of the radar and the interpretation of the data.

Part 1

A J Illingworth and I J Caylor

'Radar observations and modelling of warm rain initiation'
1988 10th Int Conf on Cloud Physics, Bad Homburg, Germany.

RADAR OBSERVATIONS AND MODELLING OF WARM RAIN INITIATION

Anthony J Illingworth
Visiting Scientist
NCAR*, Boulder
Colorado 80307, USA

and I Jeff Caylor
Dept. of Physics
UMIST
Manchester M60 1QD, UK

1. INTRODUCTION

Differential radar reflectivity observations of early echoes of rain in warm convective clouds in the UK and Alabama, USA, indicate that precipitation initially forms as raindrops greater than 4mm in size but present in concentrations of less than one per cubic meter. The differential reflectivity, ZDR, ($10 \log (Z_H/Z_V)$), where Z_H and Z_V are the radar reflectivities measured with horizontal and vertical polarizations, respectively. ZDR provides a measure of the shape of the hydrometeors, and because raindrops are oblate to a degree which depends upon their size, the magnitude of ZDR is a unique function of raindrop size (Table 1). ZDR is a ratio and so is independent of concentrations, but once the mean size is known then the conventional reflectivity, Z_H , can be used to derive an estimate of raindrop concentration (SELIGA and BRINGI, 1976).

2. RAINDROP SIZE AND CONCENTRATIONS

If we assume an exponential raindrop size distribution:

$$N(D) = N_0 \exp(-3.67 D/D_0)$$

where N is the concentration of drops of diameter D and D_0 is the equivolumetric diameter, then by summing the contributions of the various sizes of raindrops present we may calculate the values of ZDR as a function of D_0 (Table 1, final column, spectrum truncated at 8mm). The value of N_0 is then linearly dependent upon the magnitude of Z_H . In Figure 1 the solid lines are the values of Z and ZDR as D_0 varies but N_0 is kept constant. The total drop concentration is given by $N_0 D_0 / 3.67$. Many observations have shown the average raindrop size distribution to be that proposed by Marshall and Palmer with $N_0 = 8000 \text{ m}^{-3} \text{ mm}^{-1}$. A long series of radar observations of Z and ZDR (CAYLOR and ILLINGWORTH, 1987) has confirmed that the average value of ZDR of rain for a given Z does indeed lie upon the $N_0 = 8000$ curve in Figure 1.

We shall be discussing early echoes which have values of ZDR of 3 or 4dB, and would be expected to have Z values of 56 to 67dBZ for Marshall-Palmer rain. Instead the values are 30dBZ lower, implying values of N_0 reduced by a factor of 1000. For example from Figure 1 we see that a value of Z of 15dBZ accompanied by a Z_{DR} of 3dB implies a value of N_0 of only $0.8 \text{ m}^{-3} \text{ mm}^{-1}$, or a drop concentration ($D_0 = 2.5 \text{ mm}$) of 0.1 m^{-3} .

3. CHILBOLTON RADAR (UK) OBSERVATIONS

A vertical section through a young convective cloud with anomalously high ZDR is displayed in Figure 2 (for other examples and details of the radar, see ILLINGWORTH et al, 1987). Values of Z of 30dBZ are accompanied by a ZDR above 4.5dB, which imply (Figure 1) large drops (6mm) in concentrations of only one per cubic meter. This cloud persisted for twenty minutes with no great change in character; the 2700 data points obtained during this period are displayed in Figure 3, where each star represents the average value of ZDR for every 2dBZ step in Z . The solid line in Figure 3 is the $N_0 = 8000$ curve from Figure 1; showing that the low concentration of large raindrops persisted throughout the twenty minute period.

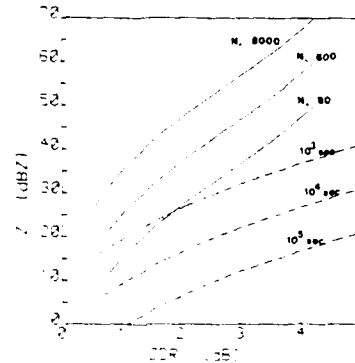


Figure 1. The variation of Z and ZDR as a function of 3 values of N_0 (solid lines). The dashed lines show the expected lifetime for a 5mm diameter drop.

TABLE 1

| Size (mm) | Axial Ratio | ZDR (dB) | D_0 (mm) | ZDR (dB) |
|-----------|-------------|----------|------------|----------|
| 4 | 0.778 | 2.49 | 1 | 0.62 |
| 5 | 0.708 | 3.48 | 2 | 2.31 |
| 6 | 0.642 | 4.42 | 2.5 | 3.03 |
| 7 | 0.581 | 5.33 | 3 | 3.56 |
| 8 | 0.521 | 6.70 | 4 | 4.22 |

Values of axial ratio (from BEARD and CHUANG, 1987) and ZDR for various sizes of raindrop. The Mie-Gans calculations are supplied by Dr Holt, Department of Mathematics, University of Essex, and apply to raindrops at 0°C and 3.0765 GHz.

*The National Centre for Atmospheric Research is sponsored by the National Science Foundation.

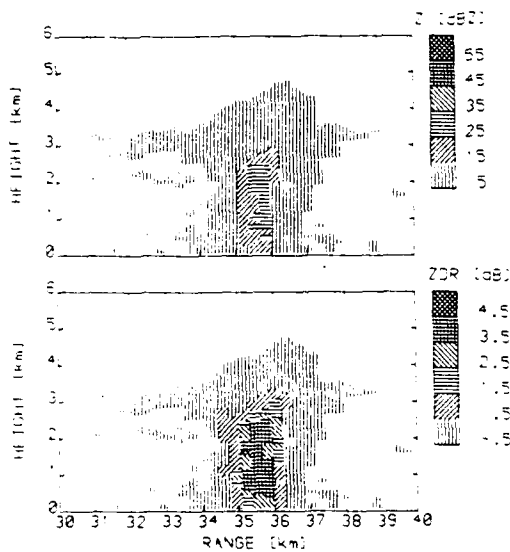


Figure 2. A vertical scan on 20 June 1980 displaying anomalously high ZDR.

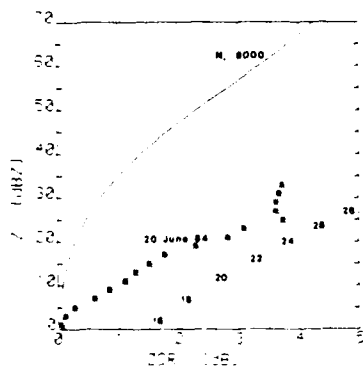


Figure 3. Averaged Z and ZDR over a 20 minute period for the cell in Figure 2. For comparison the model output as a function of time (minutes) and the Z and ZDR for a drop size distribution with $N_0 = 8000$ are shown.

4. GIANT NUCLEI MODEL

To explain such low concentrations of large raindrops, CAYLOR and ILLINGWORTH (1987) extended a suggestion (JOHNSON, 1982) that each large raindrop formed on an ultra giant nuclei ($>30\mu\text{m}$), present in the background concentration at this low level (JUNGE, 1972). Figure 3 shows the prediction of the simple model in which Z and ZDR increase as the giant nuclei sweep out cloud water of $\text{LWC } 2 \text{ g m}^{-3}$, the numbers indicate time in minutes elapsed since initiation of the model with nuclei concentrations (in units of m^{-3} per unit log interval of radius) of 10^7 for $10\mu\text{m}$ radius to 3×10^2 for $100\mu\text{m}$.

Only a few large raindrops grow, and the depletion of the cloud water is negligible. The model is linear in that increasing the LWC merely changes the time scale but not the Z/ZDR dependence; in addition, increasing the nuclei concentration merely scales up the values of Z leaving ZDR unchanged. The Chilbolton cloud persisted 20 minutes and it is not possible to give a specific age to various parts of the cloud. In view of the uncertainty of the absolute concentration of giant nuclei, the observed general dependence of Z with ZDR is consistent with the model.

5. ALABAMA DATA, NCAR CP2 RADAR

First echoes formed at temperatures above zero on many days during the 1986 MIST (Microburst Severe Thunderstorm) project. These early echoes were also normally accompanied by anomalously high values of ZDR. A particularly clear example was on 10 July, when the evolution of a very weak echo less than 2km in diameter was observed in its entirety. In 20 minutes the echo grew from zero to 20dBZ and then collapsed; the top of the radar echo reached only 5km (slightly above the freezing level), but during this time values of ZDR in the cloud increased to 4dB, the ZDR core then descended as the rain fell to ground.

Figures 4 and 5 show the specific values of each Z/ZDR data point for two successive vertical sections through the maximum echo. The numbers plotted for each point represent the height of the data to the nearest kilometer. The evolution is consistent with the model in Figure 3, in that the concentration of drops is constant and less than one per cubic meter, 5 minutes after the appearance of the echo, the value of ZDR was 3dB, growing to 4dB in the subsequent three minutes. This is consistent with the maximum drop size increasing from 4.5 to 6mm (Table 1) by sweeping out cloud water of $\text{LWC } 2 \text{ g m}^{-3}$.

6. CONCLUSIONS.

We have presented evidence that early echoes of warm clouds consist of a very few drops which grow to a large size by sweeping out cloud water. Because concentrations are so low this can happen without exhausting the supply of liquid water, and also with a negligible number of collisions causing the drops to break up. LOW and LIST (1982) found that for a collision to cause shattering, both raindrops must be larger than 1mm. For a given Do the lifetime of a large raindrop will be inversely proportional to N_0 ; in Figure 1 the dotted lines join the values of Z and ZDR for lifetimes of 1000, 10000, and 100000 seconds for a 5mm drop. The large raindrops in Figure 4 and 5 will survive for over an hour before collision-induced rupture. This situation should be contrasted to Figure 6 showing the Z/ZDR scatter plot for a normal mature cloud on 6 July 1986, the values are closer to the average $N_0=8000$ curve, and the lifetime of the larger drops is less than a minute.

Warm rain measurements in Texas (CARBONE and NELSON, 1978) and in Hawaii (BEARD et al, 1986) also indicate low values of N_0 and high D_0 . Conventional airborne instruments do not generally have a large enough sample volume to obtain meaningful statistics of the very low concentrations inferred from the radar. In Hawaii one 8mm raindrop was sampled, supporting the idea that such raindrops are indeed stable in the atmosphere if they do not undergo collisions. Drops up to 9mm are stable in low turbulence wind tunnels (PRUPPACHER and BEARD, 1970).

We suggest that convective raindrops first form on embryos which are present in concentrations of about one per cubic meter. Such embryos could be giant nuclei, or alternatively could be ice crystals. The number of ice crystals seeding such a cloud might be expected to be more variable, and to be much greater if the cloud top was higher, yet the raindrop concentrations always seem to be very low. A raindrop distribution of a few large drops would appear to be very stable, but once break-up occurs, either due to the occasional collision or spontaneously if the drops become too large, then many small fragments are produced, and the distribution rapidly and irreversibly changes to the more normal Marshall-Palmer distribution.

ACKNOWLEDGEMENTS

This research was supported by the Meteorological Office, by NERC Grant GR3/5896 and by AFOSR-87-0046. Our co-workers S M Cherry and J W F Goddard pioneered the implementation and interpretation of the ZDR data at Chilbolton. We thank Profs Bringi, Forbes, Fujita and Wakimoto for allowing us access to the MIST data. IJC acknowledges the assistance of an ORS scholarship and AJI thanks members of the FOF at NCAR for many useful discussions.

REFERENCES

- BEARD, K.V.; JOHNSON, D.B.; BAUMGARDNER, D.: *Geophys. Res. Letters*, 13 (1986) 991-994.
 BEARD, K.V.; CHUANG, D.: *J. Atmos. Sci.* 44 (1987) 1509-1524.
 CARBONE, R.E.; NELSON, L.D.: *J. Atmos. Sci.* 35 (1978) 2302-2314.
 CAYLOR, I.J.; ILLINGWORTH, A.J.: *Q. J. Roy. Meteorol. Soc.* 113 (1987) 1171-1191.
 ILLINGWORTH, A.J.; GODDARD, J.W.F.; CHERRY, S.M.: *Q. J. Roy. Meteorol. Soc.* 113 (1987) 469-489.
 JOHNSON, D.B.: *J. Atmos. Sci.* 39 (1982) 448-460.
 JUNGE, C.E.: *J. Geophys. Res.* 77 (1972) 5183-5200.
 LOWE, T.B.; LIST, R.: *J. Atmos. Sci.* 39 (1982) 1591-1618.
 PRUPPACHER, H.R.; BEARD, K.V.: *Q. J. Roy. Meteorol. Soc.* 96 (1970) 247-256.
 SELIGA, T.A.; BRINGI, V.N.: *J. App. Meteorol.* 15 (1976) 69-76.

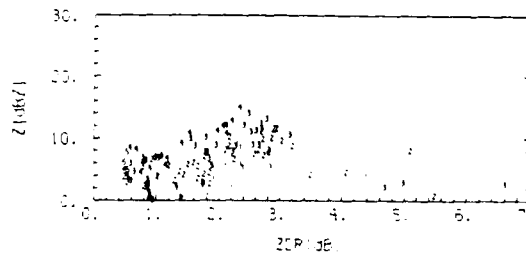


Figure 4. Scatter plot of Z and ZDR for each data point from a young echo on 10 July 1986 at 1301 CDT indicating low concentrations of large drops.

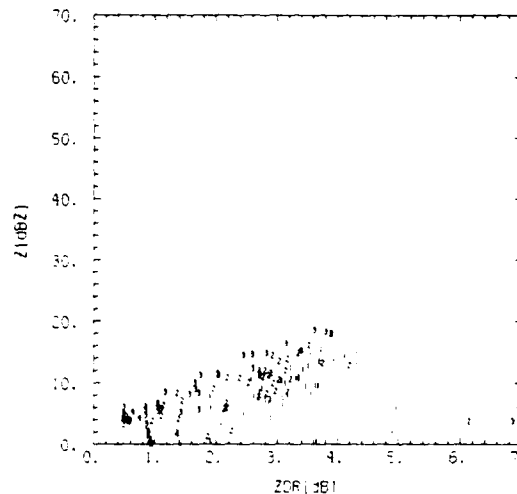


Figure 5. Values of Z and ZDR from the same cloud as Figure 4 observed 3 minutes later.

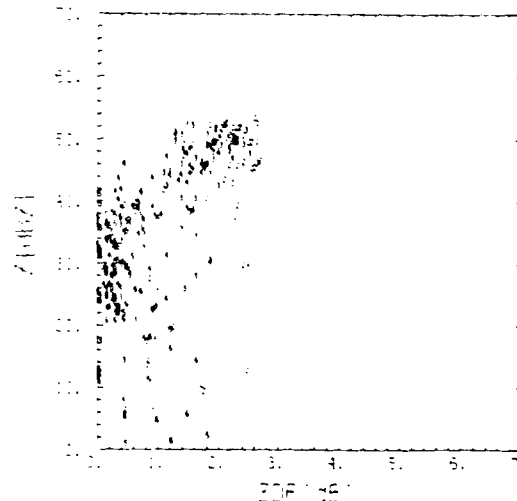


Figure 6. Z and ZDR data points from a mature convective cloud on 5 July 1986 at 1426 CDT indicating a Marshall-Palmer drop size distribution.

Part 2

A J Illingworth

'The formation of rain in convective clouds'

1988 Nature, 336, No 6201, 754-756.

The formation of rain in convective clouds

Anthony J. Illingworth*

NCAR, PO Box 3000, Colorado 80307, USA

One of the chief problems in cloud physics¹ is to explain how, in the absence of ice, small cloud droplets can coalesce to form raindrops. Cloud droplets are produced in concentrations of $\sim 10^8 \text{ m}^{-3}$ by condensation on sub-micrometre atmospheric nuclei, but, because they are so small, collisions between droplets are rare events. In mature rainclouds there are² usually about 1,000 drops per m^3 ; here, however, I present differential radar reflectivity observations which indicate that, when ice is not present, first echoes of convective showers consist of large ($> 4 \text{ mm}$) raindrops present in much lower concentrations ($< 1 \text{ m}^{-3}$). I suggest that these raindrops form on ultra-giant nuclei ($> 30 \mu\text{m}$ radius) which are present in similarly low background concentrations³. In some clouds this initial raindrop spectrum persists, whereas in other cases it changes rapidly and irreversibly to the raindrop distribution normally observed in mature clouds with many more smaller raindrops. The latter may occur when the break-up of the large raindrops becomes more common and many small satellite drops are produced.

Coalescence of small droplets in clouds may be triggered by condensation on hygroscopic salt nuclei or by mixing of drier air into the cloud; either process could produce larger droplets, which would then have a reasonable terminal velocity and be able to capture smaller droplets, thus triggering droplet growth. Paluch and Knight⁴ have reviewed the evidence for these processes. The cloud droplet concentration is at least five orders of magnitude higher than the raindrop concentration, so that it is very difficult to make direct in-cloud observations of the occasional embryonic raindrop in the radius range 50–100 μm , when so many smaller droplets are also present. Measurements of the conventional radar reflectivity, Z , are difficult to interpret in terms of both the size (d) and concentration (n) of raindrops, because Z is given by the product nd^6 summed over all raindrop sizes. Z is usually quoted in dBZ, that is in decibels over $1 \text{ mm}^6 \text{ mm}^{-3}$. A full review of the meteorological applications of radar is provided by Browning⁵.

Here we report measurements of differential reflectivity (Z_{DR}), which is defined as

$$Z_{\text{DR}} = 10 \log (Z_{\text{H}} / Z_{\text{V}}) \quad (1)$$

where Z_{H} and Z_{V} are the radar reflectivity factors measured with horizontally and vertically polarized radiation, respectively. Z_{DR} is a measure of the shape of precipitation particles. Because raindrops are oblate to a degree which depends on their size, Z_{DR} is positive for large raindrops and its magnitude is a measure of their mean size. With knowledge of the drop size, d , the drop concentration n may be calculated⁶ from the absolute value of Z_{DR} . In practice the raindrop size distribution may be well approximated by a spectrum of the form:

$$n(d) = n_0 \exp(-3.67 d / d_0) \quad (2)$$

where d_0 is the equivolumetric diameter. The value of Z_{DR} is independent of concentration and may be calculated as a function of d_0 . The value of n_0 may then be found from the observed magnitude of Z . The solid curve in Fig. 1 shows calculated values of Z and Z_{DR} for $n_0 = 8,000 \text{ m}^{-3} \text{ mm}^{-1}$; this value of n_0 was originally proposed for stratiform rain² but it now appears to describe the average properties of most rain. For individual data points and clouds not lying on this average curve, the value of n_0 may be derived by noting that Z is proportional to n_0 . The total concentration is given by $n_0 d_0 / 3.67$.

Observations of developing convection were made each day during the MIST project⁷ in 1986 using the 10-cm dual polariz-

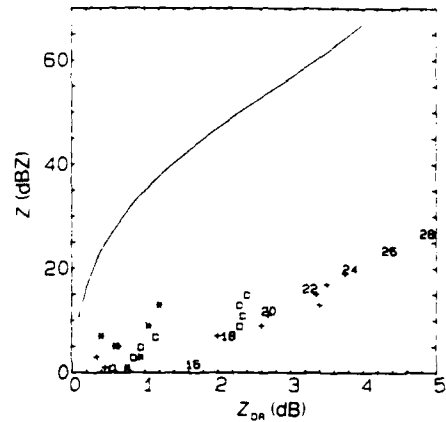


Fig. 1 Values of Z (radar reflectivity) and Z_{DR} (differential reflectivity) observed during the evolution of the echo on 10 July 1986. The solid line represents the drop concentrations for average rain, $n_0 = 8,000 \text{ m}^{-3} \text{ mm}^{-1}$ (equation 2). The observations are average values of Z_{DR} for each 2-dBZ step in Z . Symbols represent observation times: + 12:57, □ 13:01, + 13:04. n_0 scales linearly with Z , so inferred raindrop concentrations are over 30 dB (a factor of one thousand) below 'average'. The numbers indicate time in minutes elapsed since the initial evolution of the radar responses Z and Z_{DR} , during which time ultra-giant nuclei sweep out cloud water droplets.

ation CP-2 radar operated by the National Center for Atmospheric Research. The values of Z and Z_{DR} reported here are accurate to better than 1 dBZ and 0.2 dB respectively. The first echoes of 5–10 dBZ usually formed at temperatures warmer than 0°C and were accompanied by anomalously positive values of Z_{DR} , implying (Fig. 1) the presence of a very low concentration of unexpectedly large raindrops and confirming more limited UK observations^{8,9} made in 1983 and 1984 with the Chilbolton polarization radar.

A particularly well observed case occurred on 10 July 1986, when a series of 90 vertical (RH1) and horizontal (PPI) radar sections was made through an isolated echo from its initiation with $Z = 5 \text{ dBZ}$ at 12:54 CST (=GMT–6 hours) to a maximum of $Z = 20 \text{ dBZ}$ (accompanied by values of Z_{DR} near 4 dB), and terminating at 13:10 as the echo fell to the ground and disappeared. During this time the echo was unsheared, its top never rose above 5 km altitude and the horizontal cross-section never exceeded 2 km in diameter. It is not possible to plot the hundred or so data points obtained for each scan, but a summary of the evolution is provided in Fig. 1, in which the average value of Z_{DR} for each 2-dBZ step in Z is plotted for three scans at 12:57, 13:01 and 13:04. These scans are all at the same azimuth and pass through the maximum echo. We note that the maximum values of Z and Z_{DR} increase with the passage of time, but that the average values all lie on a similar curve. Plots for the intermediate scans show a smooth progression along this evolutionary curve. Increases in Z ceased at 13:04, as the main echo fell below cloud base (inferred from a nearby sonde ascent) and the plots for the scan at 13:07 are within 0.5 dB of the 13:04 data.

The evolution shown in Fig. 1 is compatible with a situation in which a very few raindrops grow by sweeping out cloud liquid water. In 3 min the maximum Z_{DR} increased from 2.4 dB to 4 dB, corresponding to an increase of the maximum diameter for monodispersed drops from $\sim 4 \text{ mm}$ to 6 mm, this occurring by collection of cloud droplets with a liquid water content of 2 g m^{-3} . The concentrations are very low; for example, a Z value of 15 dBZ accompanied by a Z_{DR} of 3 dB is equivalent, for monodispersed drops, to the presence of 4.5-mm drops at a concentration of 0.03 m^{-3} , or, for an exponential distribution, to a value of n_0 of $0.5 \text{ m}^{-3} \text{ mm}^{-1}$. The difference in concentrations predicted by the exponential and the monodispersed spectra is negligible compared with the deviation from the 'average' curve in Fig. 1. Analysis of the sonde ascent predicts a maximum adiabatic liquid water content of 3 g m^{-3} for a

*Permanent address: Department of Physics, MIST, Manchester M60 7QD, UK.

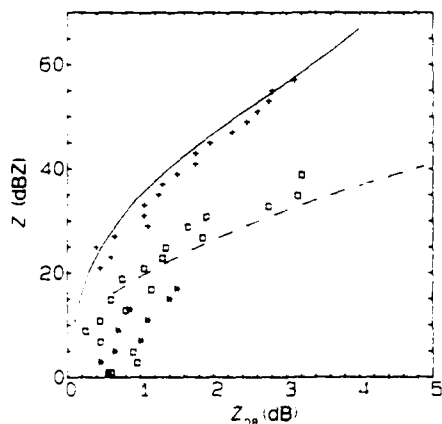


Fig. 2 The evolution of the echo observed on 28 June 1986. Solid line and averages follow the same key as in Fig. 1. Times are: \bullet 12:21, \square 12:27, $+$ 12:40. The dashed line joins the values of Z and Z_{DR} that correspond to a 5-mm raindrop which has a lifetime of 1,000 s before shattering as a result of collisions. For a given Z_{DR} the lifetime is inversely proportional to Z .

temperature of 8°C. Above this level, much drier air, with a mixing ratio of less than 2 g m^{-3} at 5°C, restricted cloud growth.

The data are in very good agreement with the time evolution predicted by a model⁸ in which ultra-giant nuclei collect cloud water and grow to raindrops. This model extends earlier work¹⁰ which showed that such a mechanism could produce a high radar reflectivity within 15–20 min. Our new model predicts the accompanying values of Z_{DR} , but does not consider the vertical structure that may result from sedimentation. The nuclei need not be hygroscopic but, because they are so large, they collect the cloud droplets with reasonable efficiency. The numbers in Fig. 1 indicate the time in minutes elapsed since initiation of the mechanism proposed in our model, for a cloud liquid water density of 2 g m^{-3} with concentrations (in units of m^{-3} per unit log interval of radius) of 1,000 for nuclei of 10- μm radius to 0.03 for 100- μm radius. These nuclei concentrations are those quoted by Junge³ for the background level found above the trade-wind inversion and are similar to the 'maritime' nucleus spectrum used by Johnson¹¹. The drop concentrations inferred on 10 July are exceptionally low; values a factor of ten higher were inferred on other days in the MIST programme. It may be that on such days nucleus concentrations closer to the ground were higher than the background levels used in the model.

When the convection was vigorous, the intensifying echo top usually rose above the 0°C isotherm and the spectra in the rain tended towards that usually observed in mature clouds, but on one occasion (28 June 1986) it was possible to observe the evolution of an echo to over 50 dBZ without ice forming in the cloud. The average values of Z_{DR} for each 2-dBZ step in Z for three successive scans are shown in Fig. 2. The time resolution is rather poor because the radar was executing 360° surveillance scans. At 12:21 the maximum Z value was 17 dBZ, associated with a Z_{DR} value of ~ 1.5 dB, and inferred concentrations are more than two orders of magnitude (equivalent to 20 dB) below the curve for 'average' rain. Six minutes later, at 12:27, Z had reached nearly 40 dBZ and Z_{DR} was ~ 3 dB, indicating that the biggest drops had grown in diameter by 2 mm. The concentration of these large drops is still two orders of magnitude below average. By 12:40 the highest Z was over 55 dBZ, but the picture is then dramatically different, the inferred raindrop size distribution being that found in mature clouds.

To support our contention that drop collisions are responsible for this abrupt change in the spectra, the dashed line in Fig. 2 represents values of Z and Z_{DR} for which a 5-mm droplet would have an average lifetime of 1,000 s before it collided with another droplet greater than 1 mm in diameter. Collisions between two raindrops which are both larger than 1 mm are generally followed by disruption and shattering to produce many small

fragments¹¹. For a given Z_{DR} , the value of d_0 is constant and the number of drops is proportional to Z ; accordingly, the lifetime of each large raindrop is inversely proportional to Z . We note that in Fig. 1 the data lie in a region where the large drops have a lifetime of several hours before they suffer collision-induced rupture. In Fig. 2 the initial concentrations are somewhat higher, and by 12:27 the drop lifetimes are slightly shorter than 20 min; finally, at 12:40 h the spectrum has changed to the 'mature' mode, with a high concentration of smaller drops, so that the large drops contributing to a Z_{DR} of 3–4 dB would have a lifetime of only a few seconds and would be continuously regenerated.

Some measurements^{12,13} made from aircraft within developing clouds have also indicated raindrop spectra different from those found in mature clouds, although Z values were higher and the spectra were not as extreme as those reported here. Measurements in Texas¹² revealed low values of n_0 in early echoes and an implied absence of collision-induced break-up. The authors attributed the low values of n_0 to drop sorting in the updraft, but this does not seem compatible with the time evolution of the Z_{DR} RHI scans from the MIST data. In Hawaii¹³ raindrops 8 mm in size were observed. The existence of such large raindrops had been questioned because in Marshall–Palmer rain they would rapidly suffer collision-induced break-up, but the authors showed that when total drop concentrations are low, the lifetimes are sufficiently long. The very low concentrations inferred from the radar data of the MIST project would be difficult to confirm by aircraft penetrations because of the limited sample volume of most precipitation-sizing probes.

Other mechanisms for the production of the raindrops must be considered. There is always the possibility that a few ice crystals (which would have a Z value below -20 dBZ and would be undetectable by radar) could fall from higher levels, melt, and then grow into large raindrops. This seems unlikely: the air was very dry at these colder levels and no bright band in Z_{DR} was observed. (It is our experience that as small ice crystals start to melt there is a sudden jump in Z_{DR} as they become wet and change their dielectric constant, followed by an equally sudden drop to zero Z_{DR} as they melt completely to become small spherical raindrops.)

In his initial report on the existence of ultra-giant nuclei, Junge³ remarked that they were so rare that they could not be important in the warm-rain process. Such a view seems eminently sensible, but this new radar evidence shows that warm rain does indeed first form in such low concentrations. It may be that a fortunate combination of collection efficiencies and droplet sizes results in just one cloud droplet in 10^6 being able to capture its neighbours and grow into a raindrop. It is evident that further modelling and observations are needed, but I propose meanwhile that cloud droplet capture by ultra-giant nuclei is a simple and equally plausible mechanism.

I thank Professors Bringi, Forbes, Fujita and Wakimoto for allowing access to the MIST data, and staff at NCAR for their assistance during my visit. This research was also supported by NERC and EOARD. NCAR is supported by the National Science Foundation.

Received 2 August; accepted 14 November 1988

1. Pruppacher H. R. & Klett J. D. *Microphysics of Clouds and Precipitation*. Reidel, Dordrecht, 1978.
2. Marshall, J. S. & Palmer, W. M. K. *J. Met. Soc.* 165, 166–194 (1948).
3. Junge, C. E. *J. Geophys. Res.* 77, 5183–5200 (1972).
4. Paluch, J. R. & Knight, J. A. *J. Atmos. Sci.* 43, 1994–1998 (1986).
5. Browning, K. A. *Rep. Prog. Phys.* 41, 761–806 (1978).
6. Neega, T. A. & Bringi, V. S. *J. Appl. Met.* 15, 89–76 (1976).
7. Dodge, J., Arnold, J., Wilson, G., Evans, J. & Fujita, T. *Bull. Am. Met. Soc.* 67, 417–419 (1986).
8. Lawson, J. T. & Illingworth, A. J. *Q. J. R. Met. Soc.* 113, 1171–1191 (1987).
9. Illingworth, A. J., Goddard, I. W. F. & Churn, S. M. *Q. J. R. Met. Soc.* 113, 469–499 (1987).
10. Johnson, D. B. *J. Atmos. Sci.* 39, 448–460 (1982).
11. Loak, T. B. & List, R. *J. Atmos. Sci.* 39, 1891–1918 (1982).
12. Mathone, R. E. & Nesjean, J. D. *J. Atmos. Sci.* 35, 212–214 (1978).
13. Beard, K. S., Johnson, D. B. & Baumgardner, D. *J. Geophys. Res. Lett.* 13, 991–994 (1986).

Part 3

A J Illingworth and I J Caylor

'Polarization radar estimates of raindrop size spectra and
rainfall rates'

1989 J Oceanic and Atmos Tech, 6, 939-949.

ABSTRACT

The differential reflectivity (Z_{DR}) measures the mean shape of hydrometeors and provides an estimate of the mean size of raindrops. Observations of Z_{DR} for rain may be combined with the conventional radar reflectivity factor (Z) and fitted to any two parameter raindrop size distribution and this information used to derive more accurate rainfall rates. In such work the precise shape of raindrops is a critical parameter. Recently available data suggest that large raindrops are more oblate than previously believed. These new shapes support the idea that Z_{DR} values above 3.5dB can be attributed to rain. Average values of Z_{DR} as a function of Z obtained in heavy rain by the Chilbolton radar agree very closely with those predicted using the new shapes. Statistics are also presented of the natural variability of raindrop spectra in heavy rain. Analytic expressions are proposed for computing rainfall rate from Z and Z_{DR} .

1. INTRODUCTION

The radar reflectivity factor, Z , of rain measured by a conventional radar is not a unique function of the rainfall rate or the mean size of the raindrops, but is given by the product ND^6 , where N is the concentration of drops of diameter D , summed over all the drop sizes present. Many different empirical relationships have been proposed relating the rainfall rate (R) to the radar reflectivity (Z). The use of one of these formulae is essentially equivalent to assuming a constant raindrop size distribution. Such relationships reflect an average long term dependence, but the actual rainfall predicted by an individual value of Z is typically in error by a factor of two because of natural fluctuations in the raindrop size spectra (Wilson and Brandes, 1979).

Polarization diversity radar provides a second observable parameter, the differential reflectivity, which is related to the mean drop size, and when this information is used in conjunction with Z , more accurate rainfall rates may be derived. The differential reflectivity (Z_{DR}) is defined as:

$$Z_{DR} = 10 \log (Z_H/Z_V) \quad (1)$$

where Z_H and Z_V are the radar reflectivity factors measured at horizontal and vertical polarizations, respectively. For spherical particles, such as small raindrops, Z_H and Z_V are equal, and Z_{DR} is zero. Larger raindrops are oblate to a degree which depends upon their size, so Z_H exceeds Z_V ; Z_{DR} is positive, and its magnitude is related to the mean raindrop size present.

When observations of both Z and Z_{DR} are available, then the data can be fitted to any two parameter raindrop size distribution. Raindrop size distributions are commonly of the exponential form:

$$N(D) = N_0 \exp (-3.67 D/D_0) \quad (2)$$

where D is the equivolumetric raindrop diameter of the oblate drops and D_0 is the volume-median drop diameter. Marshall and Palmer (1948) reported that D_0 is a function of rainfall rate and that, on the average, N_0 is $8000\text{m}^{-3}\text{mm}^{-1}$. Seliga and Bringi (1976) proposed that the value of D_0 may be derived from the magnitude of Z_{DR} , and N_0 may then be found if Z is known.

The differential reflectivity technique relies on a precise knowledge of the shapes of different sizes of raindrops. The Chilbolton radar (Cherry and Goddard, 1982) can measure Z_{DR} to an accuracy of about 0.1dB which is equivalent to a change in raindrop axial ratio of about 0.01. Most Z_{DR} measurements have been interpreted using the laboratory based equilibrium raindrop shapes of Pruppacher and Pitter (1971) who quote errors of about ± 0.03 for the axial ratios of the drops up to 4mm diameter.

In a series of comparisons of Chilbolton radar data with a ground based disdrometer (Goddard and Cherry, 1984; and Goddard, Cherry and Bringi, 1983), significantly improved agreement between the radar and disdrometer derived rainfall rates was obtained if the drops below 3mm in size were made slightly more spherical than the shapes of Pruppacher and Pitter. The proposed changes in drop shapes were within the experimental error of the Pruppacher and Pitter laboratory measurements; for example the axial ratio of a 1mm drop was changed from 0.98 to 1.00. Recently, more accurate measurements of the shape of naturally occurring raindrops using airborne shadowgraph instruments (Chandrasekar et al, 1988) have confirmed that the shapes inferred from the radar are correct and that the smaller drops are indeed slightly more spherical than suggested by Pruppacher and

Pitter. New laboratory experiments (Beard and Ochs, 1988) on 1.2 and 1.3mm drops also support this conclusion.

In this paper we direct attention to heavier rainfall with values of Z above 40dBZ and rainfall rates generally above 10mm hr^{-1} . The precise shapes of raindrops larger than 4mm are uncertain, but are important for Z_{DR} measurements in heavier rain. Doviak and Zrnic (1984) state that the maximum value of Z_{DR} due to rain should be 3.5dB. This assertion is based upon Green's (1975) formula for the axial ratio of raindrops, which is very close to the measurements of Pruppacher and Pitter. Using these shapes a 6mm drop would be associated with a Z_{DR} of 3.8dB and an 8mm drop 4.7dB; summing the weighted contribution of the various drops in a Marshall-Palmer raindrop size distribution leads to the conclusion that the Z_{DR} of rain cannot exceed 3.5dB. Doviak and Zrnic (1984) suggest that higher values of Z_{DR} result from a measurement related problem or are due to targets other than raindrops and suggest they arise from ice particles which have very oblate shapes when they melt.

Values of Z_{DR} above 3.5dB and as high as 6dB have been reported in convective showers (Illingworth et al, 1987) and in view of the above argument it seems logical to attribute such observations to melting ice particles. On closer examination other possibilities arise. Based on a statistical analysis of the high values of Z_{DR} accompanying intense echoes at altitudes where rain is to be expected, Caylor and Illingworth (1986) hypothesized that raindrops larger than 4mm are more oblate than predicted by Pruppacher and Pitter. This suggestion was prompted by two findings. Laboratory measurements (Rasmussen et al, 1984) indicate that, unless the ice particles are initially extremely oblate, then the shapes during melting are no more distorted than

those of the same sized water drop. Secondly, a limited series of aircraft measurements of large drops (Cooper et al, 1983) implied more oblate forms. Beard and Chuang (1987) have recently published more accurate computations of the shape of large drops and in Section 2 of this paper we use these new shapes to calculate the values of Z_{DR} to be expected for various raindrop size distributions. The predicted variation of the average values of Z_{DR} as a function of Z using these new shapes is compared with the actual average values observed with the Chilbolton radar. The variation in the naturally occurring spectra around these mean values is discussed in Section 3. The implications of these results for rainfall measurement are explored in Section 4.

2. THE DIFFERENTIAL REFLECTIVITY OF HEAVY RAIN

(a) Drop Shapes and Differential Reflectivity

The axial ratios for drops above 4mm proposed by Pruppacher and Pitter (1971) are compared with the more recent values obtained by Beard and Chuang (1987) in Table 1. The values of Pruppacher and Pitter have considerable scatter when experimental errors are considered, with, for example, drops between 7 and 8mm having ratios in the range 0.51 to 0.69. The uncertainties in axial ratios quoted for Beard and Chuang's model are less than 0.015. For raindrops larger than 2mm Beard and Chuang find that the axial ratio is a nearly linear function of size with a fall in axial ratio of about 0.06 for every millimeter increase in size. The 9mm drop shape entry in the table is taken from the graph in their paper and is consistent with the shape measured by Pruppacher and Beard (1970) in the low turbulence UCLA wind tunnel. The axial ratio for a 10mm diameter drop is derived by extrapolation of the linear relationship and is not supported by direct evidence.

Table 1 shows the different predicted magnitudes of Z_{DR} for the two sets of drop shapes using the simple Rayleigh-Gans theory. This is strictly only applicable to the small drops, and the Mie-Gans theory should be used when the drop diameter becomes a reasonable fraction of the radar wavelength. We are indebted to Dr. Holt of the Department of Mathematics, Essex University for the Mie-Gans calculations in Table 1, which were carried out for water drops at -10°C , 0°C and $+10^{\circ}\text{C}$ and the Chilbolton frequency of 3.0765GHz. Beard (1976) found that changes in pressure and temperature have a negligible effect on raindrop shape over all reasonable values to be found in the atmosphere. The values of Z_{DR} using the exact theory are only slightly higher than for

Rayleigh scattering apart from drops above 8mm where the divergence is considerable. Similarly, we note that temperature effects on scattering for a given drop shape are negligible for drops smaller than 8mm.

Rasmussen et al (1985) report laboratory experiments of drop shapes in the presence of a vertical electric field. Appreciable changes in axial ratio occurred only for a field above 200 kv/m and drops 4mm larger than diameter; the measurements did not encompass drops larger than 5mm or field orientations other than the vertical. It is generally believed that the field required to trigger lightning in the atmosphere is about 300 kv/m; regions where the field exceeds 200 kv/m are likely to be localised in both time and space, and are also more likely to occur where the hydrometeors are in the ice phase. The effects of electric fields on Z_{DR} are likely to be small. However, if the lightning does occur in a region with large raindrops, a localised sudden change in Z_{DR} might occur. Such a step change in Z_{DR} might be detected if the radar was not scanning but was dwelling on the lower regions of an active storm. In view of the changing sensitivity of differently sized large raindrops to field changes apparent in the results of Rasmussen et al.(1985), a quantitative interpretation of any such Z_{DR} jumps will probably not be possible.

(b) Statistical Analysis of Radar Data

A simple prediction of the values of Z_{DR} to be expected in rain is displayed in Figure 1 for a Marshall-Palmer raindrop size distribution with a value of N_0 of $8000m^{-3}mm^{-1}$. The two curves are obtained using the two drop shape models in Table 1 for different values of D_0 in Equation 2 at $0^{\circ}C$ and terminating the raindrop spectrum at 8mm. The curves diverge for values of Z

above 40dBZ; the Pruppacher and Pitter shapes lead to a maximum predicted value of 3.5dB, whereas the more oblate shapes suggest values of up to 4.5dB are possible.

The crosses in Figure 1 represent the average values of Z_{DR} for each 2dBZ step in Z , obtained from measurements in rain made with the Chilbolton radar during summer convective storms on many different days. Isolated echoes smaller than 2km in diameter were not included in the analysis. During the observation period, the freezing level was at 3km or slightly above, and so, to minimise ambiguities due to melting ice particles, data were only analysed for altitudes below 1km.

It is well established that in severe storms with intense reflectivities, values of Z_{DR} close to zero can extend down to the ground; these signatures are interpreted as hail reaching the ground (e.g. Illingworth et al, 1986). These features are usually quite localised and easy to identify, and so any cell having values at 1km altitude where Z_{DR} was below 1dB with Z above 40dBZ was excluded from the analysis. An example of the average values of Z_{DR} for every 2dBZ step in Z for such a cell is shown in Figure 2, where the effect of the hail in reducing the mean values of Z_{DR} for values of Z above 55dBZ is quite dramatic.

The Z_{DR} values for the averaged data in Figure 1 are higher than expected and it has been argued that values of Z_{DR} above 3.5dB should be attributed to raindrops containing melting ice cores (e.g. Doviak and Zrnic, 1984; Beard and Chuang, 1987). The evidence from the Chilbolton radar does not support this view. Values of Z_{DR} of up to 9dB have been observed in the bright band and are thought to result from melting snowflakes and ice crystals, but these only occur in stratiform clouds with a clearly defined melting layer. In vigorous convective storms our observa-

tions of many vertical profiles of Z and Z_{DR} indicate that, as ice particles melt, the value of Z_{DR} gradually increases from the zero value associated with graupel and hail, and reaches a maximum value reflecting the equilibrium shape of the raindrop when melting is complete. A typical profile is shown in Figure 3. The Z_{DR} profiles in convective clouds do not show a maximum associated with the final stages of melting followed by a collapse to a less oblate raindrop containing no ice. Laboratory studies of the melting of ice support this suggestion; Rasmussen et al (1984) show that ice spheres smaller than 9mm do not shed water, but that as melting proceeds they become progressively more oblate, finally assuming the shape of the equivalent diameter water drop. For spheres larger than 9mm diameter, Rasmussen et al observed that an unstable torus of liquid water built up around the equator. However, these ice spheres were tethered within a wind tunnel but a particle falling in the free atmosphere would be able to tumble and would undoubtedly shed such a torus.

Reflectivity data below 250m altitude were also excluded from the analysis in Figure 1, as these were likely to be affected by ground clutter. Even with this height restriction the quarter degree beamwidth Chilbolton radar still detected the occasional ground return, but the Z_{DR} of such returns is easy to recognise, as the values of Z_{DR} lie in the range +5dB to -5dB and change by several dB between one 300m long gate and the next (Hall et al, 1984). To suppress this clutter, a Z_{DR} reading was rejected if the change in Z_{DR} (dB) at a neighbouring gate was more than 60 .

The average values of Z_{DR} obtained, after the removal of ground clutter and ambiguities due to melting ice, are those

displayed in Figure 1. These data, together with the sample size and standard deviations are summarised in Table 2. If we assume a normal distribution then the standard errors in the mean are only significant for the values of Z in the two highest ranges; these error bars are plotted in the figure.

The use of the Beard and Chuang shapes improves the agreement between the model and the measurements, and we shall use these shapes from now onwards. The errors in axial ratio of 0.015 are equivalent to a change in Z_{DR} for the raindrops of 0.2dB, which is still larger than the estimated error of 0.1dB in the Z_{DR} measurement made by the Chilbolton radar.

(c) Analytic Forms of the Raindrop Spectrum

We have few direct observations of the concentration of the largest raindrops. The ground-based disdrometer described by Joss and Waldvogel (1967) is widely used for radar validation experiments, but the largest drop size that can be recorded is 5.3mm; even if the size range was increased, a negligible number of these larger drops would be detected because of the small sample area of the instrument. The data displayed in Figure 1 were obtained for storms within 100km range of the Chilbolton radar, but the number of such storms which would be above a single immobile ground-based disdrometer would be extremely small. This restriction does not apply to airborne instruments, and Willis (1984) reports raindrop spectra measured inside a hurricane where the rain rate was computed to be 169mm hr, but unfortunately no data are presented for drops greater than 4mm. This device sampled $2m^3$ of cloud every 10secs (1.3km of flight track); in the heaviest rain it sampled about 20 raindrops in the 4 to 5mm size range; extrapolating the exponential distribution

indicates that such a device would not obtain a significant sample of 8mm drops. Recently, Beard et al (1986) have reported finding large raindrops within warm shallow clouds over Hawaii. On one occasion the drop diameter reached 8mm and the average concentration of raindrops in the 5 to 6mm range for the observations was about one per cubic meter. It seems that earlier suggestions that collision induced break-up would limit the maximum raindrop size to a few millimeters have been overemphasised.

Although it appears that large raindrops may well be found in heavy rain, and that such large raindrops would affect the values of Z and Z_{DR} , it seems very difficult to obtain an independent means of sampling such drops to check any radar inferences. We shall adopt a different approach, and test various forms of the raindrop size distribution to see which agrees most closely with the radar data. To compute the curves in Figure 1, we assumed a D_{max} of 8mm, a constant N_0 of $8000 \text{ m}^{-3} \text{ mm}^{-1}$, and allowed D_0 to vary. We shall also explore the effect of fitting the data to a gamma distribution (Ulbrich and Atlas, 1984):

$$N(D) = N_0 D^m \exp(-(3.67+m)D/D_0) \quad (3)$$

The third parameter, m , reflects the breadth of the size distribution. The use of simplified size distributions is partially justified by the averaging of microscale features by the radar compared to disdrometer distributions.

Let us first consider the effect of truncating the exponential distribution. Both Joss and Waldvogel (1969) and Sachidananda and Zrnic (1988) used a maximum value of 6mm but, in view of the above discussion, larger values such as the 9mm used in the Z_{DR} calculations of Goddard and Cherry (1984) should be

more realistic. Drops of 9mm are stable in a low turbulence wind tunnel (Pruppacher and Beard, 1970) and so, in the absence of collisions with other raindrops, it is reasonable to suppose they would exist in natural clouds. In Figure 4 values of Z and Z_{DR} are plotted for maximum drop sizes of 8 and 10mm, with the value of N_0 kept at $8000 \text{ m}^{-3} \text{ mm}^{-1}$ throughout. The agreement of the predictions using the 10mm diameter cut-off with the average radar data is remarkable.

Figure 4 also explores the effect of the value of m in the gamma function. When $m = 0$ the gamma function reduces to the simple exponential, but some measurements indicate that natural raindrop spectra contain rather fewer of both the very large drops and the very small drops than would be the case for an exponential, and that a value of $m = 2$ is more appropriate (Ulbrich, 1983). Again N_0 is kept constant at $8000 \text{ m}^{-3} \text{ mm}^{-1}$, and the values for $D_{\text{max}} = 8$ and 10mm with $m=2$ are also plotted in Figure 4. The agreement with observation is not as good; the lower predicted values of Z_{DR} at high rain rates reflect the lower concentrations of the large raindrops in the narrower spectrum.

If four variables are used in the raindrop spectrum then, for only two observables, an infinite combination of values is possible. There is no reason, per se, to believe that the analytic form of the raindrop distribution should be the same for all rain rates, for example, N_0 can be adjusted to give the required value of Z for any value of Z_{DR} . In the absence of any other radar observable parameters, the most sensible choice for summertime convective clouds in the UK seems to be a pure exponential with a variable D_0 , but keeping N_0 at $8000 \text{ m}^{-3} \text{ mm}^{-1}$ and $D_{\text{max}} = 8$ or 10mm. A polynomial which fits these theoretical

computations and gives Z correct to 0.2dBZ is given in Table 3a.

Figure 5 compares the predicted values of Z_{DR} as a function of D_0 for a pure exponential raindrop spectrum. The polynomials which fit the curves for the Beard and Chuang shapes to an accuracy of 0.02dB in Z_{DR} are given in Table 3b. For comparison purposes we also plot the relationship $[Z_{DR} = 0.45 D_0^{1.56}]$ suggested by Seliga et al. (1986) for Green's (1975) shapes. Because this equation is constrained to pass through the origin and can have no points of inflexion, it cannot represent the dependence very accurately.

So far we have used the values of Z_{DR} computed at 0°C . Some values at $+10^\circ\text{C}$ and -10°C are presented in Table 1. Although these computations are not complete, and the change in Z_{DR} for the full Mie-Gans theory is not a simple function of temperature, the values in Table 1 indicate that there would only be a small change in the curves in Figure 1 over this temperature range. The values at -10°C are of interest when interpreting transient narrow columns of positive Z_{DR} which extend up to 2km above the freezing level in vigorous convection. We have argued (Illingworth et al, 1987) that these are due to supercooled raindrops.

These effects of temperature at S band (10cm) should be small, but seem to be more serious at C band (5.5cm). Computations at 5.5cm wavelength, but using the Pruppacher and Pitter drop shapes (Meischner, Bringi and Jank, 1988), show a pronounced resonance for 6mm drops with a maximum Z_{DR} of nearly 8dB at 20°C , falling to 4dB for 7 and 8mm. The maximum is much less marked at 0°C . The use of the Beard and Chuang shapes will modify these values, but they indicate that severe problems could arise in any quantitative analysis of high Z_{DR} regions observed at C-band.

3. VARIABILITY OF NATURAL RAINDROP SPECTRA

In the previous section we concentrated upon obtaining average values of Z_{DR} for a given magnitude of Z . Particular observations of Z and Z_{DR} do not, of course, lie on this average curve; it is this fact which enables Z_{DR} to be used as an independent observable. The curve in Figure 1 for the Beard and Chuang drop shapes represents the best available estimate of the values of Z and Z_{DR} for a value of $N_0 = 8000 \text{ m}^{-3} \text{ mm}^{-1}$ in the exponential raindrop size spectrum of Equation (2). For any particular observation of Z and Z_{DR} , the value of D_0 can be derived from Z_{DR} , and N_0 found from Figure 1, using the fact that Z scales linearly with N_0 .

Histograms of the frequency of occurrence of different values of Z_{DR} for each interval of 2dBZ in Z are plotted in Figure 6. The mean values of Z_{DR} of each histogram are those plotted in Figure 1. The width of the histograms can be used to estimate the variability of naturally occurring raindrop spectra. Histograms for values of Z less than 30dBZ are not presented because the resolution of Z_{DR} obtainable by the radar is insufficient; histograms for Z above 60dBZ are not shown because the sample sizes are too small. An asymmetry of the distributions in Figure 6 is evident, with a long tail showing that values of Z_{DR} many times the mean occasionally occur. This implies that values of N_0 are generally close to $8000 \text{ m}^{-3} \text{ mm}^{-1}$, but that on occasion much lower values occur. Figure 4 shows that non-exponential drop size spectra such as gamma functions will also contribute to the observed variability, but that the long tail in Z_{DR} cannot be explained without invoking low drop concentrations. We have drawn attention (Illingworth et al. 1987) to the anomalously high values of Z_{DR} observed in some isolated first echoes, but,

because of their limited spatial extent, such data are not included in the 'average' data. The unusual characteristics of these first echoes may be re-emphasised with reference to Figure 6. In these isolated clouds Z values of 30 and 40dbZ were accompanied by Z_{DR} values of 3 and 4dB, respectively; the statistical analysis presented in Figure 6 shows that for these two values of Z, 98% of the data in the sample were accompanied by Z_{DR} values of a lower magnitude.

In view of the skewness of the Z_{DR} histograms in Figure 6, the histograms were re-computed for $\log(Z_{DR})$. The results are displayed in Figure 7 and a greater symmetry of the distributions is apparent. This is confirmed by Table 2 which provides the values of standard deviations, skewness and kurtosis for the histograms in Figures 6 and 7. The skewness (defined as the ratio of the third moment to the cube of the standard deviation) of the $\log(Z_{DR})$ distributions is about one tenth that for the linear Z_{DR} histograms for the range of Z from 30 to 50dBZ; above 50dBZ the difference is less clear, but this may be affected by the smallness of the sample size. The kurtosis (the ratio of the fourth moment to the fourth power of the standard deviation) should be 3 for a normal distribution; higher values arise if the wings of the distribution are wider than for a normal distribution. Again, the values of kurtosis for the $\log(Z_{DR})$ histograms in the Z range 30-50dbZ are close to 3, whereas the linear Z_{DR} histograms have much greater values. Kurtosis values for Z above 60dBZ are not meaningful because of the small sample size. The data in Table 2 are for clouds on many different days. No systematic differences were apparent when the observations of individual clouds were considered.

The statistics in Table 2 of the variability of spectra may

be of use in interpreting conventional radar data and for statistical studies of problems related to electromagnetic propagation in the lower troposphere.

4. THE VARIABILITY OF RADAR DERIVED RAINFALL RATES

(a) Derivation of Rain Rate

In this section we compare various proposed relationships for deriving rainfall rates when both Z and Z_{DR} are available. Figure 8 compares the values of rain rate (R) as a function of Z and Z_{DR} using the original shapes of Pruppacher and Pitter and the new shapes of Beard and Chuang for an exponential size distribution. For a given Z_{DR} the values of R scale linearly with Z . On the Figure curves for 10 and 100 mm/hr are plotted. The new drop shapes lead to slightly lower rainfall rates for a given Z/Z_{DR} combination; for example, for a Z_{DR} of 3 and 3.7 dB the reductions are 26% and 44% respectively. The effect of using a D_{max} of 10mm is marked with the dashed line; this uncertainty over choice of truncation limit only becomes significant for Z_{DR} above 3dB, at 4dB the reduction in deduced rain rate is about 25%.

An analytic approximation to the theoretical curves in Figure 8 for a rain rate of 1 mm hr^{-1} using the Beard and Chuang shapes modified for small drops, is given in Table 3c. Measurement errors in Z_{DR} affect the precision with which rain rates may be estimated. Because of the changing gradient of the curves in Figure 8, the errors in the rainfall estimate will increase for lower values of Z_{DR} . When Z_{DR} is zero it provides only an upper bound on the mean drop size, and so, for a given Z , the Z_{DR} information merely sets a lower limit on the rainfall rate. The data presented from the Chilbolton radar in this paper have a standard error of about 0.1dB in Z_{DR} .

Several other theoretical relationships have been published recently which relate the rainfall rate to the observed values of Z and Z_{DR} and these are compared in Figure 9. The curves are for

a rain rate of 1 mm hr^{-1} , and, as in Figure 8, the rain rates scale linearly with Z. Seliga et al. (1986, Equation 35) use Green's (1975) drop shapes and suggest for Z_{DR} in dB:

$$Z(\text{dBZ}) = 27.10 + 10.40 \log(Z_{DR}) \quad (0.2 < Z_{DR} < 0.7) \quad (4a)$$

$$Z(\text{dBZ}) = 27.98 + 16.70 \log(Z_{DR}) \quad (0.7 < Z_{DR} < 2.6) \quad (4b)$$

Because we now believe that small drops are slightly more spherical than Green's formula, Equation 4 overestimates the rainfall by about 1.5dB (40%) for low values of Z_{DR} , and conversely for large values of Z_{DR} the Green shapes are insufficiently oblate and the rain rate is underestimated by about 1.5dB (30%). Seliga et al. analyse the drop size distributions measured during a three hour heavy rainfall event and compute the theoretical values of Z and Z_{DR} which would have been observed, and show that using the two observables Z and Z_{DR} should give a better estimate of rainfall rate than an empirical Z-R relationship. This argument demonstrates the validity of the technique but does not prove that the drop shapes used for Equation 4 are correct.

Z and Z_{DR} radar data for part of a single 15km x 15km PPI scan are analysed by Sachidanada and Zrnic (1987). The data are compared with the theoretical relationship for an exponential drop size distribution with a maximum size of 6mm using Green's (1975) drop shapes. For a rain rate of 1 mm hr^{-1} their Equation 8 with Z_{DR} in dB may be expressed as

$$Z(\text{dBZ}) = 21.65 + 4.86 Z_{DR} \quad (5)$$

They claim that this linear relationship fitted the theoretical curve to within 3, or 0.05dB; in view of the other theoretical curves in Figure 9, this seems difficult to understand. They comment that the observations of the scatter of

Z and Z_{DR} for the single PPI scan seem large when compared with the scatter simulated by generating random values for the drop size distribution parameters in the ranges:

$$30 < N_0 < 30,000 \quad \text{mm}^{-1} \text{m}^{-3}$$

$$-2 < m < +3$$

$$4 < D_{\max} < 6 \quad (\text{mm})$$

$$0.27 < D_0 < 1.23 \quad (\text{mm})$$

Accordingly, the observations from one part of the scan which seemed to have a particularly high scatter were discounted, although we note that the highest values of D_0 used in the simulation is equivalent to a rain rate of only 6mm hr^{-1} for Marshall-Palmer rain. Noticing that the mean value of Z for a given Z_{DR} for the remaining data seemed rather higher than expected, they suggested that the raindrops were very oblate and proposed a relationship between the axial ratio and drop diameter (D):

$$a, b = 1 - 0.64 D^{1.25} \quad (6)$$

A slight dip in the mean values of Z for higher values of Z_{DR} was interpreted in terms of drop break up. For the more oblate shapes they suggested a revised relationship for $R = 1 \text{mm hr}^{-1}$:

$$Z = 22.39 + 3.49 Z_{DR} \quad (7)$$

Our experience with the Chilbolton data is that the averages from a single PPI are highly variable and that such generalisations embodied in Equations 6 and 7 are not justified.

(b) Variability of Rain Rates for a Given Z

In order to obtain an estimate of the variability of natural rainfall for a given Z, the histograms of Chilbolton data for Z_{DR} in Figure 6 have been replotted in Figure 10. The polynomial in Table 3c has been used to convert the values of Z_{DR} to a rainfall rate. The data are summarised in Table 4, where, for a given Z,

the mean rain rate and its standard deviation are presented. We note that the standard deviation of the inferred rain rate is somewhat greater than half the mean rate, but that the distributions are skewed so that, on occasion, the inferred rain rate is many times that expected from a simple Z-R relationship. The data is taken with a sample volume which is typically a 300m cube; if this volume was increased then averaging would be expected to narrow the histograms in Figure 10.

Before applying the relationships in Table 2 the accuracy of the observations must be considered. The Chilbolton radar estimates Z_{DR} to an accuracy of about 0.1dB, introducing an error in rain rates of about 12% (that is, 0.5dB) for values of Z_{DR} above 1dB (Figure 9). When Z_{DR} values approaching zero are common, as is the case in Table 4 when Z is below 40dBZ, then the errors in the derived rainfall rate are larger.

The fundamental accuracy limiting the Z_{DR} measurement should be analysed before calculating rainfall rates. Even if we assume there are no instrumental errors due to mismatches of the channels for horizontal and vertical polarization, and that the beam is filled with rainfall with no severe reflectivity gradients across the sample volume, the accuracy of the Z_{DR} estimate is limited by the finite dwell time of the radar. Bringi et al. (1983) show that about 40-60 independent sample pairs of Z_H and Z_V are required if Z_{DR} is to be measured with a standard error as low as 0.1dB. The time to independence is related to the width of the Doppler spectrum of the target and is usually in the range 20 to 40 msec at 10cm wavelength. The Chilbolton Z_{DR} data are obtained with a time integration of 210 msec and spatial integration over four 75m range gates. If faster scanning is employed with no spatial averaging then the

number of independent samples will fall. If the number of samples is only 6, for example, the standard error in Z_{DR} will be about 0.5dB. Even for large values of Z_{DR} this would lead to an error of nearly 100% in the derived rain rate.

5. DISCUSSION AND CONCLUSIONS

The precise shape of raindrops which should be used for the interpretation of Z_{DR} measurements has been a matter of considerable debate. The radar results reported in this paper are in good agreement with the with the new, more accurate, shapes proposed for the large drops by Beard and Chuang (1987) and the Goddard, Cherry and Bringi (1983) shapes for drops below 3mm. In the absence of any third observable reflecting the value of m in the gamma distribution, the most reasonable spectrum for interpreting the Z and Z_{DR} observations is the exponential of Equation (2) with a $D_{max} = 8mm$. In heavy rain with Z values above 50dBZ there is an indication that a $D_{max} = 10mm$ could be used.

Based upon these new drop shapes and for an exponential distribution of raindrop sizes, the analytic expressions in Table 3 appear most appropriate for calculating D_0 from the observed value of Z_{DR} and for deriving N_0 and the rainfall rate from Z and Z_{DR} data. Particular attention should be paid to errors introduced into Z_{DR} by sampling limitations.

In Illingworth et al. (1987) it was argued that values of Z_{DR} of 5dB were due to a monodispersed distribution of large raindrops, and the new drop shapes discussed in this paper support their interpretation. From a radar analysis, Caylor and Illingworth (1986) hypothesised that large raindrops must be more oblate than was commonly accepted; the more oblate shapes have now been confirmed independently, and give more consistent agreement with the radar data. However, the extreme oblateness of the very large drops proposed by Caylor and Illingworth (1986) are too exaggerated, and those of Beard and Chuang (1987) should be used.

ACKNOWLEDGEMENTS

This research was supported by the Meteorological Office, by NERC grant GR3/5896 and by AFOSR-88-0121. Computing facilities were provided by the SERC under GR/D69372. One of us (IJC) acknowledges the assistance of an ORS studentship. We thank our colleagues S M Cherry and J W F Goddard for supplying the Chilbolton data and for numerous enlightening discussions.

REFERENCES

- Beard K V, (1976) Terminal velocity and shape of cloud and precipitation drops aloft. *J Atmos Sci*, 34, 851-864
- Beard K V and Chuang D (1987) A new model for the equilibrium shape of raindrops. *J Atmos Sci*, 44, 1509-1524.
- Beard D V, Johnson D B and Baumgardner D (1986) Aircraft observations of large raindrops in warm, shallow, convective clouds. *Geophys Res Letters*, 13, 991-994
- Beard K V and Ochs H T (1988) Wake-excited raindrop oscillations. Preprints 10th Int Cloud Physics Conf, Deutscher Wetterdienst, Offenbach-am-Main, 7-8
- Bringi V N, Seliga T A and Cherry S M, (1983) Statistical properties of the dual-polarization differential reflectivity (Z_{DR}) radar signal. *IEEE Trans Geo and Remote Sens*, GE-21, 215-220
- Caylor I J and Illingworth A J, (1986) Observations of the growth and evolution of raindrops using dual-polarization radar. Preprints 22nd Conf Radar Meteor, Amer Meteor Soc, 88-91
- Chandrasekar V, Cooper W A and Bringi V N, (1988) Axis ratios and oscillations of raindrops. *J Atmos Sci*, 45, 1323-1333
- Cherry S M and Goddard J W F (1982) Design features of dual polarisation radar. *URSI Open Symposium on Multiple Parameter Radar Measurements of Precipitation*, Bournemouth, UK, 23-27 Aug.
- Cooper W A, Bringi V N, Chandrasekar V, and Seliga T A (1983) Analysis of raindrop parameters using a 2D precipitation probe with application to differential reflectivity. Preprints 21st Conf Radar Meteorology, Amer Meteor Soc, 448-493
- Doviak R J and Zrnic D S (1984) *Doppler Radar and Weather Observation*, Academic Press, Orlando, Florida.
- Goddard J W F and Cherry S M, (1984) The ability of dual polarisation radar (copolar linear) to predict rainfall rate and microwave attenuation. *Rad Sci*, 19, 201-208
- Goddard J W F, Cherry S M and Bringi V N (1983) Comparisons of dual-polarization radar measurements of rain with ground-based distrometer measurements. *J Appl Met*, 21, 252-256
- Green A W, (1975) An approximation for the shape of large raindrops. *J Appl Met*, 14, 1578-1583.
- Hall M P M, Goddard J W F, and Cherry S M. (1984) Identification of hydrometeors and other targets by dual-polarisation radar. *Radio Sci*, 19, 132-140
- Illingworth A J, Goddard J W F and Cherry S M. (1986) Detection of hail by dual-polarization radar. *Nature*, 323, 431-433

Illingworth A J, Goddard J W F and Cherry S M, (1987) Polarization radar studies of precipitation development in convective storms. Q J Roy Meteorol Soc, 113, 469-489

Joss J and Waldvogel A, (1967) Ein Spektograph fur Niederschlagstropfen mit automatischer Auswertung. A raindrop spectrometer with automatic readout. Pure Appl Geophys, 68, 240-246

Joss J and Waldvogel A, (1969) Raindrop size distribution and sampling size errors. J Atmos Sci, 26, 566-569

Marshall J S and Palmer W M K, (1948) The distribution of raindrops with size. J Meteorol, 6, 243-248

Meischner P, Bringi V N and Jank T, (1988) Multiparameter Doppler radar observations of a squall line with the polarimetric DFVLR radar. Preprints 10th Int Cloud Physics Conf, Deutscher Wetterdienst, Offenbach-am-Main, 330-332

Pruppacher H R and Beard K V, (1970) A wind tunnel investigation of the internal circulation and shape of water drops falling at terminal velocity in air. Q J Roy Meteorol Soc, 96, 247-256

Pruppacher H R and Pitter R L, (1971) A semi-empirical determination of the shape of cloud and rain drops. J Atmos Sci, 28, 86-94

Rasmussen R M, Levizzani V and Pruppacher H, (1984) A wind tunnel and theoretical study of the melting behaviour of atmospheric ice particles: III Experiment and theory for spherical ice particles of radius above 500um. J Atmos Sci, 41, 381-388

Rasmussen R, Walcek C, Pruppacher H R, Mitra S K, Lew J, Levizzani, Wang P K and Barth U, (1985) A wind tunnel investigation of the effect of an external vertical electric field on the shape of electrically uncharged rain drops. J Atmos Sci, 42, 1647-1652

Sachidananda M and Zrnic D S, (1987) Rain rate estimates from differential polarization measurements. J Atm and Ocean Tech, 4, 588-598

Seliga T A and Bringi V N, (1976) Potential use of radar differential reflectivity measurements at orthogonal polarizations for measuring precipitation. J Appl Met, 15, 69-76

Seliga T A, Aydin K and Direskeneli H, (1986) Disdrometer measurements during an intense rainfall event in central Illinois: Implications for differential reflectivity radar observations. J Clim and Appl Met, 25, 835-846.

Ulbrich C W, (1983) Natural variations in the analytical form of the raindrop size distribution. J Clim and Appl Met, 22, 1764-1775.

Ulbrich C W and Atlas D (1984) Assessment of the contribution of differential polarization to improved rainfall measurements. Rad Sci, 19, 49-57

Willis P T (1984) Functional fits to some observed drop size distributions and parameterization of rain. J Atmos Sci, 41, 1648-1661.

Wilson J W and Brandes E A (1979) Radar measurements of rainfall - a summary. Bull Am Met Soc, 60, 1048-1058

TABLE 1

| Size | P-P shapes | | B & C shapes | | | | |
|------|-------------|---|--------------|---|------------------------------------|-------|-------|
| | Axial Ratio | Z _{DR} (dB) (Rayleigh Gans) | Axial Ratio | Z _{DR} (dB) (Rayleigh Gans) | Z _{DR} (dB) (Mie Gans) | | |
| | | | | | -10°C | 0°C | +10°C |
| 4 | 0.762 | 2.69 | 0.778 | 2.49 | - | - | - |
| 5 | 0.701 | 3.51 | 0.708 | 3.41 | 3.50 | 3.48 | - |
| 6 | 0.655 | 4.16 | 0.642 | 4.35 | - | 4.42 | - |
| 7 | 0.621 | 4.67 | 0.581 | 5.31 | - | 5.33 | - |
| 8 | 0.583 | 5.27 | 0.521 | 6.34 | 7.22 | 6.70 | - |
| 9 | - | - | 0.46 | 7.49 | - | 10.87 | 10.10 |
| 10 | - | - | 0.4 | 8.78 | 14.15 | 16.34 | 18.27 |

Values of axial ratio and Z_{DR} for various sizes of raindrop assuming oblate spheroid shape. The Mie-Gans calculations are supplied by Dr Holt, Department of Mathematics, University of Essex, and apply to raindrops at 0°C and 3.0765 GHz. P-P shapes refer to Pruppacher and Pitter (1971), B and C to Beard and Chuang (1987).

TABLE 2

| Z (dBZ) | LINEAR | | | | LOG | | | |
|---------|-------------------------|----------|---------------|---------------|------------------------|----------|---------------|---------------|
| | Z _{DR} (dB) | σ | Skew- ness | Kurto- sis | log Z _{DR} | σ | Skew- ness | Kurto- sis |
| 30-32 | 0.86 | 0.70 | 2.15 | 10.5 | -0.17 | 0.31 | -0.05 | 2.99 |
| 32-34 | 0.96 | 0.70 | 2.15 | 8.07 | -0.11 | 0.30 | -0.14 | 2.93 |
| 34-36 | 1.06 | 0.75 | 1.70 | 6.77 | -0.07 | 0.29 | -0.04 | 2.78 |
| 36-38 | 1.17 | 0.71 | 1.60 | 6.39 | 0.00 | 0.25 | +0.06 | 2.84 |
| 38-40 | 1.31 | 0.72 | 1.50 | 5.80 | 0.06 | 0.22 | +0.13 | 2.90 |
| 40-42 | 1.48 | 0.74 | 1.42 | 5.16 | 0.12 | 0.20 | +0.25 | 2.68 |
| 42-44 | 1.65 | 0.75 | 1.35 | 4.87 | 0.18 | 0.18 | +0.27 | 2.95 |
| 44-46 | 1.79 | 0.73 | 1.26 | 4.81 | 0.22 | 0.16 | +0.27 | 3.20 |
| 46-48 | 2.01 | 0.75 | 0.98 | 3.80 | 0.27 | 0.16 | +0.15 | 2.28 |
| 48-50 | 2.23 | 0.74 | 0.83 | 3.52 | 0.33 | 0.14 | +0.07 | 2.60 |
| 50-52 | 2.48 | 0.76 | 0.86 | 3.59 | 0.37 | 0.13 | 0.09 | 2.45 |
| 52-54 | 2.81 | 0.83 | 0.92 | 4.10 | 0.43 | 0.12 | 0.17 | 2.89 |
| 54-56 | 3.10 | 0.87 | 0.70 | 3.33 | 0.47 | 0.12 | 0.06 | 2.41 |
| 56-58 | 3.45 | 0.92 | 0.23 | 2.34 | 0.52 | 0.12 | -0.28 | 2.41 |
| 58-60 | 3.73 | 0.96 | 0.11 | 2.46 | 0.56 | 0.11 | -0.41 | 2.41 |
| 60-62 | 3.88 | 0.91 | -0.07 | - | 0.58 | 0.11 | -0.52 | - |
| 62-64 | 4.41 | 0.67 | -0.44 | - | 0.64 | 0.07 | -0.58 | - |

The average values of differential reflectivity for each 2dBZ step in Z observed in heavy rain by the Chilbolton radar. The left-hand half of the table displays the mean, standard deviations (σ), skewness and kurtosis of the distributions of Z_{DR} - see Figure 6 for the equivalent histograms. The right-hand side shows the equivalent parameters for log (Z_{DR}) - see Figure 7 for the histograms.

TABLE 3. Coefficients for the approximating polynomials. Coefficients are listed for an exponential drop size distribution with both 8mm and 10mm diameter truncation limits.

| a) $Z = \sum_k a_k ZDR$ for $N_0 = 8000m^{-3}mm^{-1}$ (Z and ZDR in units of dB) | |
|--|--|
| D_{max} | a_0 a_1 a_2 a_3 a_4 |
| 8 & 10 | 2.620 95.14 -162.8 159.0 -59.15 |
| 8 | 17.38 21.28 -4.311 0.5259 -6.070E-4 |
| 10 | 16.58 22.64 -5.020 0.6882 -0.03818 |
| | 0.1dB \leq ZDR $<$ 1.0dB 1.0dB \leq ZDR \leq 4.5dB 1.0dB \leq ZDR \leq 4.5dB |

| b) $D_0 = \sum_k a_k ZDR$ (ZDR in units of dB and D_0 in units of mm) | |
|---|--|
| D_{max} | a_0 a_1 a_2 a_3 |
| 8 & 10 | 0.4453 1.311 -0.9074 0.3863 |
| 8 | 0.04841 1.631 -0.5631 0.09509 |
| 10 | 0.5998 0.6762 -0.04640 3.804E-3 |
| | 0.1dB \leq ZDR $<$ 1.0dB 1.0dB \leq ZDR \leq 4.5dB 1.0dB \leq ZDR \leq 4.5dB |

| c) $Z = \sum_k a_k ZDR$ for $R = 1mm/hr$ (Z and ZDR in units of dB) | |
|---|--|
| D_{max} | a_0 a_1 a_2 a_3 |
| 8 & 10 | 17.86 20.57 -18.81 7.905 |
| 8 | 22.07 6.215 -0.8551 0.09013 |
| 10 | 21.79 6.586 -0.9443 0.07051 |
| | 0.1dB \leq ZDR $<$ 1.0dB 1.0dB \leq ZDR \leq 4.5dB 1.0dB \leq ZDR \leq 4.5dB |

TABLE 4

| Z (dBZ) | R (mm/hr) | σ_R (mm/hr) | n |
|------------|--------------|-----------------------|------|
| 31.0 | 4.41 | 3.94 | 3760 |
| 33.0 | 5.83 | 4.73 | 3520 |
| 35.0 | 7.96 | 5.88 | 3311 |
| 37.0 | 10.3 | 6.6 | 3347 |
| 39.0 | 13.5 | 8.1 | 3391 |
| 41.0 | 17.4 | 9.9 | 3285 |
| 43.0 | 23.1 | 13.0 | 3067 |
| 45.0 | 31.0 | 17.0 | 2871 |
| 47.0 | 40.5 | 22.7 | 2586 |
| 49.0 | 52.0 | 28.8 | 2263 |
| 51.0 | 66.2 | 35.9 | 2090 |
| 53.0 | 80.8 | 46.5 | 1871 |
| 55.0 | 102.0 | 64.0 | 1346 |
| 57.0 | 127.0 | 92.0 | 922 |
| 59.0 | 162.0 | 130.0 | 375 |

The average values of radar-inferred rainfall rate (R) for each 2dBZ step in Z, observed in heavy rain by the Chilbolton radar. Histograms of the data are shown in Figure 10. σ_R is the standard deviation and n the sample size.

LEGENDS

Figure 1

The variation of Z with Z_{DR} for an exponential drop size distribution using two drop shape models. The solid line is for the Beard and Chuang (1987) drop shapes, and the dashed-dot line is for the Pruppacher and Pitter (1971) shapes. In both cases $D_{max} = 8\text{mm}$ and $N_0 = 8000\text{m}^{-3}\text{mm}^{-1}$. The crosses are averaged Chilbolton radar data collected from summer convective clouds.

Figure 2

An example of the effect due to hail showing the significant decrease in Z_{DR} at high Z values. X represents the averaged Chilbolton data from two PPIs through a storm on 6 July 1983, where a hail shaft was identified. The two lines are theoretical Z - Z_{DR} relationships and are identical to those in Figure 1.

Figure 3

A typical vertical profile through a vigorous convective cloud showing the monotonic increase in Z_{DR} as the ice particles fall through the freezing level at 3 km and subsequently melt.

Figure 4

The relationship of Z to Z_{DR} for variations in the parameters of the gamma drop size distribution. The solid lines are $m = 0$, $D_{max} = 8\text{mm}$ and $D_{max} = 10\text{mm}$. The dotted line is $m = 2$, $D_{max} = 8\text{mm}$ and the dashed line is $m = 2$, $D_{max} = 10\text{mm}$. The Beard and Chuang drop shapes were used and $N_0 = 8000\text{m}^{-3}\text{mm}^{-1}$. The crosses are averaged Chilbolton data as in Figure 1.

Figure 5

A comparison of the various proposed relationships between Z_{DR} and D_0 .

Solid line: Beard and Chuang drop shapes for $D_{max} = 8$ and 10mm.

Dash-dot: Pruppacher and Pitter shapes for $D_{max} = 8$ mm.

Dashed line: $Z_{DR} = 0.45 D_0^{1.56}$ (Seliga et al.1986).

Figure 6

Histograms of the number of Z_{DR} values associated with 2dB intervals in Z . The data were observed for summer convective clouds in 1983 and 1984. The number in the corner of each histogram indicates the centre of the particular Z interval in units of dBZ.

Figure 7

The histograms of Figure 4 replotted with logarithmic spaced Z_{DR} bins.

Figure 8

The variation of Z with Z_{DR} expected for constant rainfall rates. The lower set of curves is for a rainfall rate of 10mm hr and the upper set is for a rate of 100mm hr. The solid line is the Beard and Chuang drop shapes and an exponential drop size distribution with $D_{max} = 8$ mm, while the dashed line is for the $D_{max} = 10$ mm. The dotted line shows the rainfall expected with the Pruppacher and Pitter shapes for an exponential distribution with $D_{max} = 8$ mm.

Figure 9

A comparison of various suggested relationships for deriving rainfall rates from Z and Z_{DR} . The curves are for rain rates of 1mm hr^{-1} .

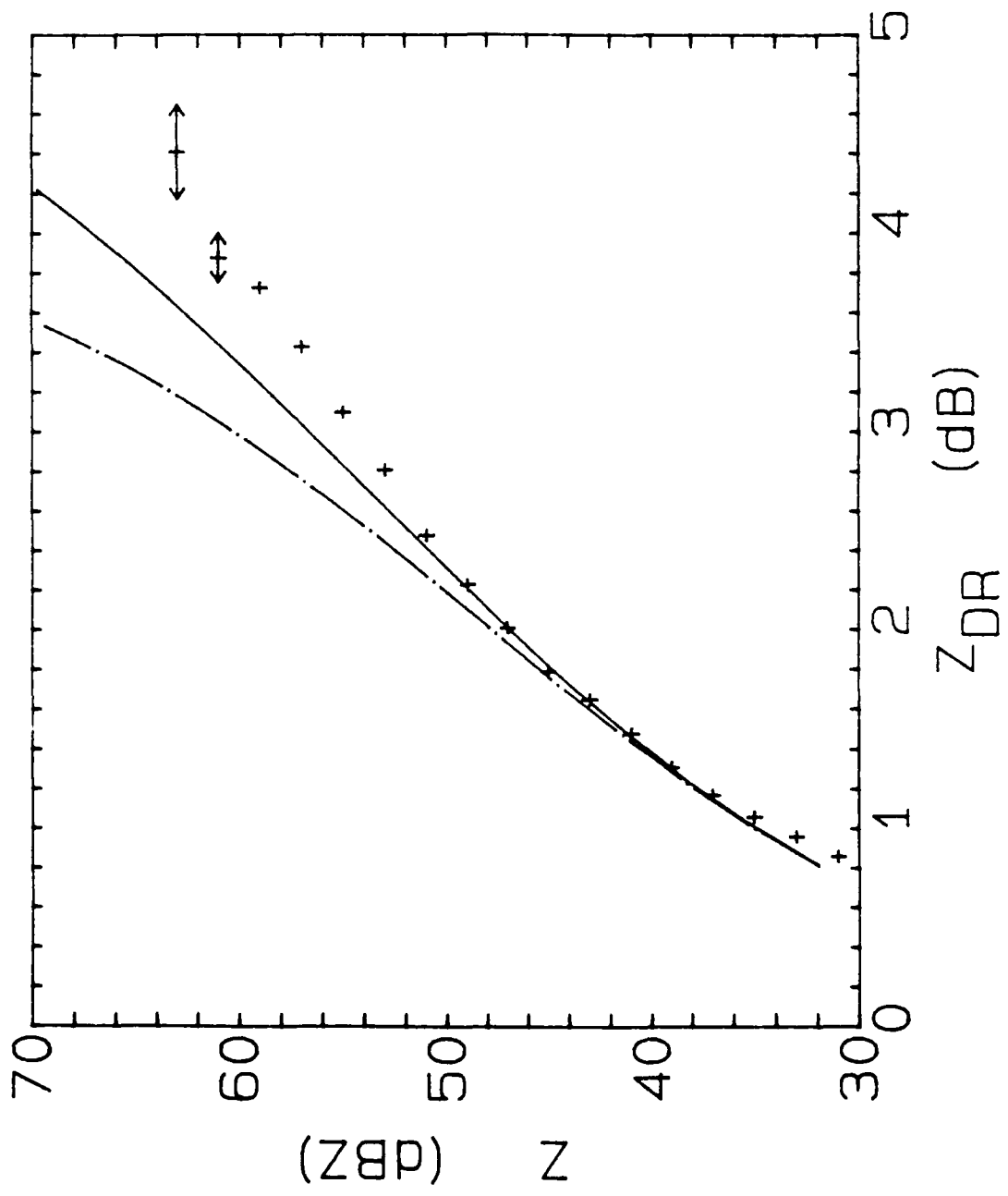
Solid lines: This study using the modified Beard and Chuang shapes.

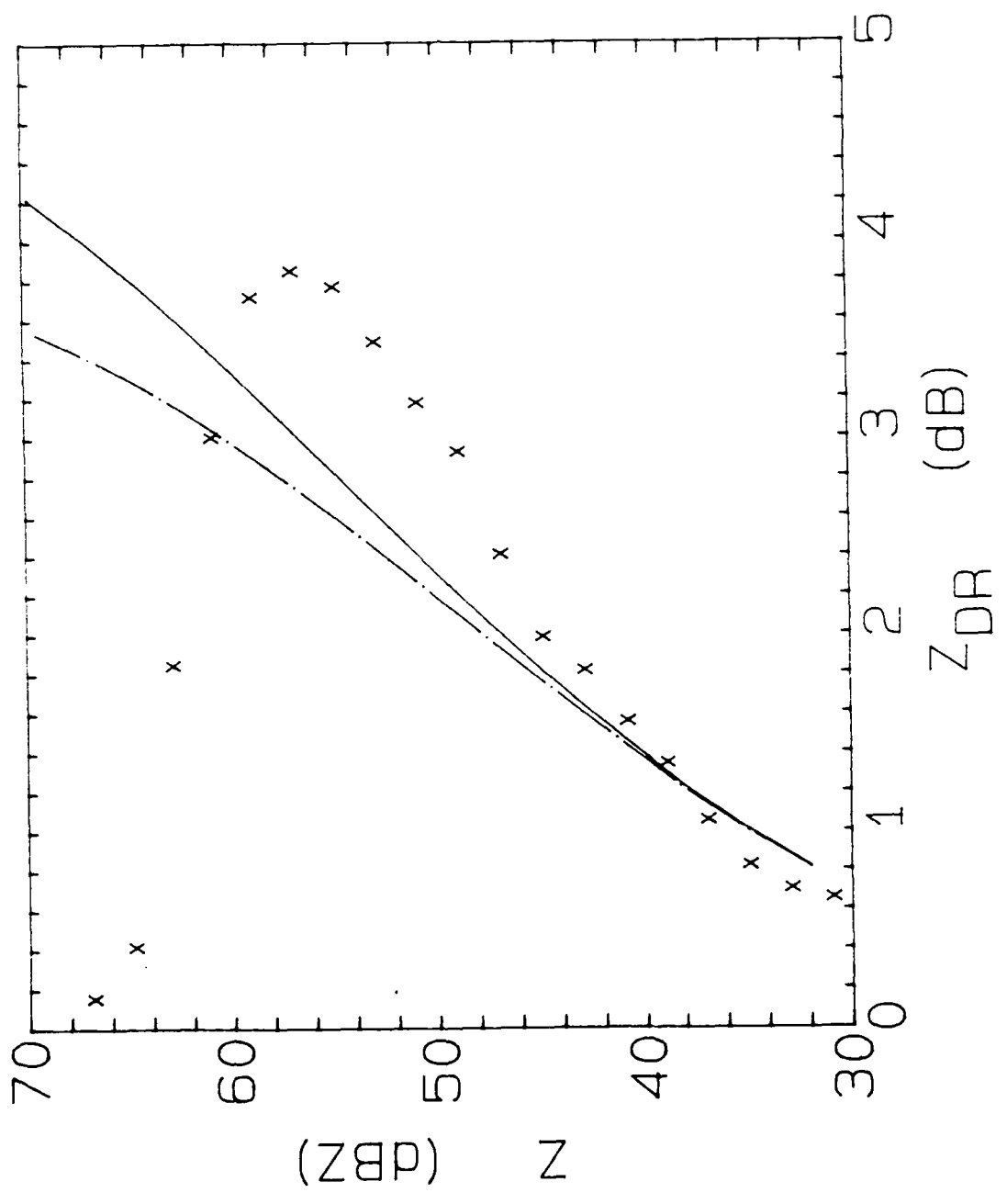
Dotted line: Seliga et al.(1986), Green's shapes, Equation 4.

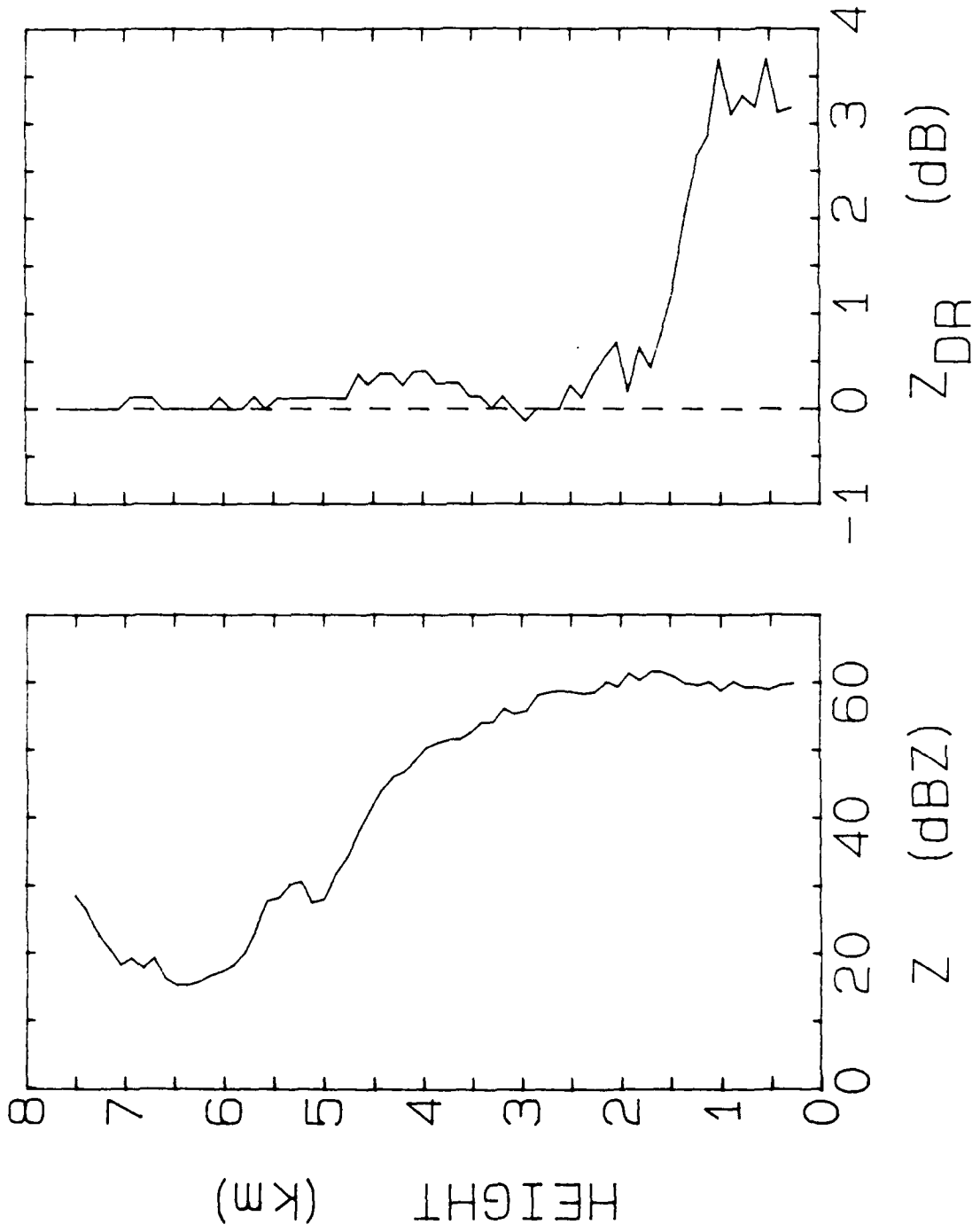
Dashed lines: Sachidananda and Zrnic (1987), Green's shapes,
Short dashes - Equation 5; Long dashes - Equation 7

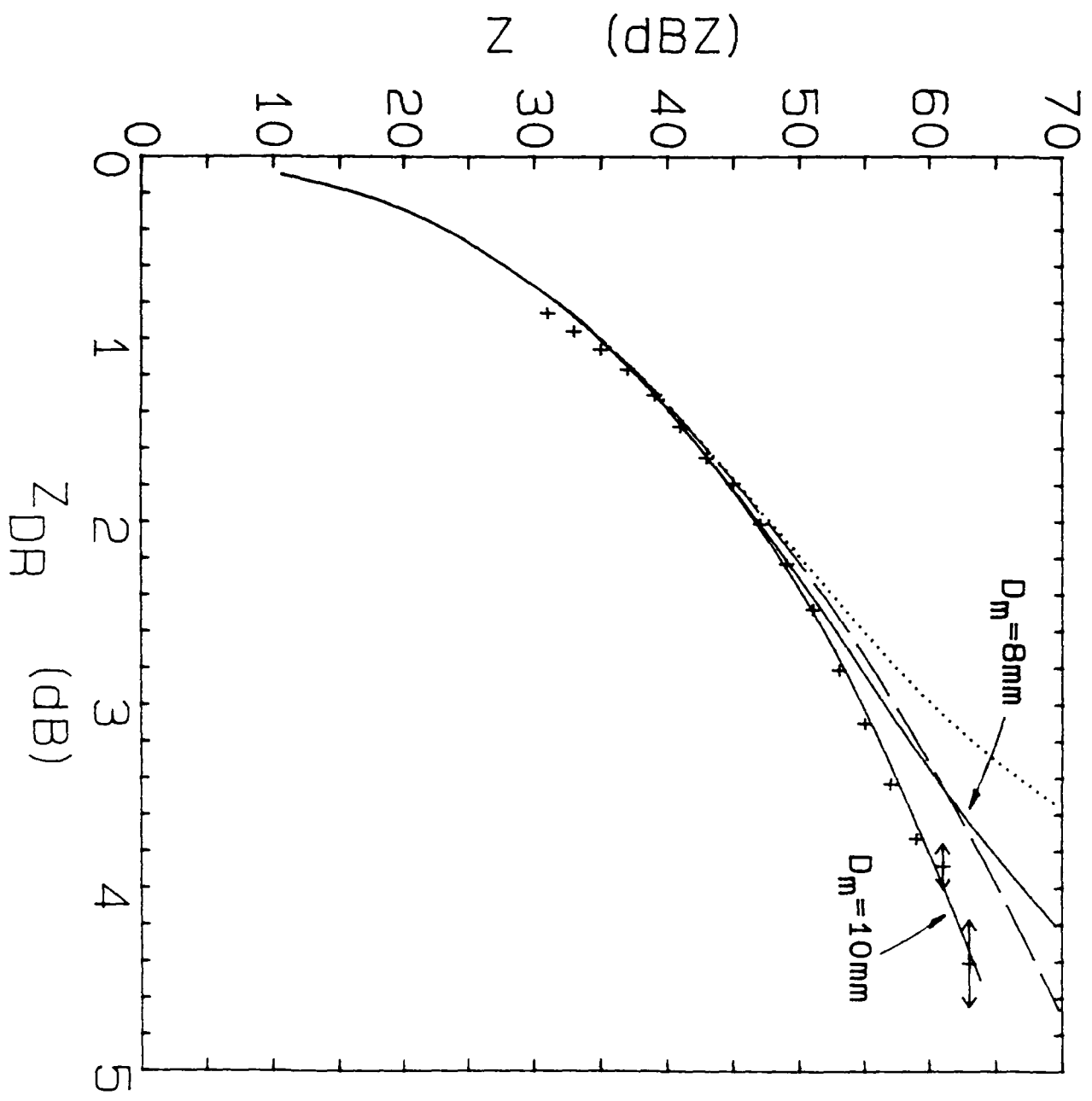
Figure 10

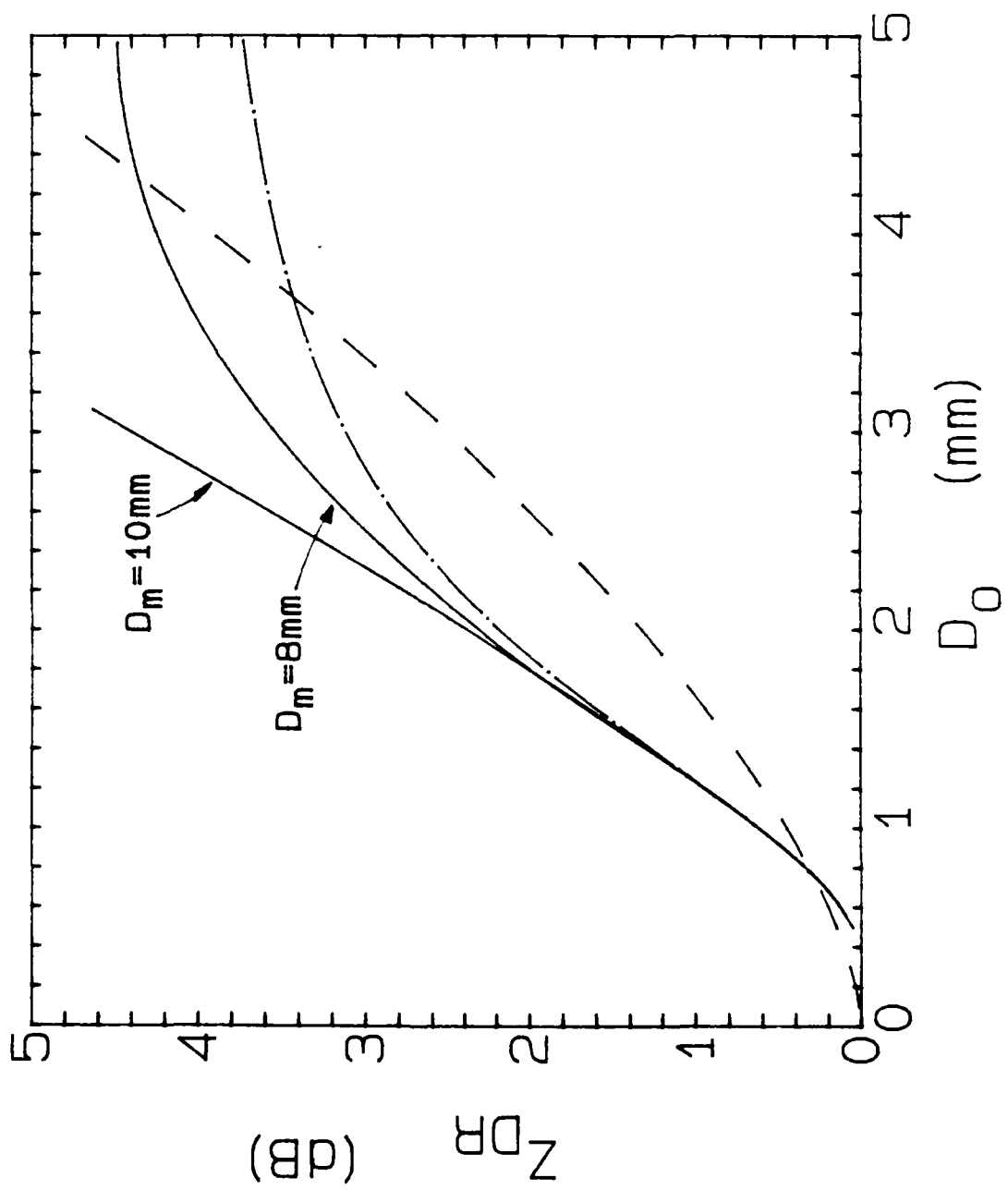
Histograms of the rainfall rates associated with 2dB intervals in Z . The data are from Figure 4, using Table 3 to compute the rainfall rate from Z and Z_{DR} .

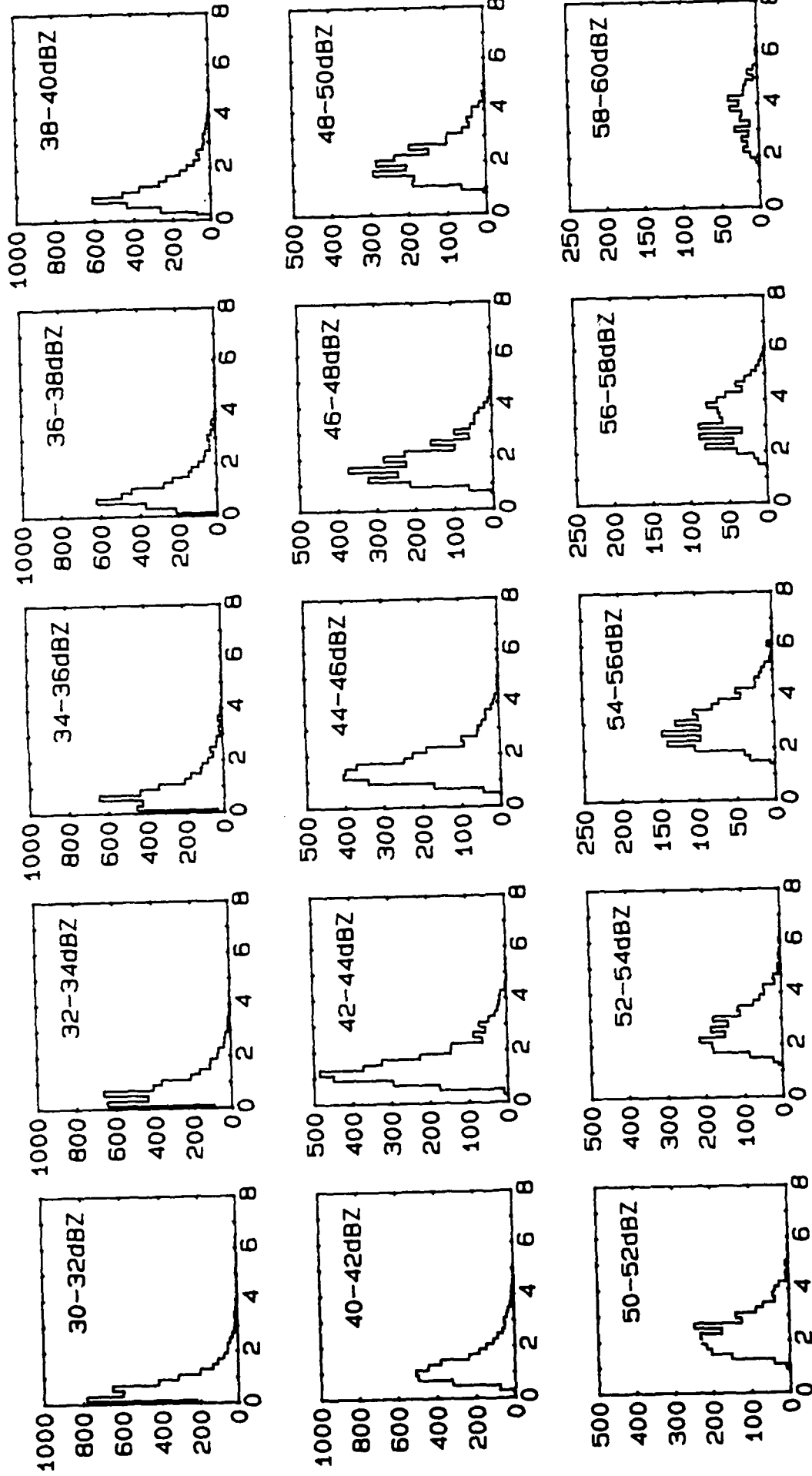






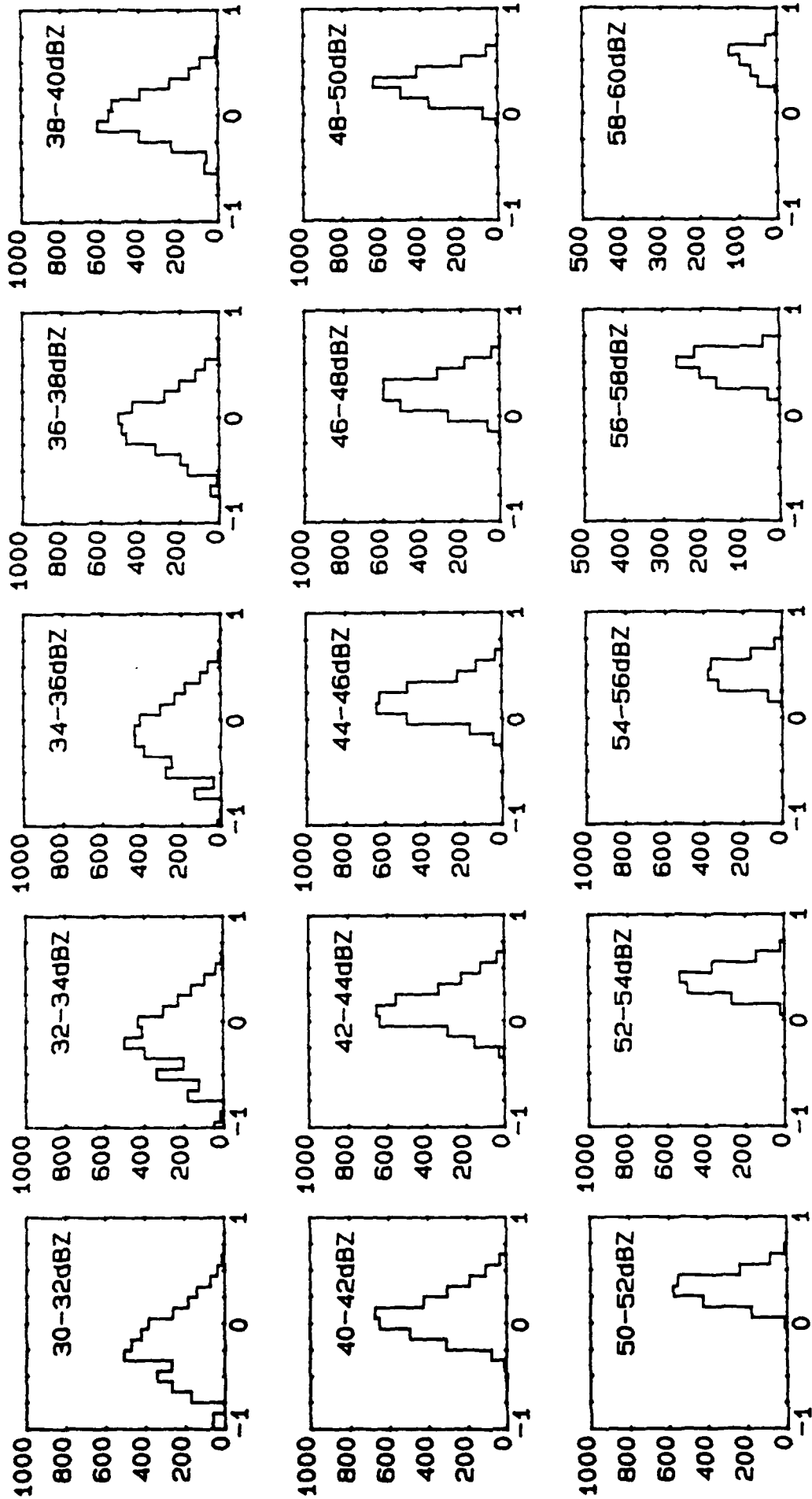






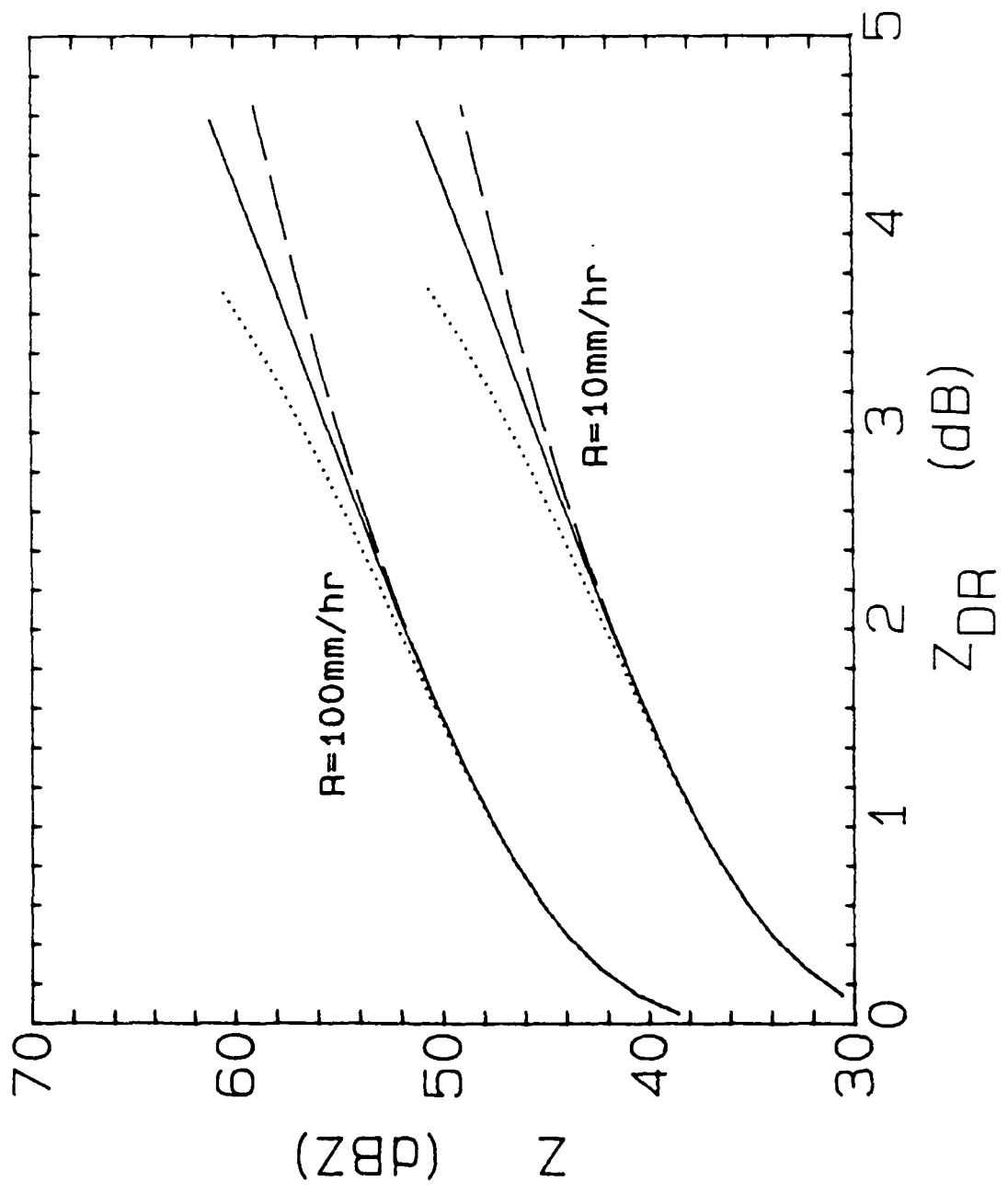
FREQUENCY OF OCCURRENCE

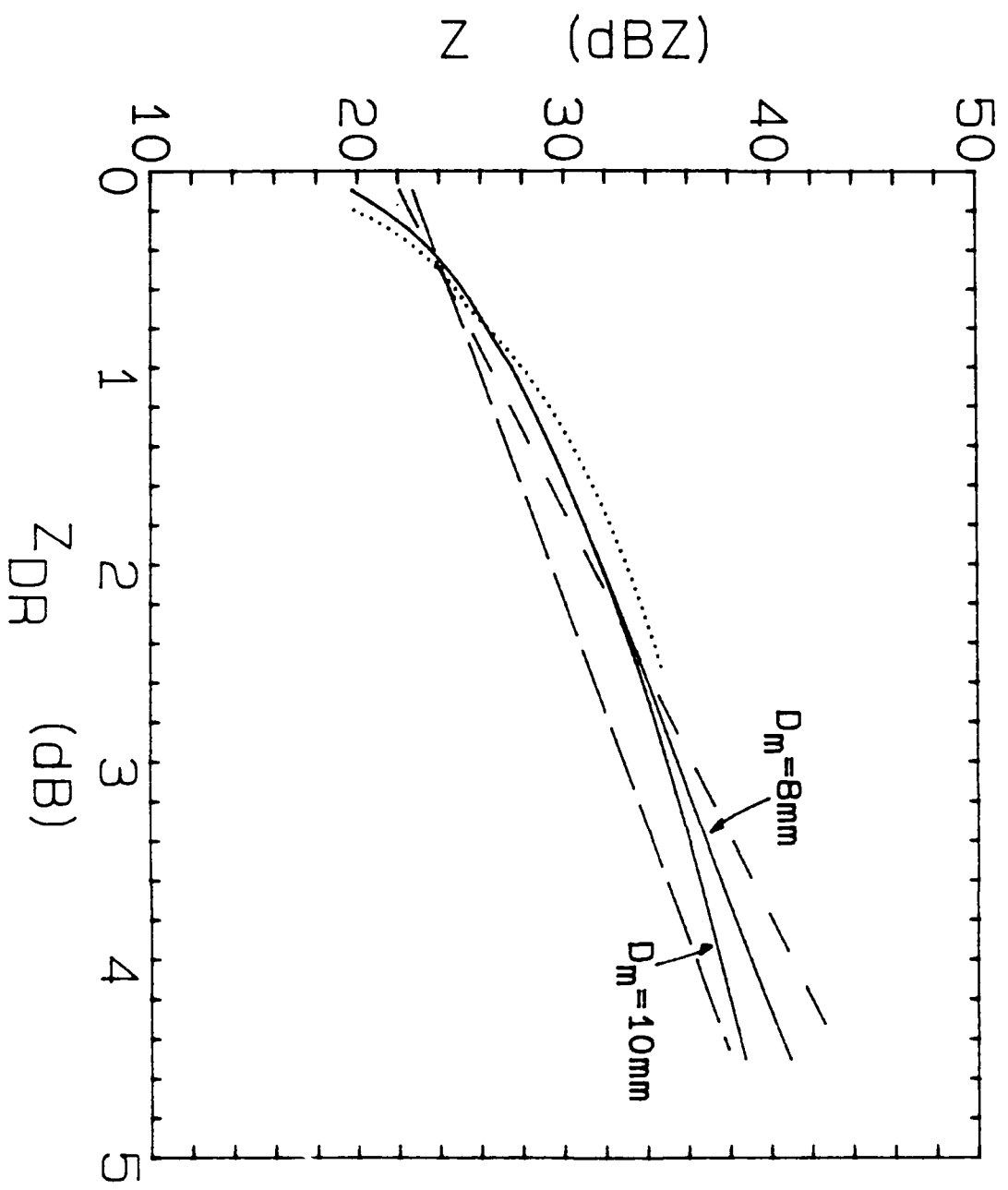
ZDR (dB)

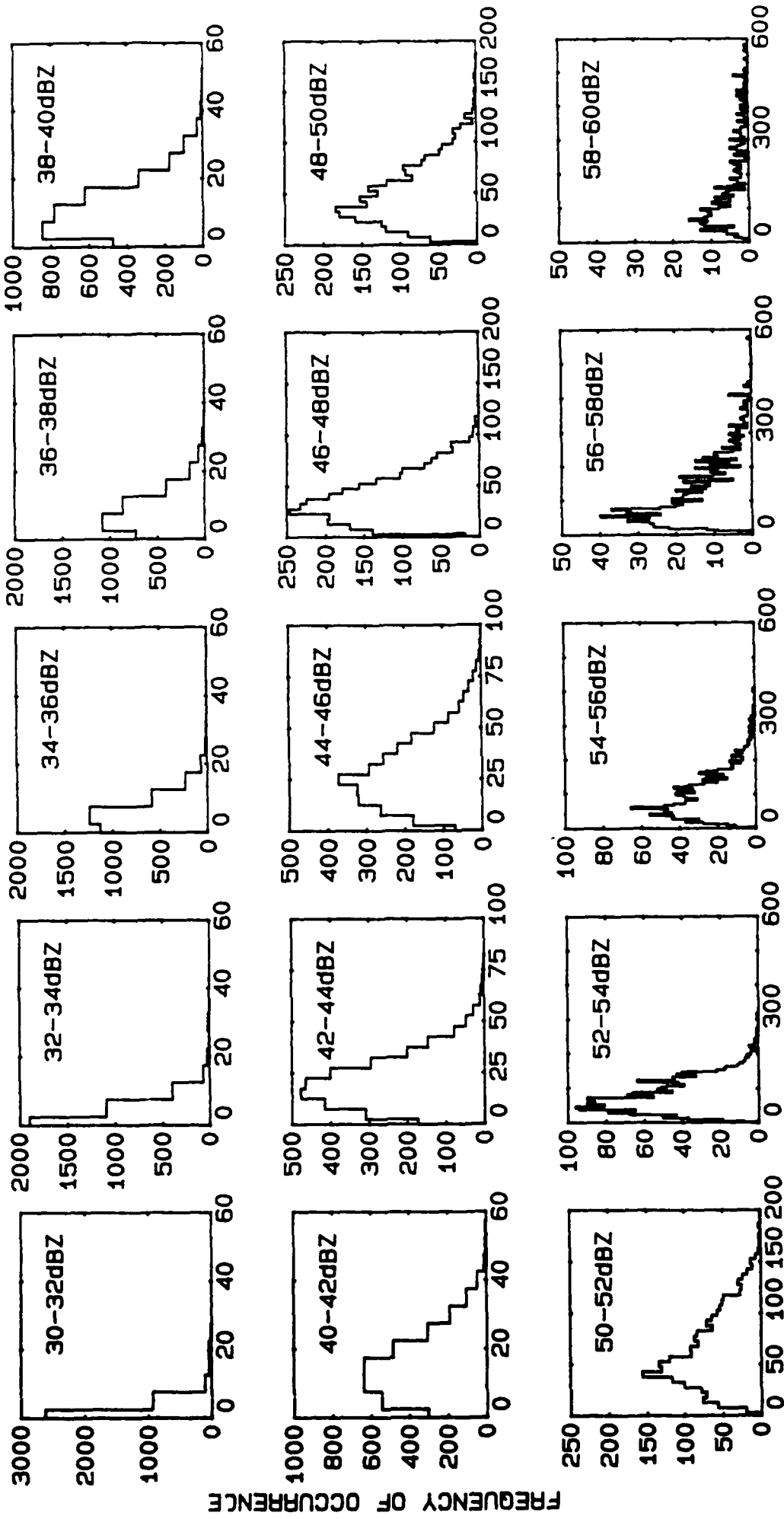


FREQUENCY OF OCCURRENCE

log ZDR (dB)







FREQUENCY OF OCCURRENCE

RAIN RATE (mm/hr)

Part 4

A J Illingworth and I J Caylor

'Identification of precipitation particles using dual
polarization radar'

1988 10th Int. Conf on Cloud Physics, Bad Homburg, Germany.

IDENTIFICATION OF PRECIPITATION PARTICLES USING
DUAL POLARIZATION RADAR

Anthony J Illingworth and I Jeff Caylor
Visiting Scientist, Dept of Physics
NCAR*, Boulder UMIST
Colorado 80307 Manchester M60 1QD, UK

1. INTRODUCTION

The S band Chilbolton radar in the UK has a quarter degree beamwidth and can transmit pulses (separation 1.6msec) which are alternately polarised in the horizontal and vertical direction. For co-polar reception we can obtain the radar reflectivity factors for the two polarizations, ZH and ZV, and then derive ZDR, the differential reflectivity ($10 \log(ZH/ZV)$). ZDR is a measure of mean shape, which for raindrops gives drop size. We shall also discuss results of the time series data obtained by recording the power received from each transmitted pulse. The cross-polar return, ZHV, and the linear depolarization ($LDR=10 \log(ZHV/ZV)$) can also be obtained, which provides information on particle fall mode. The Chilbolton antenna can detect values of LDR as low as -32dB. Results (reported elsewhere) show how the canting angle of raindrops and the mean axial ratio of tumbling graupel may be derived from LDR.

2. DIFFERENTIAL REFLECTIVITY, ZDR

The application of Z and CDR to estimate both the size and concentration of raindrops is well known (e.g. ILLINGWORTH et al, 1987). Until recently PRUPPACHER and PITTER (1970) provided the best estimate of drop shapes. Small adjustments to these shapes now appear appropriate. From CDR radar data GODDARD et al (1983) argued that millimetre drops are slightly more spherical; this suggestion has been confirmed by CHANDRASEKAR et al (1988). To explain ZDR values measured in heavy rain, CAYLOR and ILLINGWORTH (1987) postulated that drops larger than 4mm must be more oblate than the Pruppacher and Pitter shapes. BEARD and CHANG (1987) have recently confirmed that larger drops are more oblate. Direct measurements of equilibrium drop shapes are now in agreement with radar inferences, and any naturally occurring drop oscillations do not appear to bias the radar measurements.

Interpretation of the LDR at ice is more difficult (HALL et al, 1984; ILLINGWORTH et al 1987), but measurements in mature convective clouds with the Chilbolton radar consistently show LDR values within 1dB of zero, where the temperature is below freezing. Apparently in contradiction with the common observations that graupel is oblate, indicating a non-random fall mode.

3. TIME SERIES CORRELATION OF ZH AND ZV

Figure 1 shows time series data obtained at a single 75m gate in 210 milliseconds from 64 pulse pairs transmitted with alternate horizontal and vertical polarisations. Successive estimates fluctuate as the particles reshuffle in space. ZDR is normally derived by comparing the linear averages of these 64 estimates, as shown by the straight lines in the Figures. Figure 1 shows a zero ZDR for small spherical raindrops. Additional information is available from $p(H,V)$, the correlation of ZH and ZV, which here is equal to 0.99; for spheres the theoretical value is unity. Some statistical properties of $p(H,V)$ are discussed by BRINGI et al (1983).

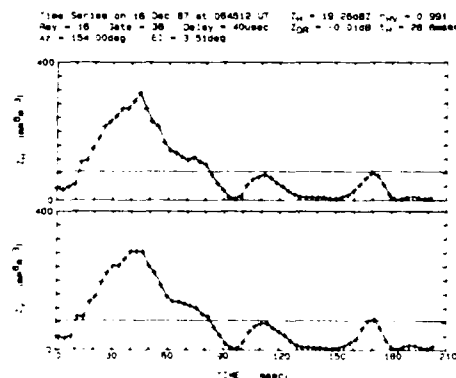


Figure 1. Time series pair showing the high correlation of ZH and ZV expected in light rain.

$p(H,V)$ will be less than one if the scattering amplitudes for the two polarizations from each particle arrive at the antenna with a non constant amplitude ratio or with a phase difference. A distribution of differently sized particles will be the most important effect in reducing $p(H,V)$. A $p(H,V)$ of 0.432 in the melting layer (Figure 2) confirms this. The bright band in Z is quite pronounced in the vertical profiles plotted in Figure 3; the maximum value of Z is 15dBZ higher than in the rain below, indicating that the particles must be of low density ice and are probably snowflakes. The ZDR profile shows a bright band in ZDR 200m below that in Z. This depression of the ZDR bright band is a common occurrence in stratiform clouds, and increases as Z becomes larger; the melting snowflake apparently reaching its maximum degree of oblateness after it has started to collapse. The low value of $p(H,V)$ in the bright band is probably caused by the coexistence of half-melted snowflakes and smaller raindrops.

A spectral analysis (Figure 4) of the time series in the melting layer (Figure 2) shows an interesting component from 40-60Hz which is greater in ZH than ZV, and is not observed in the time series for the snow above or the rain below the bright band.

We are currently developing Monte Carlo models to predict the reduction in $p(H,V)$ for the following hydrometeors:

- a) Monodispersed oblates - small phase differences between the amplitude pair from each particle due to losses or particle asymmetry.
- b) Monodispersed tumbling oblates (e.g. graupel).
- c) Polydispersed tumbling oblates (e.g. graupel).
- d) Precessing and nutating polydispersed oblates (e.g. snow and melting snow).
- e) Differently shaped aligned oblates (e.g. rain).

In rain with a ZDR of 1.5dB we have found a significant fall of $p(H,V)$ to about 0.95; but have not yet established if $p(H,V)$ can be used as an independent estimate of the breadth of the size distribution.

The lowest values of $p(H,V)$ in the low in convective clouds, should occur when the difference in the horizontal and vertical scattering amplitudes of the particle is largest; this may well occur when slightly aspherical particles enter the Mm region, and could be a way of detecting large hail in clouds. If particles are tumbling then those with axes rotated at 45deg will dominate the cross-polar return, and therefore the cross-polar time series may contain information on tumbling rates.

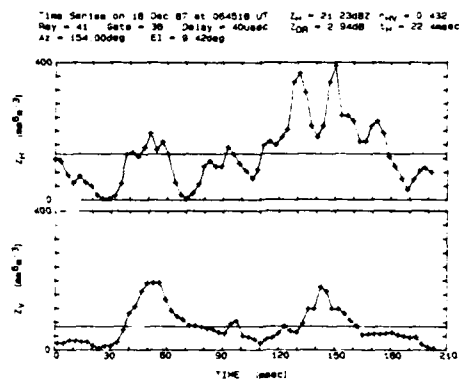


Figure 2. Time series pair observed in the melting layer of a stratiform cloud showing a lower correlation.

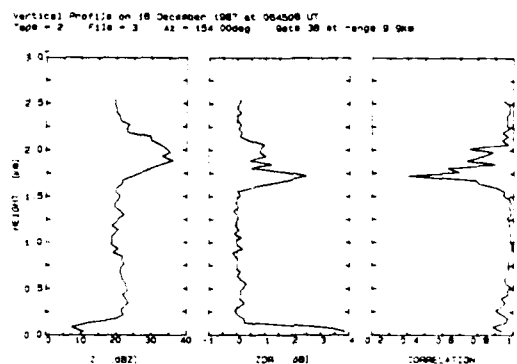


Figure 3. Profile of the vertical structure of a stratiform rain cloud from which the time series in Figures 1 and 2 are taken.

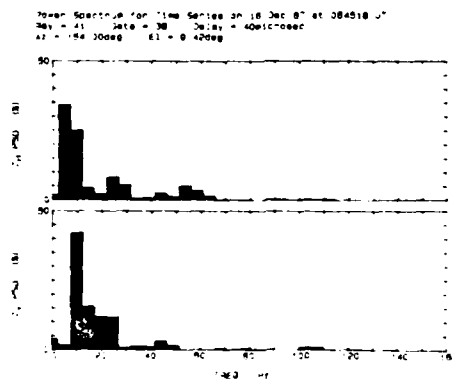


Figure 4. Normalised power spectrum for the time series of Figure 2.

4. ZDR FLARE ARTEFACTS AND IMPLICATIONS FOR DOPPLER ANALYSIS

WILSON and REUM (1988) analyse the Doppler properties of a radar artefact called a "flare echo", which extends downrange of some intense radar storm echoes. It is caused by triple scattering from a high Z region at height h , down to the ground, then back to the radar via the precipitation, thus forming a spurious echo a distance h behind the intense core. This flare has a Doppler velocity of equal magnitude to that of the core but with a reversed sign.

Figure 5, from the Chilbolton radar, has a flare echo where ZDR reaches +9dB. At a range of 87km Z reaches 70dBZ, and the flare may be identified by the column of positive ZDR inclined at 45deg to the vertical, extending from the ground at 88km range to an altitude of 4km at a range of 91km. We believe that this high value of ZDR arises because the triple scattering of the flare echo is confined to the ZH channel; for the vertical polarization the induced dipoles within the cloud should not radiate along their axes down to the ground.

Clearly such values of +9dB cannot be identified in terms of hydrometeors, but in less obvious cases positive values of ZDR towards the back of high Z regions could be erroneously interpreted as hydrometeors. ZDR artefacts caused by flare echoes should be much more widespread and intense at C and X band than at S band.

Doppler measurements are usually made using the ZH channel, but these arguments suggest that Doppler problems associated with flare echoes would be reduced if the ZV channel was used. An analysis of the MAYPOLE data, obtained by the NCAR CP2 S-band radar, reveals that the Doppler derived velocities from ZH and ZV are normally identical apart from flare regions. Further studies are underway to see if such arguments are valid at C and X band.

ACKNOWLEDGEMENTS

This research was supported by the Meteorological Office, by NERC Grant GR1 5896 and by AFOSR-87-0049. Our co-workers S.M. Cherry and J.W.F. Goddard pioneered the implementation and interpretation of the ZDR data at Chilbolton. We thank R.C. Carbone, P.H. Herzog, V.N. Bringi and T.A. Seliga for supplying us with data from the MAYPOLE '84 programme. IJC acknowledges the assistance of an IRS scholarship and AJI thanks members of the PCF at NCAR for many useful discussions.

REFERENCES

- BEARD, K.V.; CHUANG, D.: J. Atmos. Sci. 44 (1987) 1509-1524.
- BRINGI, V.N.; SELIGA, T.A.; CHERRY, S.M.: IEEE Trans Geo & Remote Sensing GE-21 (1983) 215-220.
- CAYLOR, I.J.; ILLINGWORTH, A.J.: 22nd Conf. Radar Meteorology, Amer. Meteorol. Soc. (1980) 88-91.
- CHANDRASEKAR, V.; COOPER, W.A.; BRINGI, V.N.: submitted to J. Atmos. Sci. (1988).
- GODDARD, J.W.F.; CHERRY, S.M.; BRINGI, V.N.: J. Appl. Met. 21 (1983) 252-256.
- HALL, M.P.H.; GODDARD, J.W.F.; CHERRY, S.M.: Radio Sci. 19 (1984) 132-140.
- ILLINGWORTH, A.J.; GODDARD, J.W.F.; CHERRY, S.M.: Q. J. Roy. Meteorol. Soc. 113 (1987) 469-489.
- PRUPPACHER, H.R.; PITTER, R.L.: J. Atmos. Sci. 28 (1971) 86-94.
- WILSON, J.W.; REUM, D.: J. Ocean & Atmos. Tech. (to be published 1988).

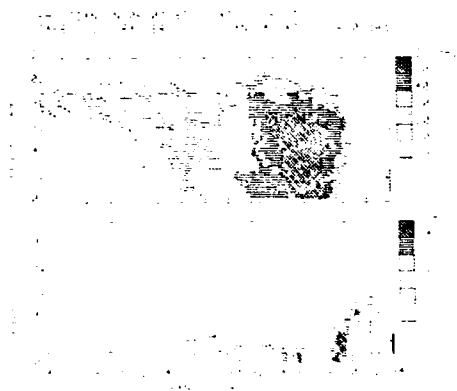


Figure 5. A vertical scan of a mature convective cloud showing a flare echo in ZDR near 88km range.

Part 5

I J Caylor and A J Illingworth

'Dual linear polarisation time series as an aid
to hydrometeor identification'

1988 IGARSS '88 Symp. Edinburgh, Sept. REF ESA SP-284.

DUAL LINEAR POLARISATION TIME SERIES AS AN AID TO HYDROMETEOR IDENTIFICATION

I J Caylor

A J Illingworth

Department of Pure and Applied Physics, UMIST
P O Box 88, Manchester M60 1QD, UK

ABSTRACT

We present radar observations of precipitation particles using a new polarization parameter, $p(H,V)$, which is the correlation of the time series of ZH and ZV (the radar reflectivity factors measured with horizontal and vertical polarization). $p(H,V)$ is very close to unity in most precipitation. In stratiform precipitation low values of $p(H,V)$ are found only in the melting layer, and so may be used as a simple means of identifying the bright band. We suggest that in convective clouds $p(H,V)$ will be low only where hailstones are large enough to enter the Mie scattering region. Our observations are made at S-band, but, because $p(H,V)$ should be little affected by propagation problems, the technique could be implemented at shorter wavelengths.

Keywords: Polarization, Time-Series, Differential-Reflectivity, Bright-Band, Hail, Correlation

The S band Chilbolton radar in the UK has a quarter degree beamwidth and can transmit pulses (separation 1.0msec) which are alternately polarized in the horizontal and vertical direction. From the copolar reception we can obtain the radar reflectivity factors for the two polarizations, ZH and ZV, and then derive ZDR, the differential reflectivity ($10 \log(ZH/ZV)$). ZDR is a measure of mean shape, which for raindrops gives drop size. The application of Z and ZDR to estimate both the size and concentration of raindrops is well known; interpretation of the ZDR of ice is more difficult (Hall et al., 1984, Illingworth et al., 1987), but measurements in nature convective clouds with the Chilbolton radar consistently show ZDR values within 0.1dB of zero. We shall discuss results of the time series data obtained by recording the power received from each transmitted pulse.

Figure 1 shows time series data obtained at a single 75m gate in 210 milliseconds from 64 pulse pairs transmitted with alternate horizontal and vertical polarizations. Successive estimates fluctuate as the particles reshuffle in space. ZDR is normally derived by comparing the linear averages of these 64 estimates, as shown by the straight lines in Figure 1; in this case ZDR is zero for the small spherical raindrops in the light rain. Additional information

is available from $p(H,V)$, the correlation of ZH and ZV, which here is equal to 0.99; for spheres the theoretical value is unity. Some statistical properties of $p(H,V)$ are discussed by BRINGI et al (1983). Sachidananda and Zrnic (1985) show theoretically that values of $p(H,V)$ in rain should be close to unity.

Figure 1. Time Series in light rain on 16/12/87
 $Z_H=19.28dBZ$ $Z_{DR}=0.01dB$ $r_{HV}=0.991$ $t_H=28.8msec$

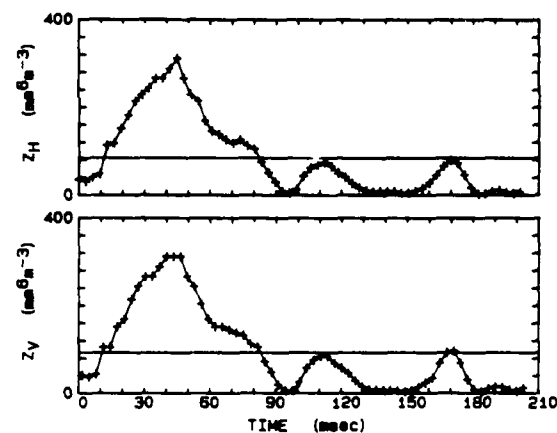
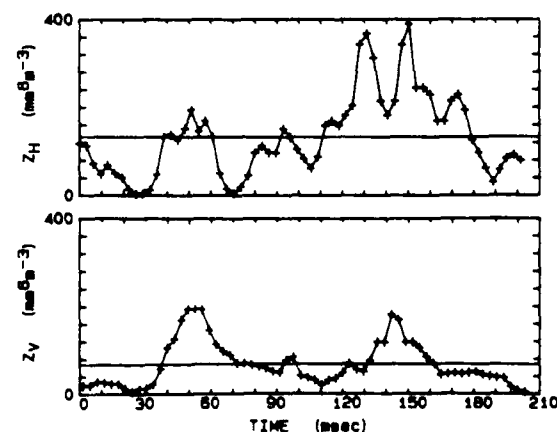


Figure 2. Time Series in bright band on 16/12/87
 $Z_H=21.23dBZ$ $Z_{DR}=3.34dB$ $r_{HV}=0.432$ $t_H=22.4msec$



One factor reducing $p(H,V)$ will be if the various particles in the sample volume have different ratios of scattering cross-sections for the two polarizations. A distribution of particles with different shapes will be the most important effect in reducing $p(H,V)$. A $p(H,V)$ of 0.432 in the melting layer (Figure 2) confirms this. The bright band in Z is quite pronounced in the vertical profiles plotted in Figure 3; the maximum value of Z is 15dBZ higher than in the rain below, indicating that the particles must be of low density ice and are probably snowflakes. The ZDR profile shows a bright band in ZDR 200m below that in Z. This depression of the ZDR bright band is a common occurrence in stratiform clouds, and increases as Z becomes larger; the melting snowflake apparently reaching its maximum degree of (electromagnetic) oblateness after it has started to collapse. The low value of $p(H,V)$ in the bright band is probably caused by the coexistence of half-melted snowflakes and smaller raindrops.

The power spectra for the time series for ZH and ZV in rain are identical (e.g. Figure 4), but in the melting layer (Figure 5) there are usually some higher frequency components which are greater in ZH than ZV. These may result from the greater contribution of the oblate snowflakes with low terminal velocities leading to a broader Doppler spectrum in ZH, or, alternatively, fluttering of the oblate semi-aligned snowflakes modulating ZH more than ZV.

Our measurements in the ice in convective clouds generally show high values of $p(H,V)$. When values of decorrelation times (t_c) fall below 20 msec it is necessary to interpolate the data so that the ZH and ZV sampling is effectively simultaneous. We expect low values of $p(H,V)$ to be confined to regions containing large hail. Ground observations of hail show that the axial ratio rarely exceeds 0.9. Laboratory scattering experiments on such particles which are large enough to enter the Mie region, reveal that their scattering cross-sections should change by up to 10dB as they tumble; this should give rise to low values of $p(H,V)$.

The melting layer observations lend support to this proposed hail detection algorithm. We observe high $p(H,V)$ in heavy rain with a ZDR of 2.5dB although a distribution of drop shapes must be present, but an equally high ZDR in the melting layer is accompanied by low $p(H,V)$. We are investigating theoretically if this implies such a large range of scattering amplitudes that we need to invoke Mie scattering from the larger half melted snowflakes in the bright band.

ACKNOWLEDGEMENTS

This research was supported by the Meteorological Office, by NERC Grant GR3/5896 and by AFOSR-88-0121. Our co-workers S M Cherry and J W F Goddard pioneered the implementation and interpretation of the ZDR data at Chilbolton.

REFERENCES

1. Bringi V N, Seliga TA & Cherry S M 1980, IEEE Trans Geo & Remote Sensing GE-21 (1983) 215-220.
2. Hall M P H, Goddard J W F & Cherry S M 1984, Radio Sci. vol 19, 132-140.
3. Illingworth A J, Goddard J W F & Cherry S M 1987, Q J Roy Meteorol Soc vol 113, 469-489.
4. Sachidanada M & Zrnic D S 1985, Rad Sci vol 20, 907-922.

Figure 3. Vertical profile on 16/12/87 at 064508 UT
Tape=2 File=3 Az=154.0deg Range=8.8km

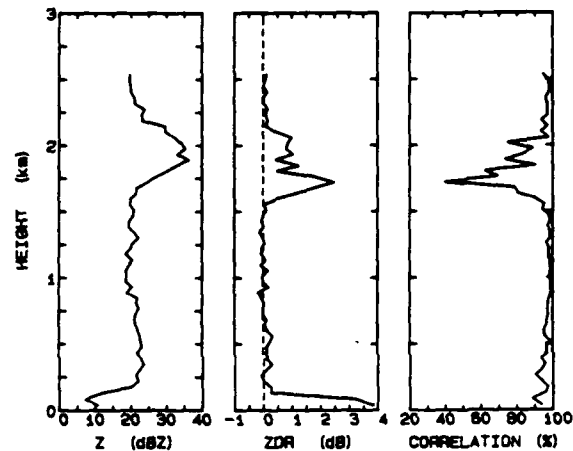


Figure 4. Power spectrum for light rain on 16/12/87
Ray=20 Gate=38 Az=154.0deg E1=4.5deg R=8.8km

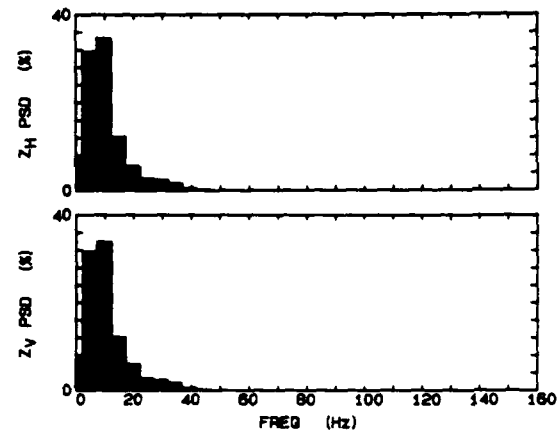
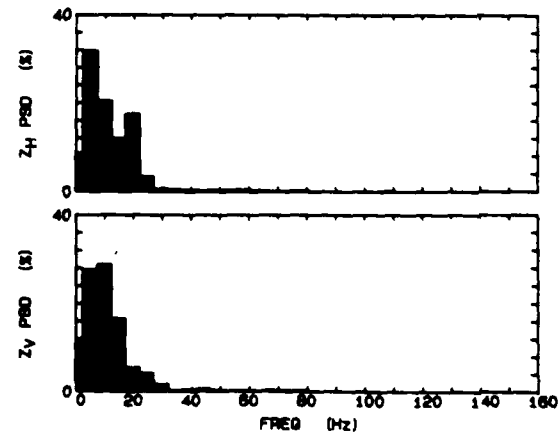


Figure 5. Power spectrum for bright band on 16/12/87
Ray=41 Gate=38 Az=154.0deg E1=9.4deg R=8.8km



Part 6

I J Caylor and A J Illingworth

'Identification of the bright band and hydrometeors
using co-polar dual polarization radar'

1989 24th Conf. on Radar Meteorology, Tallahassee, Florida.

IDENTIFICATION OF THE BRIGHT BAND AND HYDROMETEORS
USING CO-POLAR DUAL POLARIZATION RADAR

I Jeff Caylor and Anthony J Illingworth

Department of Physics, UMIST
Manchester, UK

1. INTRODUCTION

Polarization radar measurements can provide information on the characteristics of precipitation particles which is unavailable from the simple reflectivity measurement. We discuss means of measuring raindrop sizes and concentrations, raindrop canting angles, and we outline techniques for differentiating between the various forms of frozen hydrometeors (snow, graupel and hail) and for rapid identification of the bright band.

The S-band (10cm) Chilbolton radar (Goddard and Cherry, 1987) situated in Hampshire in the UK has a 25m dish (quarter degree beamwidth) and is the largest steerable meteorological radar in the world. The radar can transmit (and receive) pulses every 1.6msec which are alternately polarized in the horizontal and vertical directions. The pulses are 0.5msec long with a peak power of 500kW, and the return is digitised every 500nsec to give a 75m range resolution. In this paper we present observations (introduced by Illingworth and Caylor, 1988a) of (a) The differential reflectivity, ZDR, which measures mean hydrometeor shape, and (b) the co-polar correlation $\rho^2(H,V)$, which reflects the variety of particle shapes present. A companion paper (Illingworth and Caylor, 1989) discusses a third parameter, (c) the Linear Depolarization Ratio, LDR, which is affected by the fall mode of the particles. We shall also report results of the cross-polar correlation and the frequency spectra of the co- and cross-polar time series.

2. DEFINITION OF TERMS AND EXAMPLES OF DATA

Figure 1 shows time series data for 210 msec obtained at a single 75m gate from 64 pulse pairs transmitted with alternate horizontal and vertical polarizations. Reception is co-polar (or parallel) to the transmitted polarization so the 64 samples are of ZH and ZV, the reflectivities for horizontal and vertical polarization respectively. Successive estimates of ZH and ZV fluctuate as the particles re-arrange in space, the decorrelation time of each time series being related to the width of the Doppler spectrum of the scattering particles.

The differential reflectivity, ZDR, is defined as

$$ZDR = 10 \log (ZH/ZV) \quad (1)$$

where ZH and ZV are the averages (linear power) of the 64 samples, as shown by the straight lines in Figure 1; this data is for heavy rain

and has a ZDR of 2.76dB. ZDR is particularly useful for distinguishing ice from rain and for measuring the mean shape of the raindrops (see Section 3).

Time Series on 13 July 1988 at 155425 UT
Ray=148 Gate=30 Az=253.0deg El=2.4deg R=13.5km
ZH=46.05dBZ ZDR=2.76dB ρ_{HV} =0.992 t_H =19.2msec

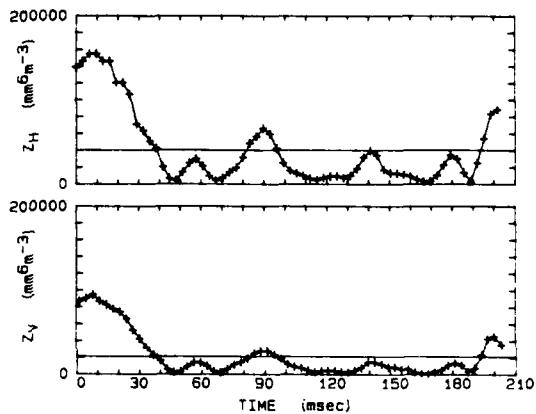


Figure 1
ZH and ZV time series taken in heavy rain.

Additional information can be derived from the correlation of the two time series in ZH and ZV, which we call the co-polar correlation ($\rho^2(H,V)$). Previously the average values of ZH and ZV have been computed in real time and the time series data has not been recorded. For the heavy rain in Figure 1 ρ^2 is 0.99 (see Sections 4 and 5).

3. ZDR, THE DIFFERENTIAL REFLECTIVITY

In rain ZDR provides a measure of the mean raindrop shape. Raindrops become more oblate with increasing size, so ZDR is positive and the magnitude of ZDR is related to the mean raindrop size. The application of Z and ZDR for estimating both the size and concentration of raindrops is well known (e.g. Seliga and Bringi, 1976). Until recently Pruppacher and Pitter (1971) provided the best estimate of drop shapes. Small adjustments to these shapes now appear appropriate. From ZDR radar data Goddard and Cherry (1983) argued that millimeter sized drops are slightly more spherical than previously believed; this suggestion has been confirmed

by the aircraft measurements of drop shapes by Chandrasekhar et al (1988) and the laboratory measurements of Beard and Ochs (1988). To explain high ZDR values measured in heavy rain Caylor and Illingworth (1987) postulated that drops larger than 4mm must be more oblate than the Pruppacher and Pitter shapes; Beard and Chuang (1987) have recently confirmed that larger drops are indeed more oblate. Direct measurements of equilibrium drop shapes are now in agreement with radar inferences, and any naturally occurring drop oscillations do not appear to bias the radar measurements. An analysis of these drop shapes and their effect on estimates of drop size distributions and rainfall rates is given by Illingworth and Caylor (1988b). Z and ZDR measurements indicating that first echoes in warm convective clouds consist of a low concentration of large raindrops are discussed by Illingworth (1988).

The theoretical precision of the ZDR measurement is analysed by Bringi et al (1983), and Figure 2 (from their equation 7) predicts how the number of independent samples and the copolar correlation, p , limit the accuracy of ZDR. For the time series in Figure 1, there are 10 independent samples, $p^*(H,V)$ is 0.99, so the predicted standard error in the ZDR estimate is 0.25dB. To increase the accuracy of rainfall estimates, ZDR must be measured to an accuracy of 0.1dB. Figure 2 implies that 40 independent samples are needed if $p=0.99$; the Chilbolton radar achieves this by spatial averaging over four adjacent 75m range gates.

Interpretation of the ZDR of ice is more difficult (Hall et al, 1984, Illingworth et al 1987) because ZDR varies with axial ratio, shape, fall mode and dielectric constant. Figure 3 shows the values of ZDR as a function of axial ratio, for Rayleigh scattering from oblate spheroids of water and ice with their major axes aligned in the horizontal. Our experience with the Chilbolton radar is that ZDR values in convective clouds are within 0.1dB of zero, indicating tumbling ice, or, at the other extreme, aligned graupel with a mean axial ratio of less than 0.95. In stratiform clouds the values of ZDR in ice are variable, and although zero is the most common, values of up to 3dB occur, particularly where Z tends to be low. High ZDR values, locally up to 6dB, can be found in the melting layer.

4. MEASUREMENT PROBLEMS FOR THE CO-POLAR CORRELATION

Two practical problems arise in estimating the correlation: the finite signal to noise ratio (SNR) and the non-simultaneous sampling of ZH and ZV. Bringi et al (1983) show that for a finite SNR the measured value p^* is related to the true value of p by:

$$p^* = p (1 + 1/\text{SNR})^{0.5} (1 + \text{ZDR}/\text{SNR})^{0.5} \quad (2)$$

For values of ZDR close to 0dB, a true value of $p=1$, is reduced to 0.999 for an SNR of 30dB, and 0.99 for 20dB. The reduction of the correlation due to non-simultaneous sampling is given by (Zrnica et al, 1988):

$$p^* = p \cdot p(l) \quad (3)$$

where $p(l)$ is the decorrelation of the H or the V time series after one pulse delay. In practice, because of measurement errors, Equation 3 can occasionally lead to corrected values of $p(H,V)$ which are slightly larger than unity. We prefer to use a third order polynomial fit and interpolation to estimate the coincident values, although it is computationally more intensive. Sorting of many hundreds of time series in rain at altitudes between 250m and 1km and with a SNR better than 20dB, reveals that for a decorrelation time (τ) of 13msec the average value of p^* is 0.95, but rises to 0.97 after interpolation; the average improvement using equation 3 is similar. For a τ of 25msec the average value of p^* is 0.97 which rises to 0.98 after interpolation; for longer values of τ corrections for non-simultaneous sampling are not significant.

The drop in correlation due to Doppler effects will be more serious at shorter wavelengths, although this can be mitigated by the use of a higher PRF. The extreme narrowness of the Chilbolton beam minimises Doppler broadening

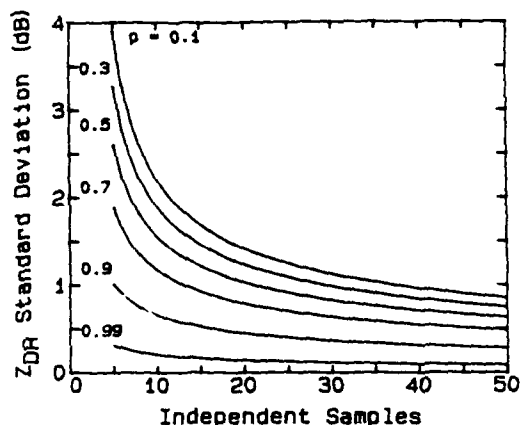


Figure 2
Standard deviation of ZDR as a function of the number of independent samples and correlation.

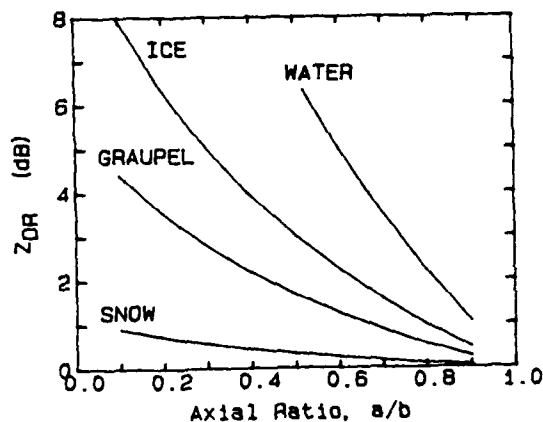


Figure 3
ZDR as a function of axial ratio for oblate spheroids.

due to wind shear, and data are always taken with antenna elevations below 15° . If elevations any higher are used then the Doppler spread introduced because of the raindrops' terminal velocities will lead to very short decorrelation times and compromise any measurements of the co-polar correlation.

In their theoretical study Sachidananda and Zrnic (1985) predict that the correlation in rain should be at least 0.995. Jameson and Dave (1988) and Bebbington et al (1987) have demonstrated that the linear correlation may be derived from circular polarization measurements. In this case simultaneous reception of the two circularly polarized is possible, but it is not obvious how the accuracy of the derived value for linear correlation is limited by the transformation from circular to linear and by the algorithms which correct for propagation effects.

5. CO-POLAR CORRELATION RESULTS

The measured values of linear co-polar correlation in most precipitation are not significantly different from unity. Theoretically in rain with a large ZDR there should be a reduction in correlation due to the variety of drop shapes. We find that when ZDR is 2.5dB the average value of the ρ^2 is about 0.97, but these high ZDRs tend to occur in more turbulent conditions, and it is not clear how much of the reduction is due to the inadequacy of our correction algorithm. Ideally, the drop in correlation should be related to the width of the raindrop spectra, and could provide a value of m if a gamma function is used to describe the raindrop spectrum, but any effect seems to be masked by measurement errors.

An example of a time series measured in snow is shown in Figure 4. In this case the value of ρ^2 reaches the exceptionally high value of 0.999, aided no doubt by the SNR of 50dB for these data. The only region where appreciable reductions occur is in the bright band as demonstrated in Figure 5 where ρ^2 falls to 0.31. The low correlation in the bright band is probably caused by the coexistence of large oblate wet snowflakes and spherical raindrops.

Conventional radars scanning in PPI mode are used to estimate rainfall, but when the beam intersects the bright band the rainfall is overestimated. Smith (1986) has suggested algorithms for bright band identification which involve comparing PPI at two elevations. Our data in stratiform cloud show that a value of ρ^2 below 0.8 is an excellent detector of the bright band; the efficiency of the algorithm is easily verified by examining RHI scans where the bright band can be clearly seen from the Z structure. The use of the correlation method has several advantages:

- It is unaffected by differential attenuation and so, in contrast to ZDR, should be applicable at shorter wavelengths.
- Only a short time series is required to estimate ρ^2 , thus overcoming the long dwell times needed to measure ZDR.
- The correlation is unaffected by differential phase shifts.

We suggest that in convective clouds the value of ρ should fall when the hail particles are large enough for Mie scattering to occur. This idea is based upon the observations that all hail particles are slightly aspherical and tumble as they fall. Consequently the vertical and horizontal cross sections of the individual tumbling hailstones will vary by up to 15dB (Atlas and Wexler, 1963). At 10cm Mie scattering should be rare, but for a 3cm radar the drop in correlation should be an indication that hail has reached a diameter of about 1cm. In addition to the advantages itemized for the melting band, this algorithm should work equally well for wet and dry hailstones. Thus far the maximum Z we have observed in ice is about 40dBZ (but see, Zrnic et al, 1988).

Time Series on 29 May 1988 at 160418 UT
Ray=51 Gate=62 Az=290.0deg El=11.3deg R=9.3km
 $Z_H=25.47$ dBZ $Z_{DR}=0.01$ dB $\rho_{HV}=0.999$ $t_H=22.4$ msec

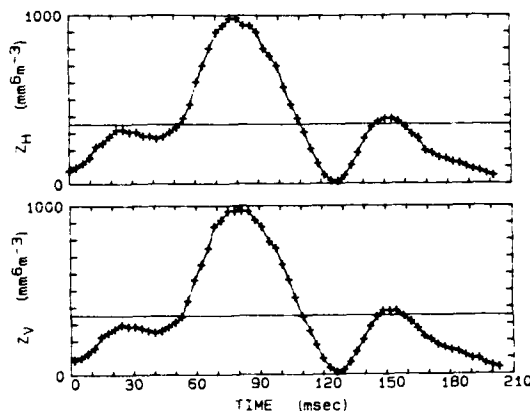


Figure 4
Time series for ice above the melting layer.

Time Series on 29 May 1988 at 160418 UT
Ray=24 Gate=62 Az=290.0deg El=5.4deg R=9.3km
 $Z_H=25.43$ dBZ $Z_{DR}=2.52$ dB $\rho_{HV}=0.312$ $t_H=12.8$ msec

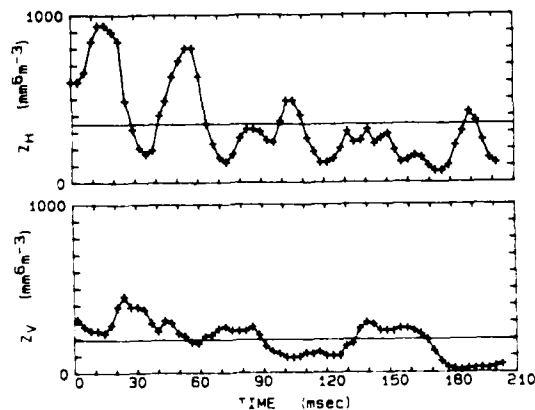


Figure 5
ZH and ZV time series in the bright band.

6. ZDR FLARE ARTEFACTS AND IMPLICATIONS FOR DOPPLER ANALYSIS

Wilson and Reum (1988) analyse the Doppler properties of a radar artefact called a "flare echo" which extends downrange of some intense radar storm echoes. It is caused by triple scattering from a high Z region at a height h , down to the ground, then back to the radar via the precipitation, thus forming a spurious echo a distance h behind the intense core. The Doppler velocity of this flare is related to the terminal velocity of the particles in the core.

Figure 6, from the Chilbolton radar, has a flare echo where ZDR reaches +9dB. At a range of 87km Z is 70dBZ, and the flare may be identified by the column of positive ZDR inclined at 45 deg to the vertical, extending from the ground at 88km range to an altitude of 4km at a range of 91km. We believe that this high value of ZDR arises because the triple scattering of the flare echo is confined to the ZH channel; for the vertical polarization the induced dipoles within the cloud should not radiate along their axes down to the ground.

Clearly, such values of +9dB cannot be interpreted in terms of hydrometeors, but in less obvious cases positive values of ZDR towards the back of high Z regions could be erroneously ascribed to hydrometeors. ZDR artefacts caused by flare echoes should be much more widespread and intense at C and X band than at S band.

Doppler measurements are usually made using the ZH channel, but these arguments suggest that Doppler problems would be reduced if the ZV channel was used. An analysis of the MAYPOLE data, obtained by the NCAR CP2 S-band radar, reveals that the Doppler derived velocities from ZH and ZV are normally identical apart from in the flare regions where there are large differences.

ACKNOWLEDGEMENTS

This research was supported by NERC Grant GR3/5896 and by AFOSR-86-0121. Our co-workers S M Cherry and J W F Goddard pioneered the implementation and interpretation of the ZDR data at Chilbolton. We thank R E Carbone, P H Herzegh, V N Bringi and T A Seliga for supplying us with data from the MAYPOLE 84 program. IJC acknowledges an ORS scholarship and AJI thanks members of the FOF at NCAR for many useful discussions.

REFERENCES

- Atlas D and Wexler R: *J Atmos Sci*, 20,48 (1963)
 Beard K V and Chuang D:
J Atmos Sci 44, 1509-1524 (1987)
 Beard K V and Ochs H T:
 Proc Xth Int Cloud Phys Conf, Deutscher Wetterdienst, Offenbach-am-Main (1988)
 Bebbington D H O, McGuinness R and Holt A R:
IEE Proc 134 H5,431-437 (1987)
 Bringi V N, Seliga T A and Cherry S M: *IEEE Trans Geo & Remote Sensing* GE-21 (1983)
 Caylor A J and Illingworth A J:
Q J Roy Meteorol Soc, 113, 1171-1191 (1987)
 Chandrasekhar V, Cooper W A, Bringi V N:
J Atmos Sci, 45, 1323-1333 (1988)

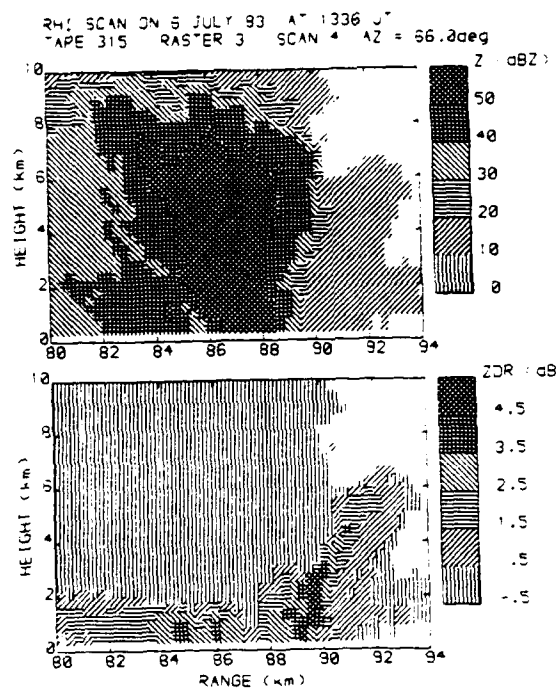


Figure 6
 Z and ZDR for an RHI with a flare echo at 88-91km.

- Goddard J W F and Cherry S M:
Rad Sci, 19, 252-256 (1983)
 Goddard J W F and Cherry S M:
IEE Conf Pub No 274, London (1987)
 Hall M P M, Goddard J W F and Cherry S M:
Radio Sci 19, 132-140 (1984)
 Illingworth A J and Caylor I J:
 Proc Xth Int Cloud Phys Conf, Deutscher Wetterdienst, Offenbach-am-Main (1988a)
 Illingworth A J and Caylor I J:
 Submitted to *J Ocean & Atmos Tech* (1988b)
 Illingworth A J and Caylor I J:
 These proceedings (1989)
 Illingworth A J, Goddard J W F and Cherry S M:
Q J Roy Meteorol Soc 113,469-489 (1987)
 Illingworth A J: Accepted for publication in *Nature* (1988).
 Jameson A R and Dave J H:
J Atmos & Ocean Tech, 5,405-415, (1988)
 Pruppacher H R and Pitter R L:
J Atmos Sci, 28,86-94 (1971)
 Sachidananda M and Zrnica D S:
J Atmos & Ocean Tech, 4, 588-598(1984)
 Seliga T A and Bringi V N:
J Appl Met, 15, 69-76, (1976)
 Smith C J:
J Atmos & Ocean Tech, 3, 129-141 (1986)
 Wilson J W, Reum D: *J Ocean & Atmos Tech*, 5, 197-205 (1988)
 Zrnica D S, Balakrishnan N, Sachidananda M: *Proc IGAARS Symp, Edinburgh, ESA SP-284* (1988)

Part 7

A J Illingworth and I J Caylor

'Cross polar observations of the bright band'.

1989 24th Conf on Radar Meteorology, Tallahassee, Florida.

PREPRINTS: 24th Conference on Radar Meteorology,
 American Meteorol Soc, Florida March 1989

CROSS POLAR OBSERVATIONS OF THE BRIGHT BAND

Anthony J Illingworth and I Jeff Caylor

Pure and Applied Physics, UMIST,
 Manchester M60 1QD, UK

1. INTRODUCTION

In this paper we present cross-polar radar measurements in precipitation and discuss the vertical profiles of three polarization parameters through the bright band. The specification of the S-band Chilbolton radar and an introduction to the various polarization parameters is given in a companion paper (Caylor and Illingworth, 1989, referred to as C&I), which concentrates on the differential reflectivity (ZDR), and the correlation between the co-polar received signals for vertically and horizontally polarized transmission ($p^2(H,V)$). We now consider the additional information available in the cross-polar (or orthogonal) linearly polarized returns.

Figure 1 shows time series data for 210 msec obtained at a single 75m gate from 64 pulse pairs, for each pulse the reception alternates between the co-polar and the cross-polar. The linear depolarization ratio LDR is defined as:

$$LDR = 10 \log (ZVH/ZH) \quad (1)$$

where ZVH is the average (linear power) of the 64 estimates of the cross polar return (transmit vertical, receive horizontal), and ZH is the same average for the co-polar (horizontal) return. For the time series in Figure 1 the value of LDR is about -31dB. LDR senses particle fall mode and, as we shall see, is an excellent detector of wet ice. It is also possible to estimate the cross-polar correlation ($p^2(VH,H)$) between the two time series, which for Figure 1 is only -0.08.

2. LINEAR DEPOLARIZATION RATIO

The earliest LDR data were taken by Browne and Robinson (1952) at wavelengths of 3.2cm and 8mm who detected an enhanced cross-polar return from the bright band. More recent observations at 3cm are reported by Herzegh and Conway, (1986). Herzegh and Jameson (1988) propose a correction algorithm for the propagation problems that occur at these wavelengths, which are caused by the progressive depolarization of the incident radiation as it passes through precipitation, and result in a rise in the apparent values of LDR with increasing range.

The first measurements of LDR at 10cm wavelength were made with the Chilbolton radar in the summer of 1988 (Goddard et al, 1988). At this wavelength propagation problems appear to be minimal, and theoretical interpretation is simplified because Rayleigh scattering may be assumed for most precipitation particles.

Precipitation particles will depolarize incident radiation only when they are aspherical and have no axis of symmetry parallel to the incident polarization. If we consider oblate

particles, then the strength of the depolarized signal is dependent upon the ratio of the polarizabilities along their major and minor axes, that is to say, it is a function of the value of ZDR the particles would have if they were aligned. For randomly tumbling particles the value of LDR is given by (Atlas et al, 1953):

$$LDR = (1 - 2\sqrt{ZDR} + ZDR)/(3 + 4\sqrt{ZDR} + 8ZDR) \quad (2)$$

where ZDR is the value the particles would have if they were aligned. Equation (2) is plotted (solid line) in Figure 2. The cross polar isolation of the Chilbolton antenna is so good that LDR levels down to at least -32dB can be measured (dotted line in the Figure). The values of ZDR as a function of axial ratio for oblate spheroids of water, solid ice, graupel and snow are given in Figure 3 of C&I. If randomly tumbling particles are to give a measurable LDR, their value of ZDR (if aligned) must be at least 0.8dB. This suggests that because of its low dielectric constant the depolarization of snow should be very low; for a density of $0.1g\ cm^{-3}$ the axial ratio of tumbling snow would have to be less than 0.15 to be detectable. For tumbling graupel (density 0.5) to give a measurable LDR, an axial ratio of less than 0.73 is required; this may occur occasionally. As soon as these particles become wet, the dielectric constant will rise and the cross-polar return will be much larger. The values of LDR for spheroids with a constant canting angle are also plotted in Figure 2, the two dashed curves are for angles of 5° and 10° randomly distributed about the vertical axis; these values are lower than for the same particles randomly tumbling, and should be applicable to raindrops.

Time Series on 13 July 1988 at 155512 UT
 Ray=20 Gate=30 Az=253.0deg El=2.4deg R=13.5km
 $Z_H=48.37dBZ$ $LDR=-30.67dB$ $r_{HV}=-0.085$ $t_H=9.6msec$

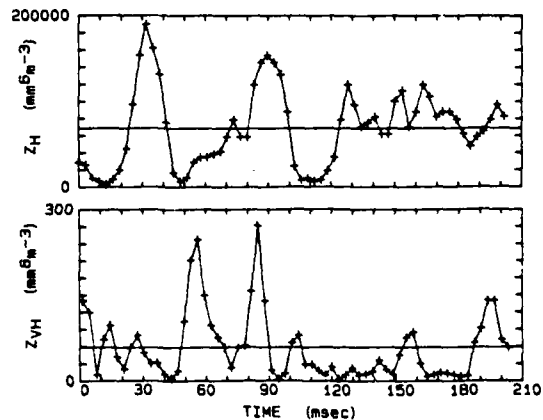


Figure 1. The co- and cross-polar time series in heavy rain

Values of LDR in light rain are limited by the isolation of the antenna to less than -32dB, with some measurements as low as -34dB. When the rain has a ZDR of above 1.5dB it is possible to detect a cross-polar return which tends to increase as ZDR rises. First results indicate that values are consistent (Figure 2) with a constant canting angle of 10° randomly distributed about the vertical axis, or, more realistically, for a Gaussian distribution of such canting angles with a standard deviation of about 5° . Such low canting angles reduce the values of ZDR of the rain by less than 0.1dB (Goddard et al, 1988). These LDR values are significantly lower than the -26 to -29dB reported at 3cm by Herzegh and Conway (1986); the 3cm values could be affected by propagation effects, lower antenna isolation, or non-Rayleigh scattering by the large raindrops.

Values in ice again tend to be at the antenna limit. During 1988 no regions of ice with Z exceeding 40dBZ were sampled, but on some occasions LDR values of -30dB were observed, consistent with tumbling graupel (density 0.5) with an axial ratio of about 0.66, or, more likely, solid ice with an axial ratio of 0.8. Much higher values are to be expected for hail in wet growth (see measurements by Herzegh and Conway, 1986). When hailstones become so large that Mie scattering theory applies, the values of LDR should also rise because, even for axial ratios of 0.9, the differences in the polarizability along the major and minor axes of the hailstone can be a factor of ten (Atlas and Wexler, 1963). By far the most interesting LDR data were obtained for melting ice particles as described below.

3. VERTICAL SECTIONS AND PROFILES

The two colour plates show RHI scans of Z, ZDR and LDR. In Plate 1 we believe the ice particles to be snow, whereas in Plate 2 it is suggested that graupel is present. The data for these two plates are taken at very short range to maximise the power in the cross-polar channel. In Plate 1 the system noise at a 7km range is equivalent to a Z of about -20dBZ and at 14km range to -14dBZ; if there is to be significant power in the cross polar channel for all types of precipitation, then the Z value in the main channel should be at least 15dBZ and 20dBZ at these two ranges, respectively. An additional advantage of operating at short ranges is that at 10km the beamwidth is only 50m. The ZDR and LDR data are not recorded simultaneously, but for sequential scans are separated by about 30secs; comparisons were only made when the Z values had not changed appreciably in this period.

LDR measurements are very sensitive to ground clutter as shown in Plate 1, where the LDR values below 300m are high and very variable from gate to gate. The ground scatters isotropically (Skolnik, 1980) and only a small ground component is required to dominate the cross-polar signal from the precipitation. The ZDR data in Plate 1 are unaffected because the co-polar signals are so much higher; ground clutter is very easy to identify from ZDR (Hall et al, 1984).

In Plate 1 the LDR values in the dry ice and the rain (ZDR up to 1dB) are both at the antenna limit. The most striking feature is the uniformly high values of LDR of about -16dB in the melting

Figure 2. Values of LDR for canted and tumbling oblate spheroids

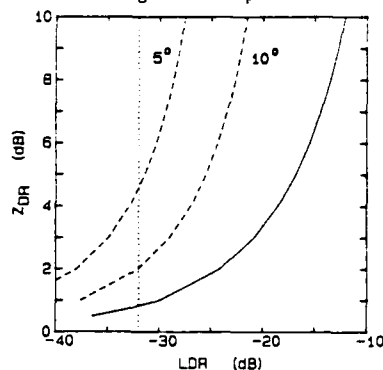
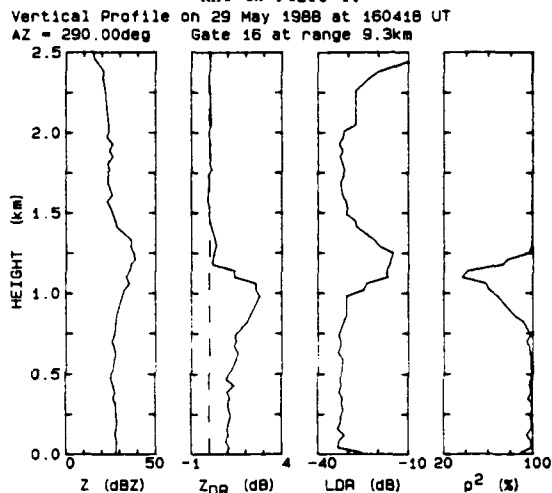


Figure 3. Vertical profiles at 9.3km for the RHI in Plate 1.



layer, which are equivalent to wet tumbling spheroids with an axial ratio of 0.55. Figure 3 depicts a vertical profile of Z, ZDR, LDR and the co-polar correlation $\rho^2(H,V)$ at a range of 9.3km for the data in Plate 1. From this and other profiles we note that the bright band in LDR and Z cover the same constant height range, whereas the bright band in ZDR occurs up to 50m lower, with the larger depressions occurring where Z is greater. The values of correlation are very high in the ice (Figure 5 of C&I is the time series at a height of 1.85km), the slightly lower values in the rain below are probably measurement related and caused by the shorter decorrelation time. The low levels of correlation are found only in the bright band and coincide with the ZDR bright band, at 1.3km LDR and Z are high but ρ^2 is still unity. All these data point to the melting of low density oblate ice:

- An axial ratio of 0.55 is deduced from LDR.
- Z values rise 10dBZ, wetting of solid ice gives only 7dB rise.
- There is a maximum in ZDR - the half melted particles are more oblate than the fully melted spherical raindrops.
- The low correlation indicates the coexistence of very different shapes, such as oblate half melted flakes and raindrops.

We conclude that the particles are snowflakes, but the evidence on the change of fall mode of the flakes as they melt is harder to disentangle. When melting first starts at 1.5km height the flakes are undergoing a predominantly tumbling or spinning motion (see the lab studies of Mitra et al (1988)), although the slight rise in ZDR to 0.3dB implies that there is a small degree of alignment. p^2 is still unity because the particles are the same shape. At about 1.2km, the degree of alignment becomes much greater, as the central pores of the oblate snowflakes start to fill in with water, and the fall mode is stabilised. Over the next 200m some flakes collapse to spherical raindrops, causing a fall in Z , and p^2 falls because we have a variety of oblate and spherical shapes. Subsequently, below 1km all the half-melted flakes collapse to more spherical raindrops, ZDR falls and p^2 rises as the particles once again all have the same shape.

The low values of p^2 in the bright band limit the accuracy of the ZDR measurement. Even though the shorter decorrelation time in the bright band allows us to take 20 independent samples in the 210msec time series, Figure 2 of C&I (from Bringi et al, 1983) shows that if p is 0.6, then the standard deviation of ZDR will be about 1dB. This should be contrasted with the situation in the rain or snow, where, although only ten samples are gathered in a single time series, for $p=0.99$ the ZDR error is only 0.2dB. For the profiles in Figure 3 the values of Z , ZDR and LDR are obtained by spatial averaging over four adjacent 75m range gates; reducing the error in ZDR to 0.1dB and Z to 0.7dBZ.

The second colour Plate shows a very different situation. There is a monotonic increase in ZDR when melting occurs and no maximum is evident, and the LDR maximum on melting is about -26dB with the altitude of this maximum varying by up to 500m. The correlation is high everywhere, with the slight reduction from unity in the rain again being a measurement problem. From the colour plate we note that the LDR is finite in regions of the rain where ZDR is high; this has been interpreted in terms of finite canting angles in the previous section. Some areas of the ice have a finite return also, values of -30dB indicating higher density more oblate particles. Figure 4 is a vertical profile at a range of 13.8km through the rain with the highest ZDR in the Plate, where the rain has a ZDR between 2 and 2.5dB and LDR is about -29dB. There is strong evidence that the ice particles are high density slightly oblate graupel particles:

- (a) An LDR of -26dB implies tumbling wet particles with axial ratio 0.83. Dry ice particles of this shape would not give a detectable LDR even for a density of 0.9.
- (b) ZDR increases monotonically - the oblate graupel particles melt and progressively assume the shape of the equilibrium raindrop, the collapse stage to less oblate raindrops noted in Figure 3 is absent.
- (c) The correlation is high everywhere indicating that there is not a mixture of particles having very different shapes.

After correcting 3cm data for propagation effects, Bringi et al. (1986) derived an LDR of -24 to -26dB for melting graupel.

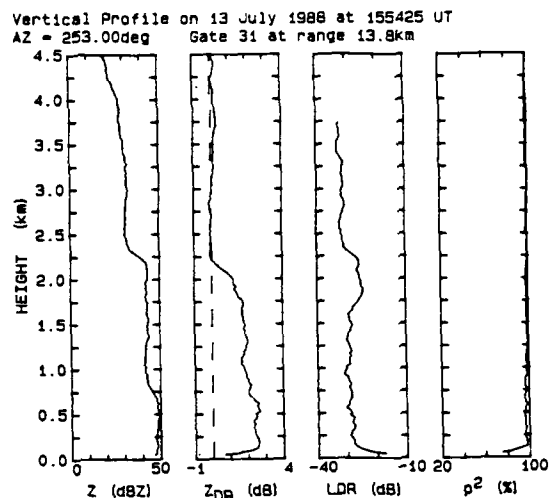


Figure 4. Vertical profiles at 13.8km for the RH1 in Plate 2.

The values of LDR and Z start to rise at 2.4km, and LDR reaches its maximum value after about 200m, where ZDR is still only slightly positive. The profiles are consistent with tumbling graupel particles which stabilise as melting progresses. Another feature, absent in Plate 1, is that the altitude of the LDR bright band varies by up to 500m, with the maximum heights occurring where Z is greatest. The peak values of LDR appear to be independent of altitude. The height at which ZDR starts to increase follows the same pattern. This variation of the altitude of the LDR bright band is difficult to explain. It may be that where Z is greater the temperature of the surface of the graupel is a few degrees higher and so wet growth starts sooner; this could arise if the high Z regions have higher LWC and larger graupel particles.

The different magnitudes of LDR in the bright band should be a reliable indicator of the type of precipitation in the ice above. Although the LDR measurement requires good antenna performance, the very high values of LDR in the bright band should be reasonably easy to detect. The LDR measurement itself can be simpler than ZDR, in that no rapid switching of the polarization of the transmitted power is required, and the two receive channels do not need to be so precisely matched.

We are currently analysing 2D probe data taken from the Met Office C-130 when flying near or just above the melting layer on several days in 1988. On 13 July 1988 the aircraft was struck by lightning while penetrating a region with a Z below 40dBZ. The strike occurred where the LDR bright band indicated a 6km region of graupel embedded in a widespread area having an LDR snow bright band. This is consistent with current ideas on electrification; cloud electrification occurs where graupel and ice crystals exist, and triboelectric charging of the aircraft by collisions with crystals should further enhance the electric field so that a discharge may be triggered by the aircraft. In regions of snow bright band any small ice crystals would tend to be captured by the snowflakes.

4. CROSS CORRELATION AND THE SPECTRA OF THE TIME SERIES.

A typical power spectrum of the two co-polar time series (Fig 5 in C&I) in the snow bright band for the profile in Figure 3 is displayed in Figure 5. Higher frequency components are present in the ZH spectrum than in that for ZV. The value of ZDR was 2.76dB, so ZH is weighted more by the oblate half melted snowflakes while ZV is reflecting more the signal from the raindrops. We suggest that the high frequency fluctuations in ZH are caused by the rapid oscillatory and spinning motion of the melting snowflakes (Mitra et al, 1988) modulating the values of the scattering cross sections; the slower variation in ZV are caused by the changes in phase of the scattered signals as the particles move in space. The same features are present when several time series are averaged together. Ten series and a dwell time of 2.5-seconds are usually needed to obtain reliable spectra; this leads to very slow scan rates for a quarter degree beamwidth antenna.

The values of the correlation between the co-polar and the cross-polar returns ($\rho^2(VH,H)$) are generally not significantly different from zero and do not appear to contain useful information. However when the antenna limit is reached the correlation can rise to 0.3 to 0.5, presumably caused by the signal from the main channel leaking through the antenna into the cross-polar channel. The spectra for the two time series in Figure 1 in heavy rain are plotted in Figure 6. This illustrates the widespread finding that the ZVH spectrum has much higher components than the ZH spectrum, and that the low frequency maximum in the ZH spectrum is absent in the cross-polar spectrum. The ZVH spectrum reflects the rare of oscillations, spinning and tumbling of the particles. The high frequency tail in the ZVH spectrum above 80Hz is probably caused by system noise; for this spectrum the ZH signal to noise ratio was 16dB and that for the cross-polar channel was 25dB.

5. CONCLUSIONS

Based on the work presented in this paper and C&I we suggest:

- Low values of the co-polar correlation can be used for rapid identification of the bright band.
- Low values of the co-polar correlation in vigorous convective clouds could indicate the presence of large hail.
- LDR measurements in rain are consistent with a Gaussian distribution of canting angles with a standard deviation of 5° .
- LDR values in the bright band can be used for distinguishing between snow and graupel.

ACKNOWLEDGEMENTS

This research was supported by NERC Grant GR3/5896 and by AFOSR-86-0121. Our co-workers S M Cherry and J W F Goddard pioneered the implementation and interpretation of the ZDR and LDR data at Chilbolton. IJC acknowledges an ORS scholarship.

Figure 5. Spectra of the co-polar time series in the melting layer.

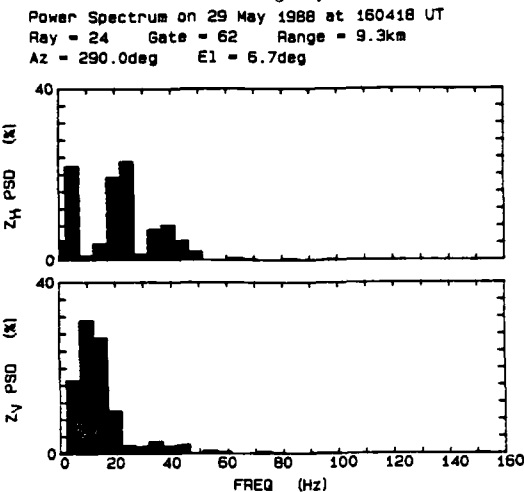
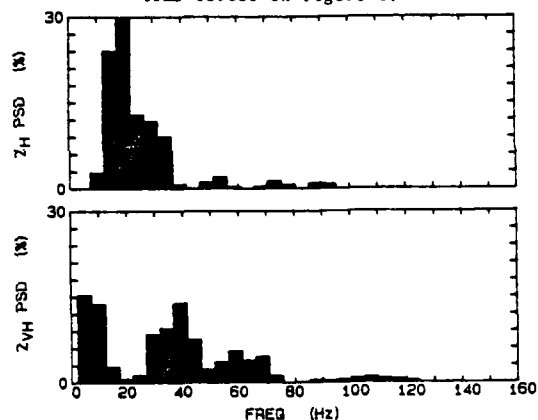


Figure 6. Cross and co-polar spectra for the time series in Figure 1.



REFERENCES

- Atlas D., Kerker M., & Hitchfield W: J Atmos and Terr Phys, 3,108-119. (1953)
Atlas D and Wexler R: J Atmos Sci, 20,48 (1963)
Bringi V N, Selig T A & Cherry S M: IEEE Trans Proc 134 H5, 431-437 (1983)
Bringi V N, Rasmussen R M, Vivekanandan J: J Atmos Sci, 43,2545-63 (1986)
Browne I C, Robinson N P: Nature,170,1078-9(1952)
Caylor I J & Illingworth A J: These Procs (1989)
Goddard J W F, Cherry S M & Holloway K: Proc IGAARS Symp, Edinburgh, ESA SP-284 (1988)
Hall M P M, Goddard J W F & Cherry S M: Radio Sci 19, 132-140 (1984)
Herzogh P H & Conway J W: Proc 23rd Radar Met Conf, Amer Meteorol Soc, Boston, 55-58, (1986)
Herzogh P H & Jameson A R: Proc Xth Int Cloud Phys Conf, Deutscher Wetterdienst, Offenbach-am-Main (1988)
Jameson A R and Dave J H: J Atmos & Ocean Tech, 5,405-415, (1988)
Mitra S K, Vohl O, Pruppacher H R: Proc Xth Int Cloud Phys Conf, Deutscher Wetterdienst, Offenbach am Main (1988)
Skolnik M I: Introduction to radar systems, McGraw-Hill (1980)

Figure 1. RHI on 29 May 1988 indicating the presence of aggregates or snowflakes.

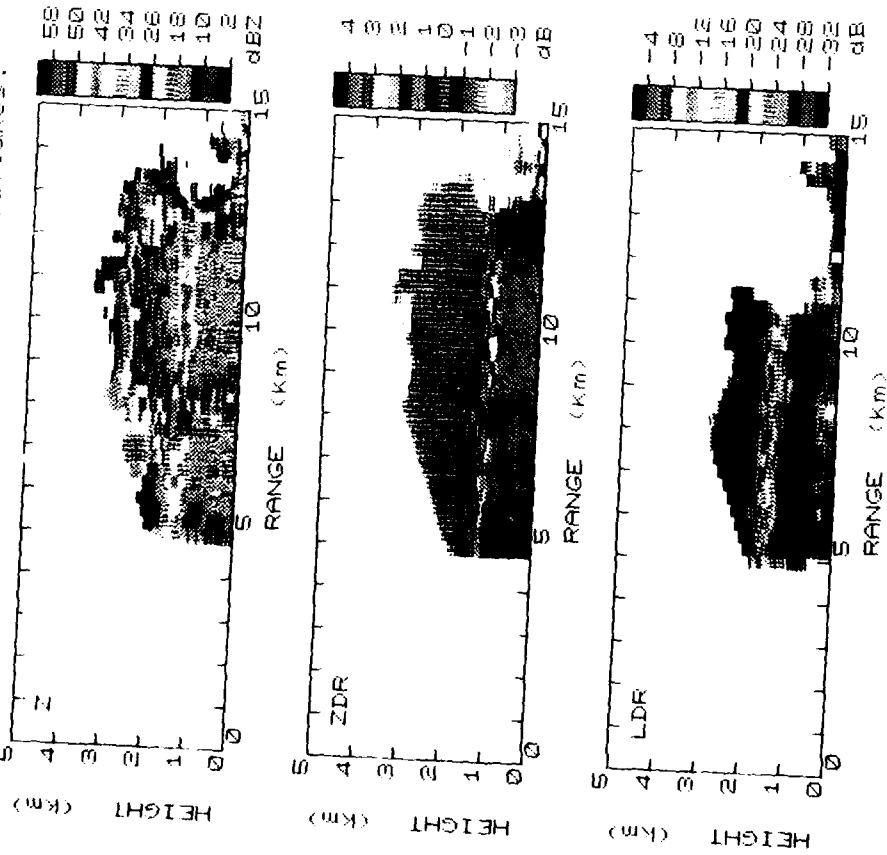
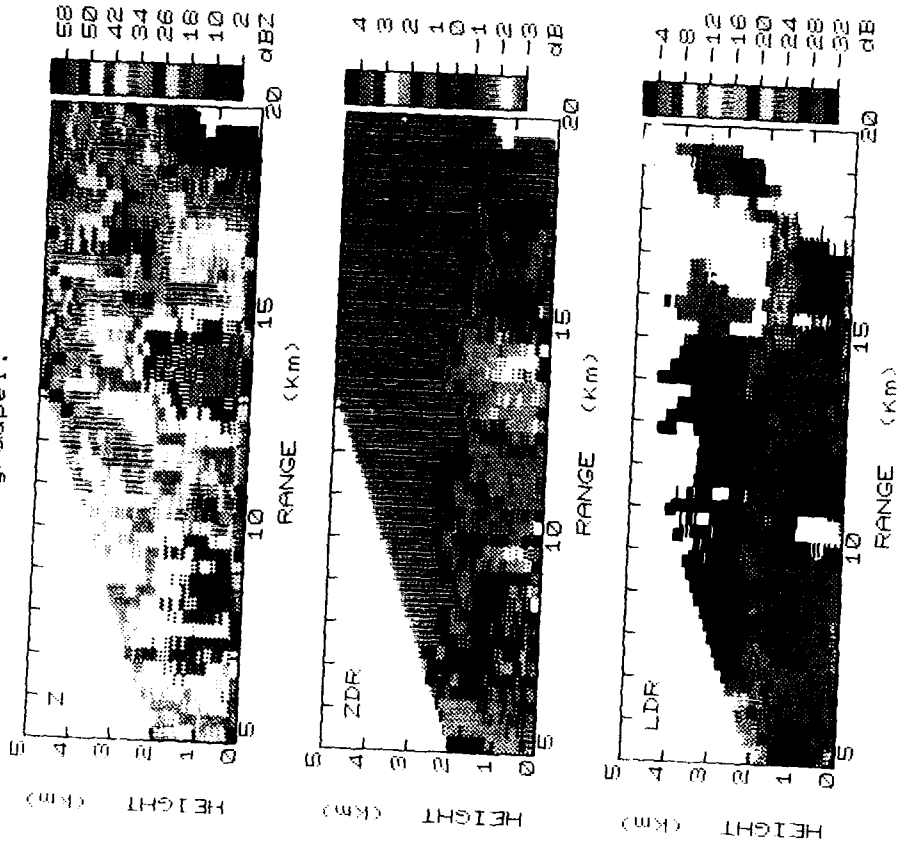


Figure 2. RHI on 13 July 1988 indicating the presence of graupel.



Part 8

S E Hopper, A J Illingworth and I J Caylor

'Bright band errors in rainfall measurement: identification and correction using linearly polarised radar returns'

Int Symp on Hydrol Appl of Weather Radar, Salford, UK 1989.

BRIGHT BAND ERRORS IN RAINFALL MEASUREMENT: IDENTIFICATION
AND CORRECTION USING LINEARLY POLARIZED RADAR RETURNS

S E Hopper, A J Illingworth and I J Caylor
Dept of Physics, UMIST, Manchester, M60 1QD, UK

ABSTRACT

A principle source of error in rainfall rates derived from the radar reflectivity (Z) is caused by the enhanced radar return due to melting snowflakes in the bright band. We present observations made by the narrow beamwidth S-band Chilbolton radar which involve transmission of horizontally and vertically polarized radiation and reception of the co-polar and cross-polar return signals. The linear depolarization ratio (LDR) is defined as the ratio of the cross-polar to the co-polar return. The high values of Z in the bright band are accompanied by values of LDR above -18dB; in echoes where no bright band is present the values of LDR are everywhere below -20dB.

1. INTRODUCTION

The conventional radar reflectivity, Z , is proportional to ND^6 , where N is the concentration of particles of diameter D , summed over all sizes. Z is usually expressed in units relative to the signal from a 1mm raindrop per cubic meter, even though from Z alone it is not possible to distinguish rain from ice and the reflectivity of a raindrop is about 7dB higher than the equivalent mass of ice. Neither can Z be used to differentiate between the various forms of frozen hydrometeors (snow, hail, hailstones etc), or to measure the sizes and concentrations of raindrops. Z is usually converted into a rain rate, R , using an empirical relation of the form:

$$Z = 284 R^{1.47} \quad (1)$$

which, for a given R , is equivalent to assuming a constant size distribution of raindrops. Some of the problems in estimating rainfall using Equation 1 are demonstrated in Figure 1, which is a vertical section of Z through stratiform rainfall observed by the quarter degree beamwidth Chilbolton radar.

The most notable feature in Figure 1 is the layer of enhanced reflectivity or 'bright band' at about 1.1km altitude. At a range of 45km the value of Z reaches 43dBZ leading (via Equation 1) to an estimated rain rate of about 18mm/hr. Values below 150m are affected by obscuration of the radar beam, but from 200m to 800m, in the rain, the value of Z is only 28dBZ, equivalent to a rainfall rate of only 1.7 mm/hr. The bright band leads to an overestimate of R by a factor of ten.

The enhanced return in the bright band is caused by large, low density wet snowflakes which reflect microwaves as if they were giant raindrops. Dry snowflakes have a lower return because of their low dielectric constant; below the bright band Z falls due to two factors; when the snowflakes melt completely they collapse to smaller raindrops and, secondly, the raindrop concentration falls as the terminal velocity increases.

Other problems are evident from Figure 1. The Z values at altitudes greater than 2.5km are lower than in the rain, much of the growth and

RHI SCAN ON 13/01/88 AT 014216 UT
TAPE 5113 RASTER 204 SCAN 3 AZ 260.00deg

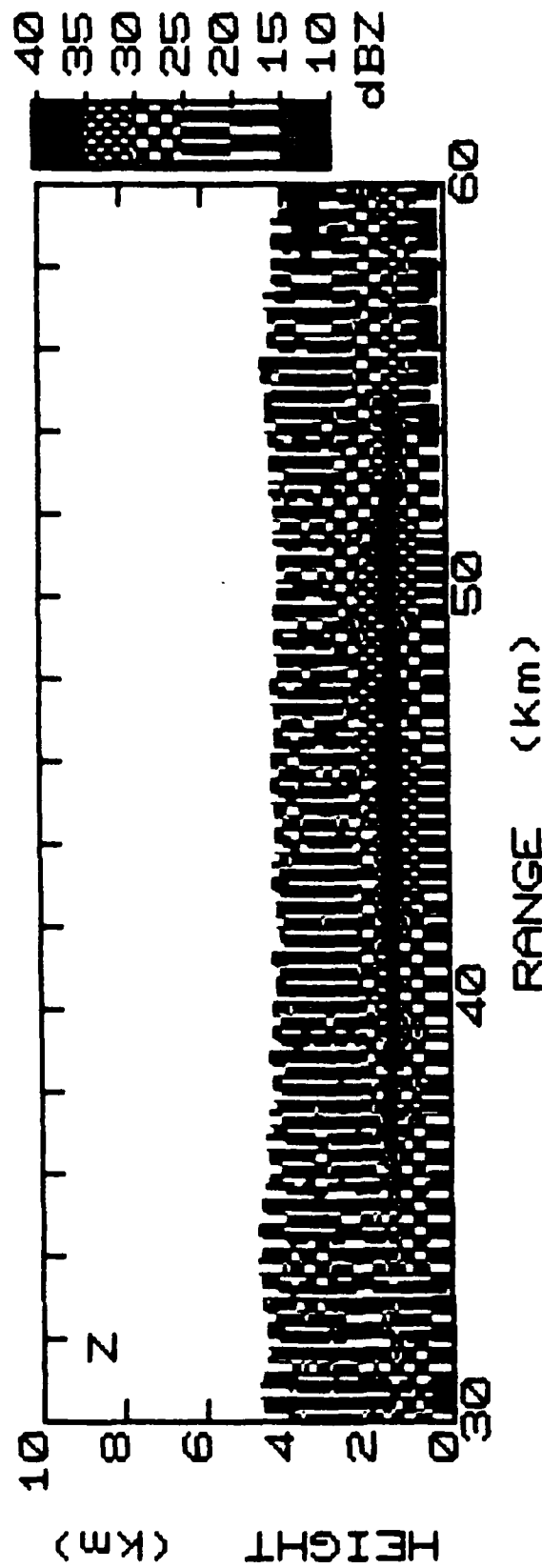


Figure 1. An example of the structure of the radar reflectivity (Z) for stratiform precipitation with a well defined bright band.

aggregation of the ice occurring at lower levels. Consequently, the higher elevation scans of a one degree beamwidth radar will underestimate rainfall at larger distances (1), while sampling of the rain alone with the lower elevation scans without ground clutter and /or obscuration is difficult, because, in the UK, the melting layer is usually below 2km.

Ground based rain gauges can provide localised real-time information for correcting bright band errors (2). Most radar networks scan in PPI mode to obtain a complete spatial coverage, and in truly stratiform rain the bright band should be recognisable as a concentric ring of enhanced reflectivity centred on the radar. Smith (3) has suggested an automatic means of identifying the bright band by comparing the range of the maximum values of Z at a particular azimuth for two different beam elevations. However, in practice the height of the bright band can change, the precipitation is never stratiform and, in the UK at least, quite vigorous showers often have bright bands. In this paper we demonstrate a means of uniquely identifying the bright band by analyzing the cross-polar radar return.

2. THE CHILBOLTON POLARIZATION RADAR

The Chilbolton radar operates at S-band (10cm) and, with a 25m dish, is the largest steerable meteorological radar in the world, having a beamwidth of only a quarter of a degree. Earlier reports (4,5,6) have considered the implementation and interpretation of differential reflectivity (ZDR), we now analyze observations made in 1988 of a new parameter, the linear depolarization ratio (LDR).

The differential reflectivity (ZDR) provides an estimate of mean hydrometeor shape. It is defined as

$$ZDR = 10 \log(ZH/ZV) \quad (2)$$

where ZH and ZV are the radar reflectivities measured at horizontal and vertical polarizations respectively. For small raindrops or tumbling ice particles, ZH and ZV are equal and ZDR is zero. The theoretical values of ZDR for oblate particles with their minor axes aligned in the vertical are plotted in Figure 2; ZDR increases with greater oblateness and higher dielectric constant. In heavier rain ZDR is positive and reflects the mean shape (and hence the size) of the raindrops. The ZDR of ice is more complex (6). Because of the low dielectric constant, dry snowflakes have a ZDR close to zero, but wet snowflakes can have high positive values. Graupel tends to tumble and so be associated with a zero ZDR value.

The linear depolarization ratio, LDR, is a measure of the hydrometeor fall mode and appears to be an excellent indicator of wet ice. It is defined as

$$LDR = 10 \log(ZVH/ZH) \quad (3)$$

where ZVH is the (horizontal) cross-polar return from a vertically polarised transmitted pulse, and ZH (as in Equation 2) is the co-polar (horizontal) return for horizontally polarized transmission. A cross polar return occurs only when oblate hydrometeors fall with their major or minor axis at an angle to the vertical. Computations of LDR for tumbling oblate spheroids (Figure 3) and are consistent with the Chilbolton observations (7). Snowflakes have such a low dielectric constant that even if they are very oblate their LDR is below the antenna limit of -32dB, oblate dry hail or graupel could have a value up to -20dB if the axial ratio were as low as 0.5, but LDR values above -20dB can only realistically occur for wet tumbling ice particles. Such high values are restricted to the bright band. Raindrops give rise to a very low cross-polar return.

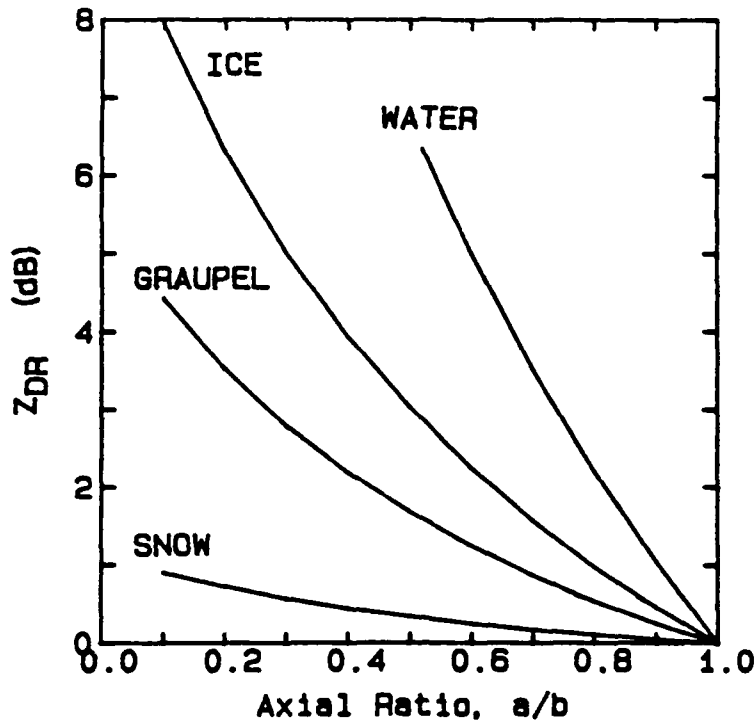


Figure 2. ZDR values as a function of axial ratio for various precipitation particles, assuming the major axis is horizontal.

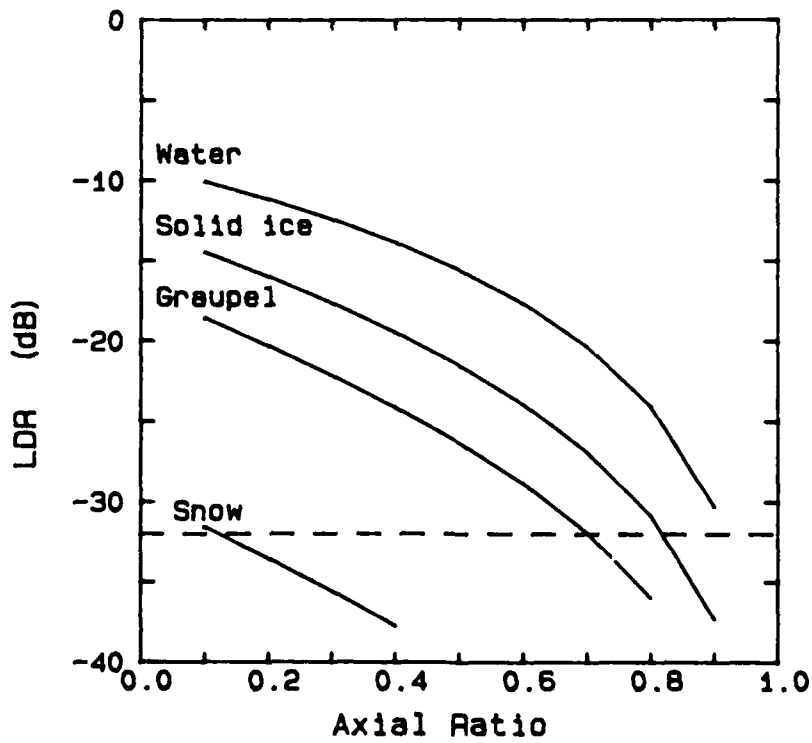


Figure 3. LDR values for randomly tumbling particles as a function of axial ratio.

3. COMPARISON OF ECHOES WITH AND WITHOUT BRIGHT-BANDS

An RHI through widespread stratiform precipitation is displayed in Figure 4, where the reflectivity does not exceed 30dBZ in the rain but reaches 40dBZ at 2km altitude in the bright band. At this height the oblate melting snowflakes give a clearly visible bright band in ZDR with values reaching 2dB. However automatic recognition of the ZDR bright band can be difficult. ZDR values in the rain at 10-20km range reach 0.5dB, and in heavier rain can be much higher. We also note in Figure 4 the positive ZDR values above 3km altitude; this low Z region presumably containing aligned high density ice crystals.

It is much easier to identify the Z bright band from the LDR data. The maximum values of Z coincide with the peak LDR of about -15dB, which is consistent with wet tumbling snowflakes having an axial ratio of about 0.5 (Figure 3). In contrast LDR values in the rain are near the antenna limit of -32dB, and reach about -27dB in the low Z ice region above 3km where the ZDR indicated high density crystals. Figure 4 also shows that ground clutter results in LDR values above -10dB near to the ground. Because LDR involves measuring the low-power cross-polar return it is much more susceptible to ground clutter than is Z or ZDR.

Figure 5 illustrates an example of a heavy shower with a horizontal extent of about 25km. The Z values in the rain are higher than in Figure 4, but the enhancement of Z in the bright band is over 10dB. Again the presence of the bright band can be most easily identified by the values of LDR which exceed -16dB.

A vigorous shower with no bright band is depicted in Figure 6 and it is clear that the polarization parameters have a quite different character: the LDR values are much lower than for the bright band case in Figures 4 and 5. We believe that the data in Figure 6 indicate the presence of graupel. The dry tumbling graupel gives negligible LDR, but melting occurs at about 2km altitude and LDR rises to about -25dB. This weak "LDR graupel bright band" is consistent (Figure 3) with tumbling wet ice with an axial ratio of 0.8. In the heavy rain the LDR is just detectable and is explicable in terms of a canting angle of about 5 degrees. Values of ZDR are low for the tumbling dry ice, but rise monotonically as the graupel melts and assumes the equilibrium shape of the large raindrops. This vertical profile in ZDR should be contrasted with the bright band case in Figures 4 and 5, where a maximum in ZDR is caused by the low density oblate wet snowflakes, which subsequently, on complete melting, collapse to more spherical raindrops.

It should be emphasised that, in the UK at least, the presence of a bright band is not restricted to stratiform clouds with low Z. In some showers Z values can reach 50dBZ in the bright band, while others, with no bright band, have lower peak values of Z.

4. LDR STATISTICS

In order to test our hypothesis that the peak value of LDR in a vertical profile is related to the increased reflectivity in the bright band, the results from scans on 11 different days in 1988 are summarised in Figure 7. The altitude of the maximum value in LDR (which is found in all types of cloud) is used to fix the melting level. The enhancement of Z (ΔZ) is then estimated by comparing the Z at the melting level with the Z in the

RHI SCAN ON 29/11/88 AT 120130 UT
TAPE 5148 RASTER 58 SCAN 1 AZ 285.00deg

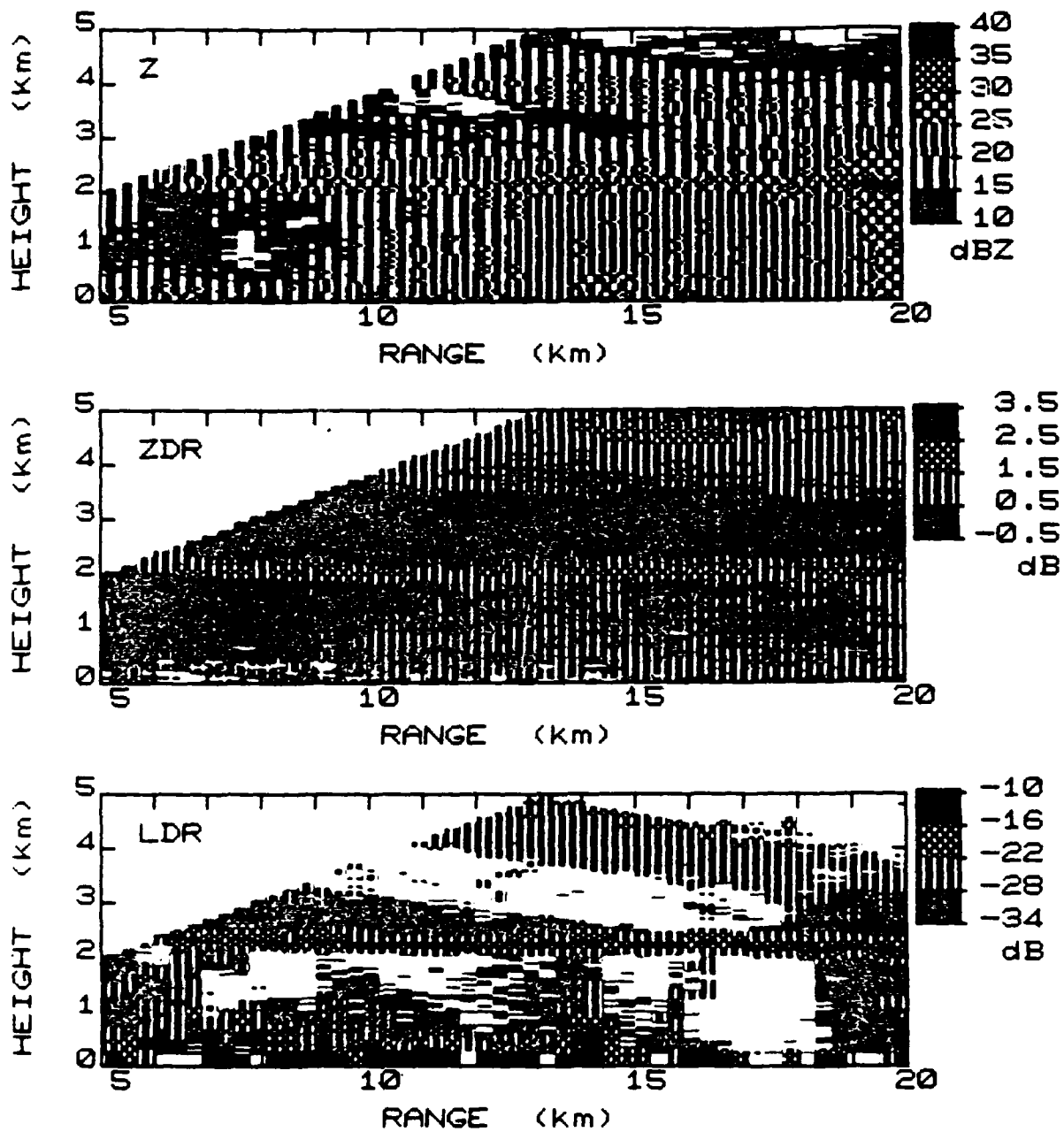


Figure 4. A typical RHI scan through stratiform cloud on 29 November 1988 with a bright band for Z, ZDR and LDR.

RHI SCAN ON 29/05/88 AT 155541 UT
TAPE 7150 RASTER 52 SCAN 2 AZ 255.00deg

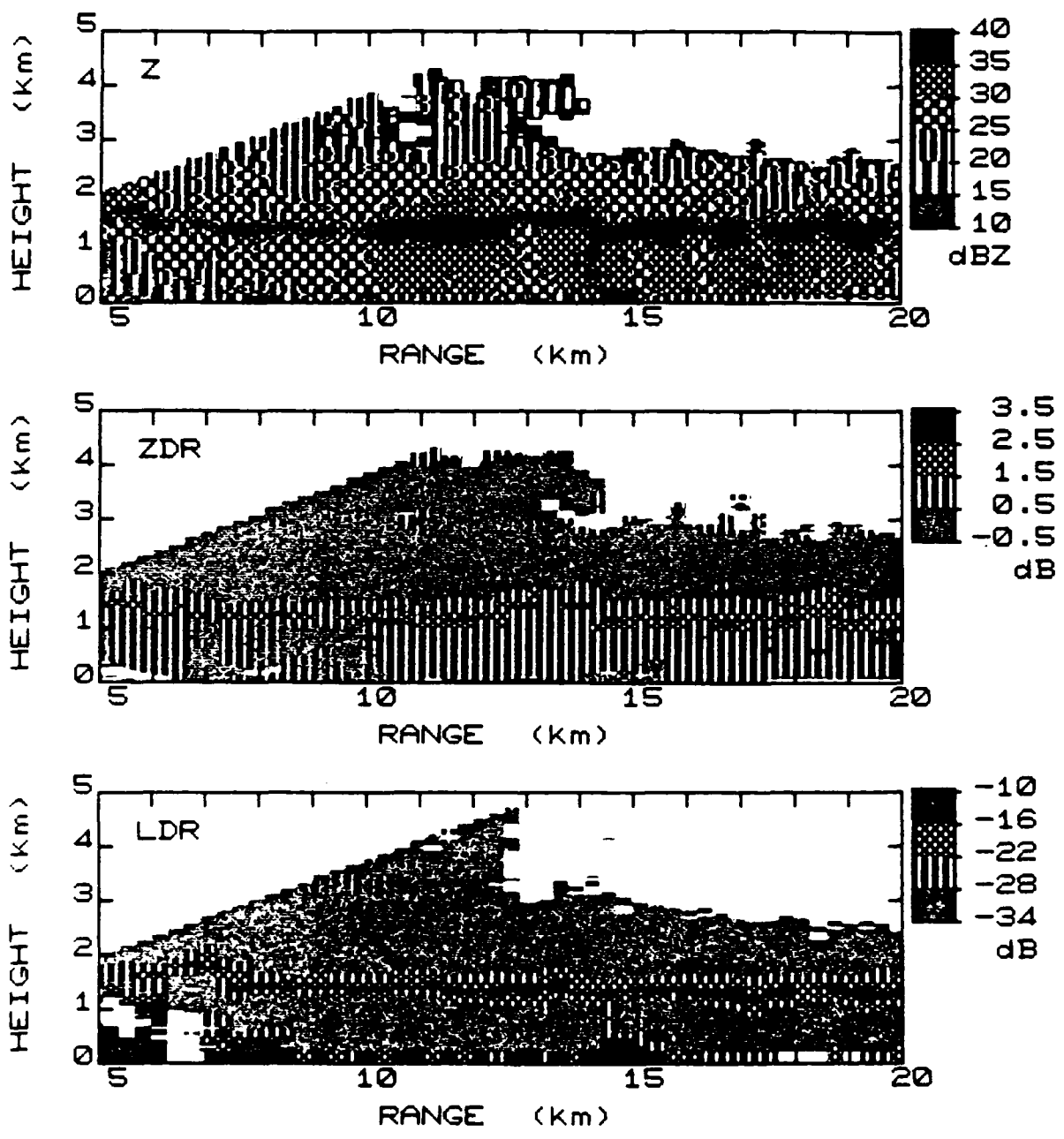


Figure 5. An RHI scan of Z, ZDR and LDR through a vigorous shower with a bright band. 29 May 1988.

RHI SCAN ON 13/07/88 AT 155423 UT
TAPE S131 RASTER 22 SCAN 1 AZ 253.00deg

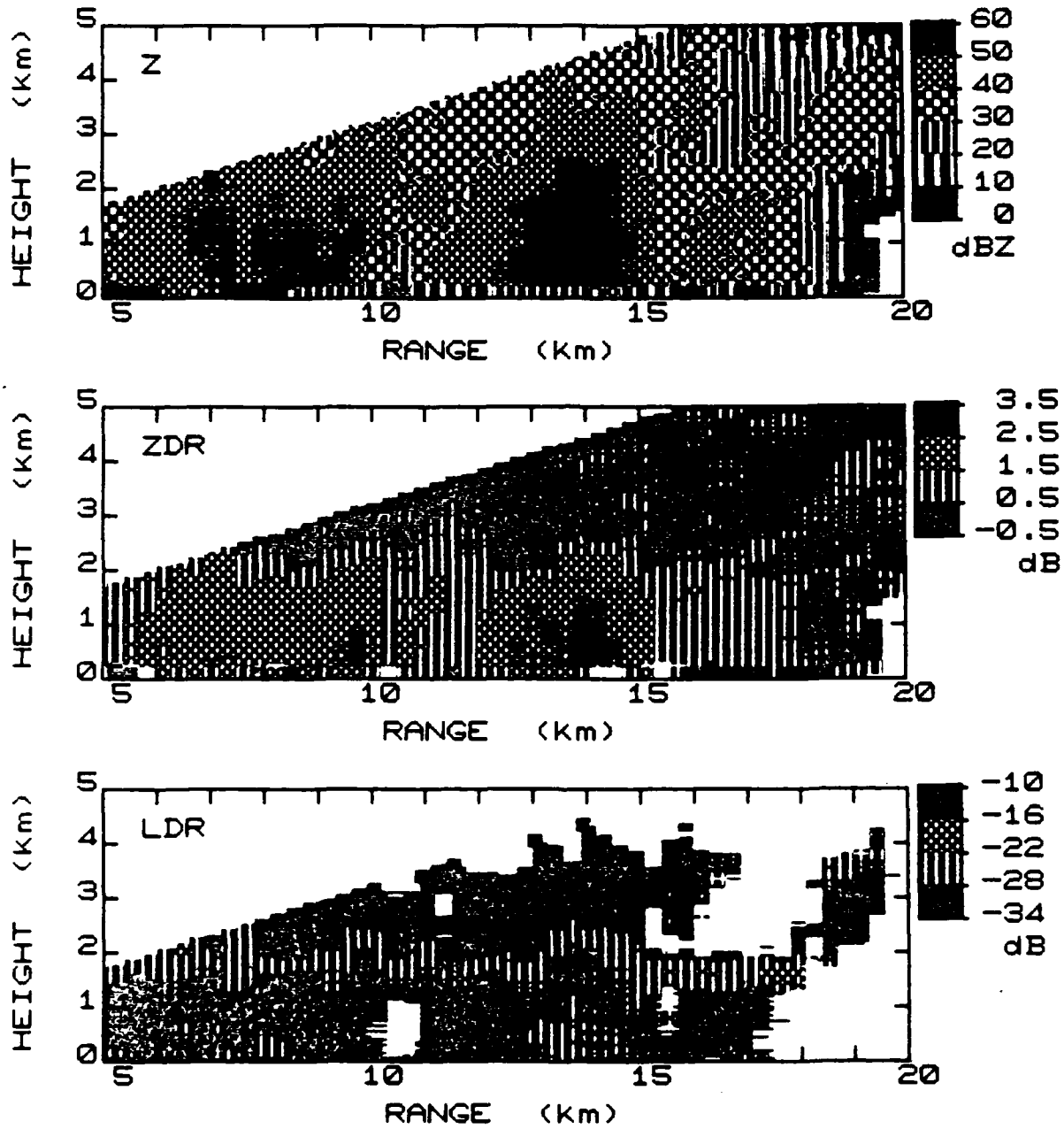


Figure 6. A typical RHI scan through a convective cloud on 13 July 1988 with no bright band for Z, ZDR and LDR.

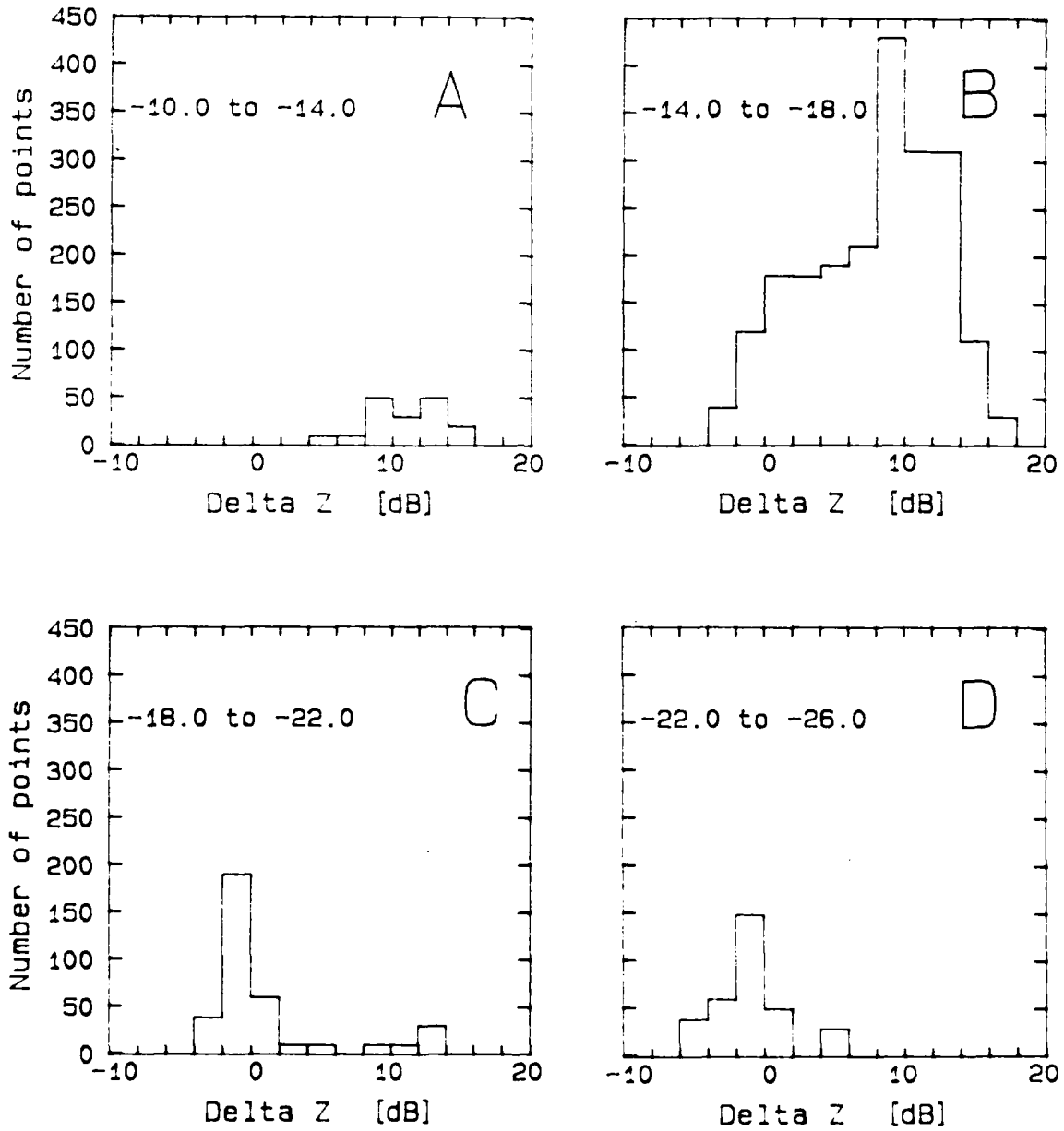


Figure 7. Histograms of the enhancement of the reflectivity in the bright band (ΔZ) as a function of LDR in the bright band.

rain 500m below. Histograms of the enhancement of the reflectivity in the bright band are plotted for each 4dB increment in LDR. For most vertical profiles the peak LDR values are in the range -14 to -18dB and in these cases the enhancement of Z is, on average, about 10dB. Less common, in this UK sample, are the peak values of LDR in the range -18 to -22dB and -22 to -26dB where the Z enhancement is essentially zero and no bright band is present.

It should be stressed that in 1988 there were no observed cases of deep vigorous convection. Measurements of LDR at 3cm (8) suggest that hail in wet growth can give high LDR values, although the measurements at this wavelength are affected by propagation problems. For the observations discussed in this paper the depth of the bright band is greater than the beamwidth of the Chilbolton radar. In future we will analyze the effect on the LDR measurements for a one degree beamwidth radar which is only partially filled by the bright band.

5. DISCUSSION AND CONCLUSION

Several factors need to be considered if the LDR technique is to be implemented on conventional C-band radars. The LDR measurement has the advantage that no fast switching of the transmitted signal is needed. However, the cross-polar signal power is very low, and a signal to noise ratio of more than 20dB is required if an LDR of down to -20dB is to be detected. We also note that the low power cross-polar signal is much more sensitive than Z and ZDR to ground clutter contamination. Finally, and most importantly, the LDR signal is affected by propagation and attenuation problems at shorter wavelengths. Correction algorithms may be possible at C-band.

These observations suggest that high values of the linear depolarization ratio are associated with the presence of melting snowflakes and can be used to identify the bright band. This parameter may also be of use in identifying anomalous propagation and ground clutter, both of which should have high values of LDR.

ACKNOWLEDGEMENTS

This work was supported by AFOSR 89-0121, NERC GR3/5896 and the Meteorological Office. We also thank John Goddard of RAL who implemented the LDR parameter on the Chilbolton radar.

REFERENCES

- (1) Joss J and Waldvogel A (1989) Preprints 24th Radar Meteorol Conf, Amer Meteor Soc, Boston, 682-688.
- (2) Smith C J (1986) J Atmos Ocean Tech, 3, 129-141.
- (3) Collier C G (1986) J Hydrol, 83, 207-223.
- (4) Cherry S M and Goddard J W F (1982) URSI Symposium on Multiple Parameter Radar Measurement of Precipitation, Bourne, UK.
- (5) Hall M P M, Goddard J W F, and Cherry S M (1984) Radio Sci, 19, 132-140.
- (6) Illingworth A J, Goddard J W F and Cherry S M (1987) Q J Roy Meteorol Soc, 113, 469-489.
- (7) Illingworth A J and Caylor I J (1989) Preprints 24th Radar Meteorol Conf, Amer Meteor Soc, Boston, 323-327.
- (8) Herzegh P H and Jameson A R (1989) Preprints 24th Radar Meteorol Conf, Amer Meteor Soc, Boston, 315-317.

Part 9

I J Caylor, J W F Goddard, S E Hopper and A J Illingworth

'Bright band errors in radar estimates of rainfall:
identification and correction using polarization diversity'

1989 COST-73 Int Semin on Weather Radar Networking, Brussels.

BRIGHT BAND ERRORS IN RADAR ESTIMATES OF RAINFALL:
IDENTIFICATION AND CORRECTION USING POLARIZATION DIVERSITY

I J Caylor, J W F Goddard[†], S E Hopper, and A J Illingworth
Dept of Physics, UMIST, Manchester, M60 1QC, UK
[†]RAL, Chilton, Didcot, OXON, OX11 0QX, UK

Summary

A principle source of error in rainfall rates derived from the radar reflectivity (Z) is caused by the enhanced radar return due to melting snowflakes in the bright band. We present observations of two S-band polarization radar parameters which enable the bright band to be simply identified. The technique involves transmission of horizontally and vertically polarized radiation and reception of the co-polar and cross-polar return signals. The linear depolarization ratio (LDR) is defined as the ratio of the cross-polar to the co-polar return and $p(H,V)$ as the correlation of the time series of the horizontal and vertical co-polar return. The high values of Z in the bright band are accompanied by values of LDR above -18dB and $p(H,V)$ below 0.8. In echoes where no bright band is present the values of LDR are everywhere below -20dB and the correlation is always close to unity. We discuss potential problems in implementing these techniques for C-band radars with one degree beamwidths, and also consider how they could be used to identify spurious echoes from ground clutter and anomalous propagation.

1. INTRODUCTION

A major source of error in deriving the rainfall rate (R) from the radar reflectivity (Z) arises from the enhanced radar return occurring in the melting layer or 'bright band'. The value of Z typically increases by 10dB when low density snowflakes become wet and scatter microwaves as if they were giant raindrops. This error in Z in an empirical Z - R relationship would lead to a fivefold overestimate of the rainfall.

Most radar networks scan in PPI mode to obtain a complete spatial coverage, and in truly stratiform rain the bright band should be recognisable as a concentric ring of enhanced reflectivity centred on the radar. Smith (1) has suggested an automatic means of identifying the bright band by comparing the range of the maximum values of Z at a particular azimuth for two different beam elevations. However, in practice the height of the bright band can change, the precipitation is never stratiform and, in the UK at least, quite vigorous showers often have bright bands. Ground based rain gauges can provide localised real-time information for correcting bright band errors (2). In this paper we demonstrate a means of uniquely identifying the bright band using two new polarization parameters. We shall also consider how such techniques could be implemented on C-band radars with smaller antennas.

2. THE CHILBOLTON POLARIZATION RADAR

The Chilbolton radar operates at S-band and, with a 25m dish, is the largest steerable meteorological radar in the world, having a beamwidth of only a quarter of a degree. Earlier reports (3,4,5) have considered the implementation and interpretation of differential reflectivity (ZDR), but here we discuss observations made in 1988 of two new parameters (LDR and $p(H;V)$) which are described below.

2.1 DIFFERENTIAL REFLECTIVITY

The differential reflectivity (ZDR) provides an estimate of mean hydrometeor shape. It is defined as

$$ZDR = 10 \log(ZH/ZV) \quad (1)$$

where ZH and ZV are the radar reflectivities measured at horizontal and vertical polarizations respectively. For small raindrops or tumbling ice particles, ZH and ZV are equal and ZDR is zero. Positive values of ZDR occur for oblate particles of high dielectric constant when ZH exceeds ZV. In heavier rain ZDR is positive and reflects the mean shape (and hence the size) of the raindrops. The ZDR of ice is more complex (5). Because of the low dielectric constant, dry snowflakes have a ZDR close to zero, but wet snowflakes can have high positive values. Graupel tends to tumble and so be associated with a zero value.

2.2 LINEAR DEPOLARIZATION RATIO

The linear depolarization ratio, LDR, is a measure of the hydrometeor fall mode and appears to be an excellent indicator of wet ice. LDR is defined as:

$$LDR = 10 \log(ZVH/ZH) \quad (2)$$

where ZVH is the (horizontal) cross-polar return from a vertically polarised transmitted pulse, and ZH (as in Equation 1) is the co-polar (horizontal) return for horizontally polarised transmission.

A cross polar return occurs only when oblate hydrometeors fall with their major or minor axis at an angle to the vertical. Computations of LDR for tumbling oblate spheroids are plotted in Figure 1 and are found to be consistent with the Chilbolton observations (6). Snowflakes have such a low dielectric constant that even if they are very oblate their LDR is below the antenna limit of -32dB, oblate dry hail or graupel could have a value up to -20dB if the axial ratio were as low as 0.5, but LDR values above -20dB can only realistically occur for wet tumbling ice particles. Such high values are restricted to the bright band. Raindrops give rise to a very low cross-polar return.

2.3 CO-POLAR CROSS CORRELATION

The estimates of ZH and ZV in equation (1) are made from the true linear average (over 210msec) of the return at one 75m gate from 64 successive pulse pairs transmitted with alternate horizontal and vertical polarization. The standard error in ZDR is reduced to 0.1dB by spatial averaging over four adjacent 75m gates. The co-polar cross correlation ($p(H;V)$) is the correlation of these two time series in ZH and ZV.

Observations (7) show that the correlation is generally close to unity in rain and dry ice, with low values being confined to the bright band. Low values of correlation are thought to indicate that a variety of hydrometeor shapes is present. We believe that the low values in the bright

band are caused by the coexistence of oblate half-melted snowflakes with nearly spherical raindrops.

3. COMPARISON OF ECHOES WITH AND WITHOUT BRIGHT-BANDS

An RHI through stratiform precipitation is displayed in Figure 2; where the reflectivity does not exceed 30dBZ in the rain but reaches 40dBZ at 2km altitude in the bright band. At this height the oblate melting snowflakes give a clearly visible bright band in ZDR with values reaching 2dB. However automatic recognition of the ZDR bright band can be difficult. ZDR values in the rain at 10-20km range reach 0.5dB, and in heavier rain can be much higher. We also note in Figure 2 the positive ZDR values above 3km altitude; this low Z region presumably containing aligned high density ice crystals.

It is much easier to identify the Z bright band from the LDR data. The maximum values of Z coincide with the peak LDR of about -15dB, which is consistent with wet tumbling snowflakes having an axial ratio of about 0.5 (Figure 1). In contrast LDR values in the rain are near the antenna limit of -32dB, and reach about -27dB in the low Z ice region above 3km where the ZDR indicated high density crystals. Figure 2 also shows that ground clutter results in LDR values above -10dB near to the ground. Because LDR involves measuring the low-power cross-polar return it is much more susceptible to ground clutter than is Z or ZDR. The bright band can also be identified via the correlation parameter. Although data is limited to a 5km range window values of correlation below 90% are restricted to the bright band.

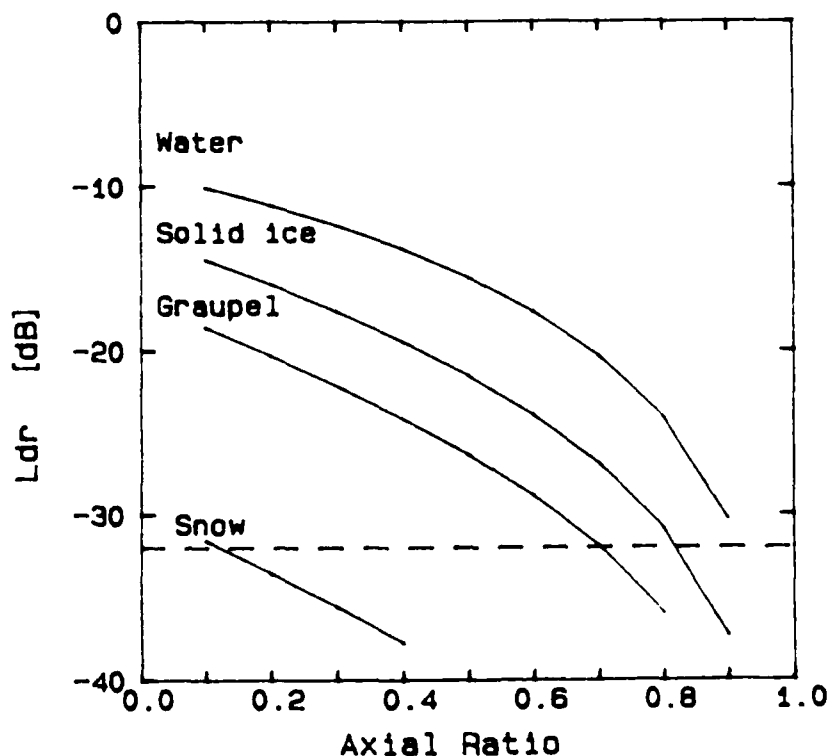


Figure 1. LDR values for randomly tumbling particles as a function of axial ratio.

RHI SCAN ON 29/11/88 AT 120130 UT
 TAPE 5148 RASTER 58 SCAN 1 AZ 285.00deg

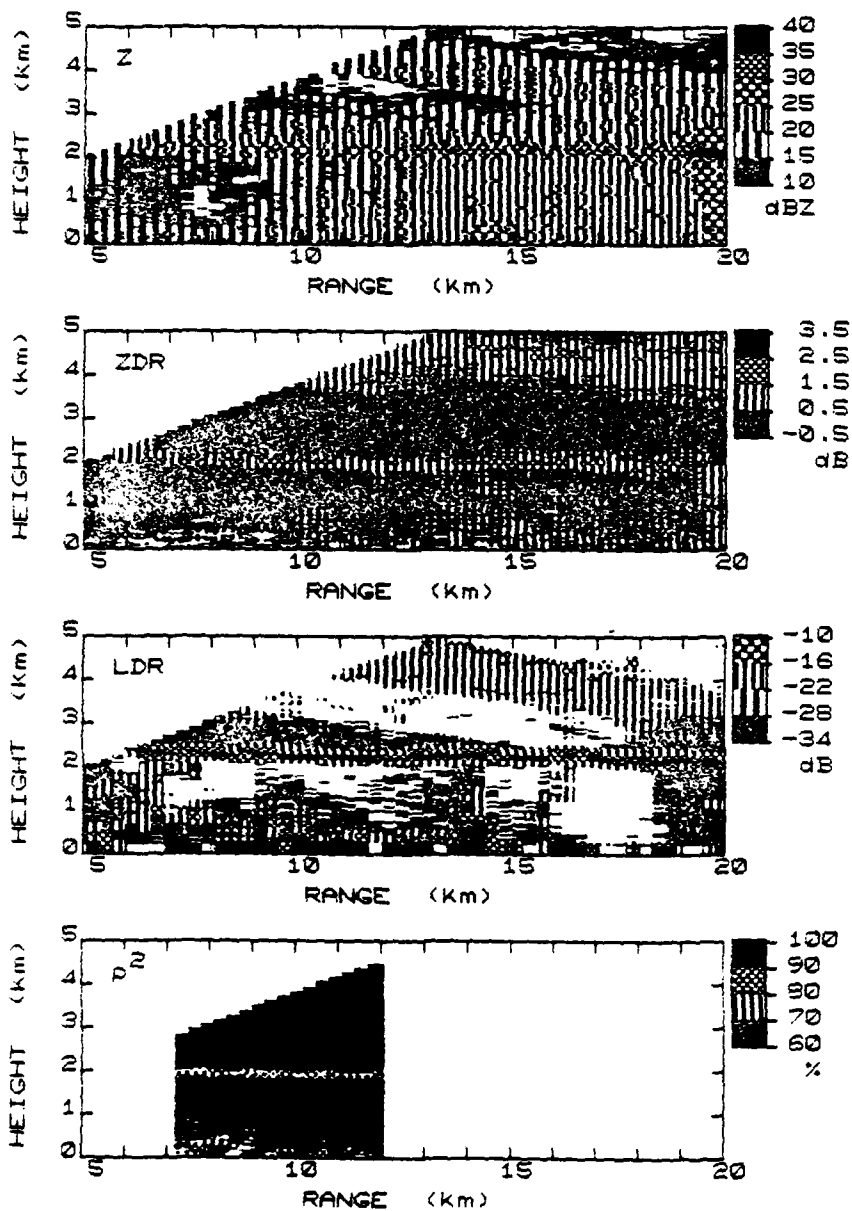


Figure 2. A typical RHI scan through stratiform cloud on 29 November 1988 with a bright band for Z, ZDR, LDR, and p(H,V).

A vigorous shower with no bright band is depicted in Figure 3 and it is clear that the polarization parameters have a quite different character: the correlation is high everywhere while the LDR values are much lower than for the bright band case in Figure 2. The different vertical profiles through these two clouds are plotted in Figures 4 and 5. We believe that the vigorous shower with no bright band in Figures 3 and 5 contains graupel. The dry tumbling graupel gives negligible LDR, but melting occurs at about 2km altitude and LDR rises to about -25dB. This weak "LDR graupel bright band" is consistent (Figure 1) with tumbling wet ice with an axial ratio of 0.8. In the heavy rain the LDR is just detectable and is explicable in terms of a canting angle of about 5 degrees. Values of ZDR are low for the tumbling dry ice, but rise monotonically as the graupel melts and assumes the equilibrium shape of the large raindrops. These profiles should be contrasted with the bright band case in Figure 4, where a maximum in ZDR is caused by the low density wet snowflakes. In the graupel case the correlation is everywhere above 90% as there is no great variety of shapes present.

Figures 6 and 7 display how the value of LDR is related to the enhanced value of Z in the bright band. The altitude of the maximum value in LDR (which is present in all types of cloud) is used to fix the melting level. The enhancement of Z (ΔZ) is then estimated by comparing the Z at the melting level with the Z in the rain 500m below. In Figure 6, for the bright band case in Figures 2 and 4, the ΔZ enhancement in the bright band for ranges out to 60km is about 10dB, and is accompanied by an LDR value of about -15dB. In Figure 7 these parameters are plotted for both the graupel cloud in Figures 3 and 5 at a range of 10-20km, and for a second shower beyond 40km which does have a bright band. In the graupel clouds the mean ΔZ enhancement is close to zero and LDR values are in the range -20 to -25dB, while for the more distant cloud the bright band increase in Z of about 10dB is associated with higher LDR values of -15dB.

It should be emphasised that, in the UK at least, the presence of a bright band is not restricted to stratiform clouds with low Z. In some showers Z values can reach 50dBZ in the bright band, while others, with no bright band, have lower peak values of Z.

4. LDR STATISTICS

In order to test our hypothesis that the value of LDR is related to the increased reflectivity in the bright band, the results from scans on 11 different days in 1988 are summarised in Figure 8. Histograms of the enhancement of the reflectivity in the bright band are plotted for each 4dB increment in LDR. For most vertical profiles the peak LDR values are in the range -14 to -18dB and in these cases the enhancement of Z is, on average, about 10dB. Less common, in this UK sample, are the peak values of LDR in the range -18 to -22dB and -22 to -26dB where the Z enhancement is essentially zero and no bright band is present.

It should be stressed that in 1988 there were no cases of very deep vigorous convection. Measurements of LDR at 3cm (8) suggest that hail in wet growth can give high LDR values, although the measurements at this wavelength are affected by propagation problems. We hope to examine such cases in the future. For the observations discussed in this paper the depth of the bright band is greater than the beamwidth of the Chilbolton radar. In future we will analyze the effect on LDR and correlation

RHI SCAN ON 13/07/88 AT 155423 UT
TAPE 5131 RASTER 22 SCAN 1 AZ 253.00deg

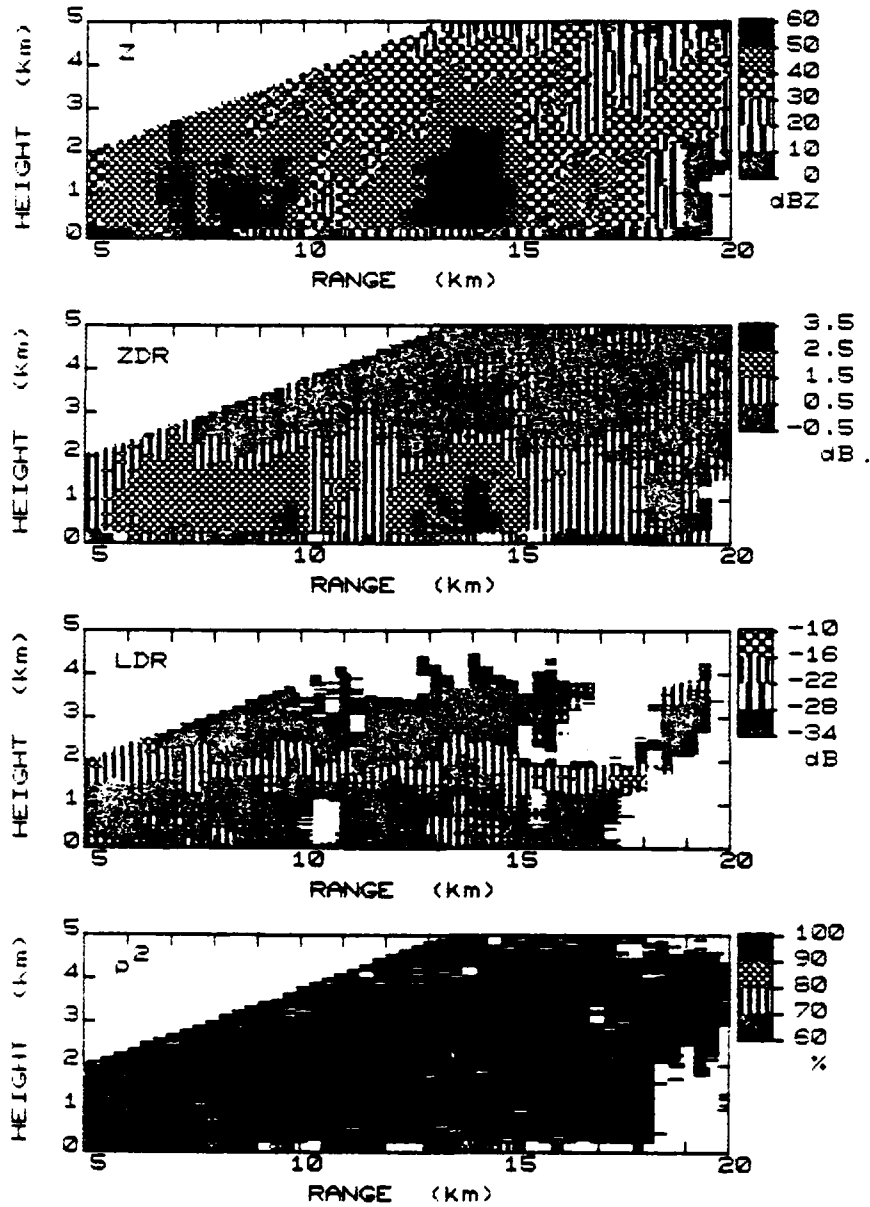


Figure 3. A typical RHI scan through a convective cloud on 13 July 1988 with no bright band for Z, ZDR, LDR and $p(H,V)$.

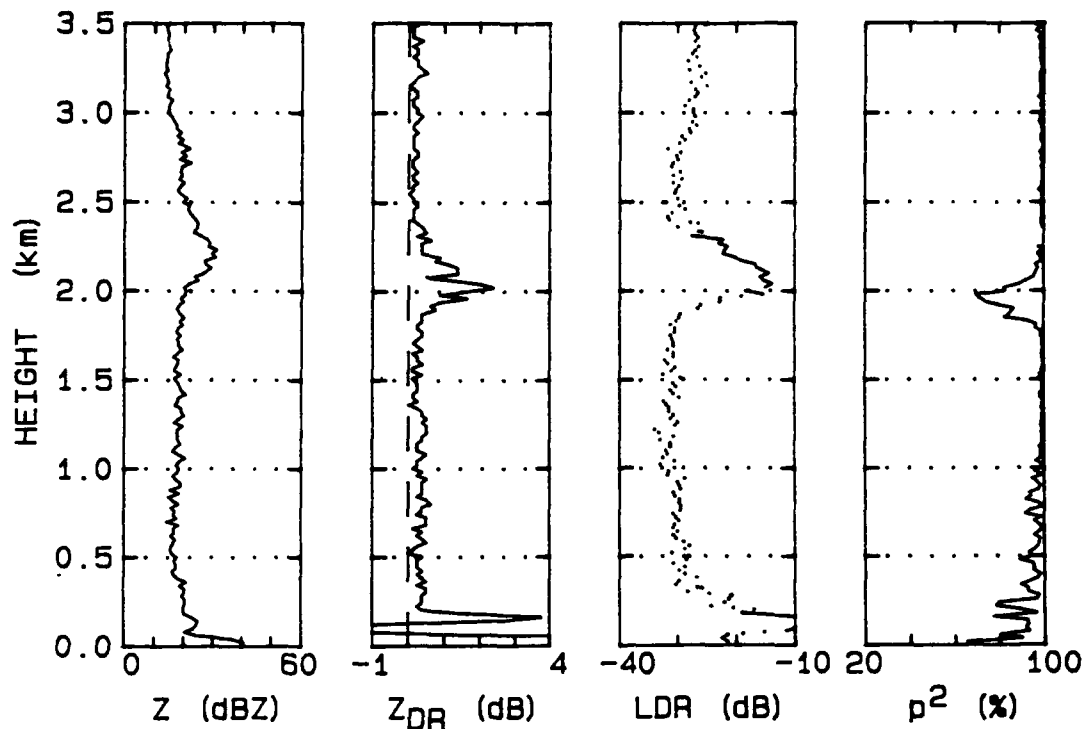


Figure 4. Vertical profile at 9.6km range for the RHI in Figure 2.

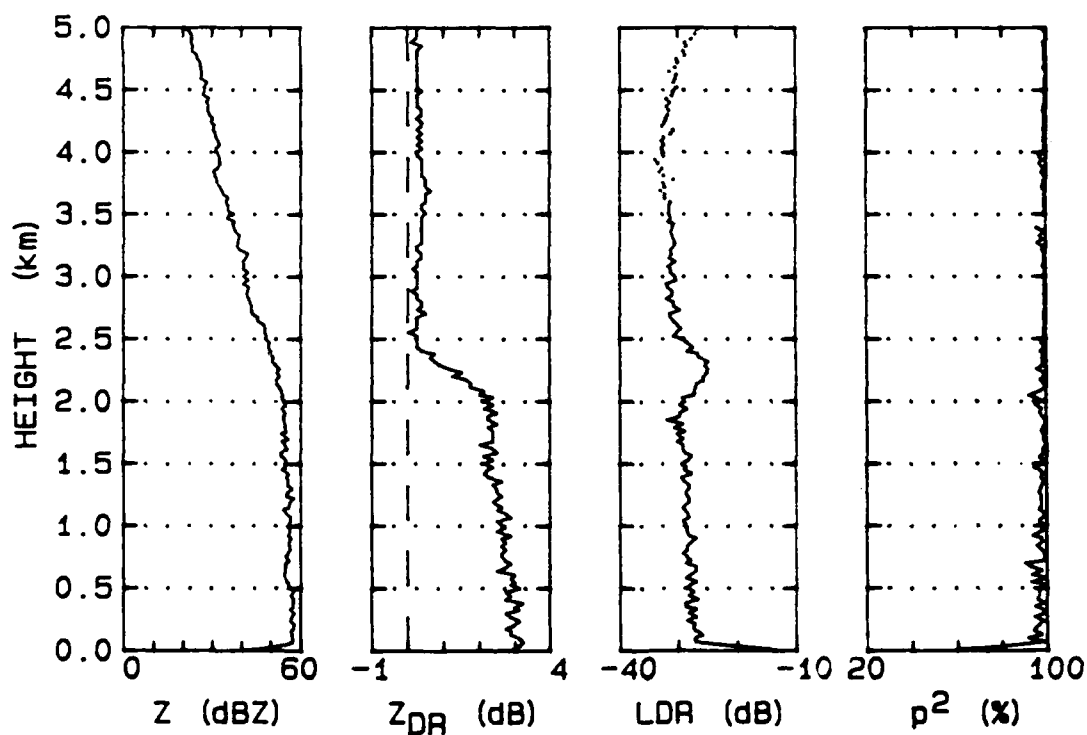


Figure 5. Vertical profile at 13.8km range for the RHI in Figure 3.

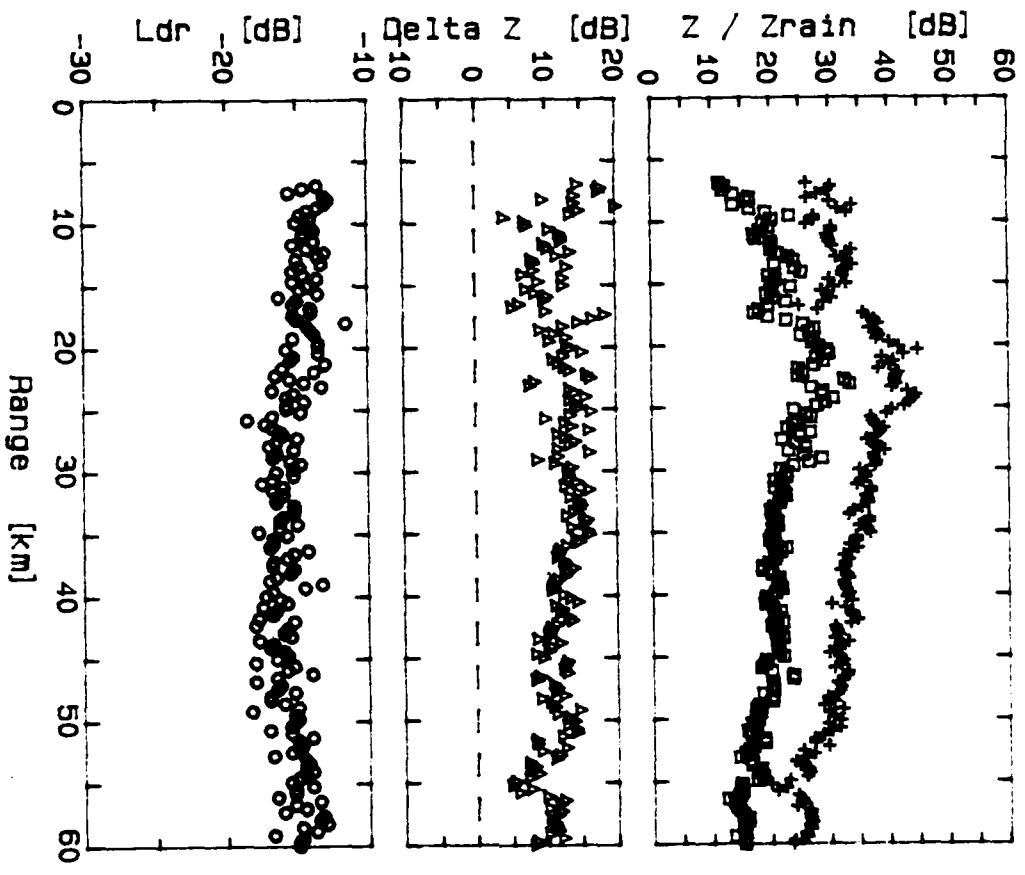


Figure 6. The enhancement of (ΔZ) of Z in the bright band (+) compared to the rain below (□) as a function of LDR in the bright band (○) for the scan in Figure 2.

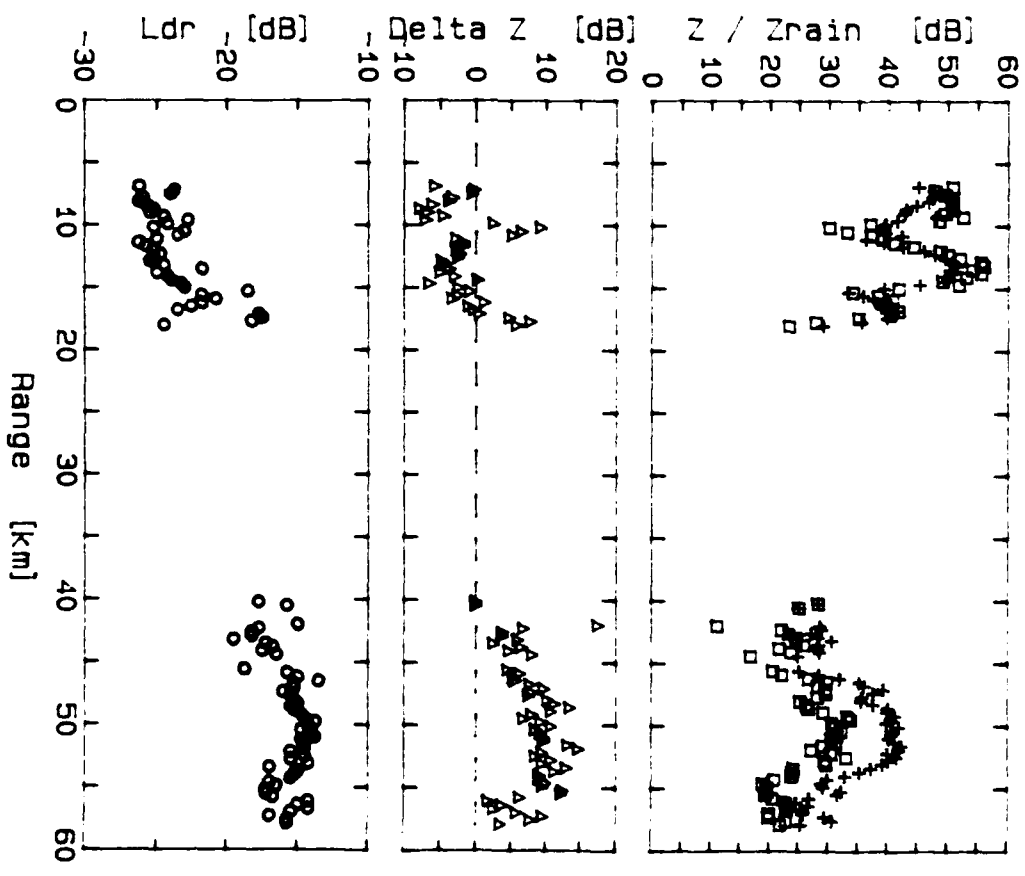


Figure 7. The enhancement of (ΔZ) of Z in the bright band (+) compared to the rain below (□) as a function of LDR in the bright band (○) for the scan in Figure 3.

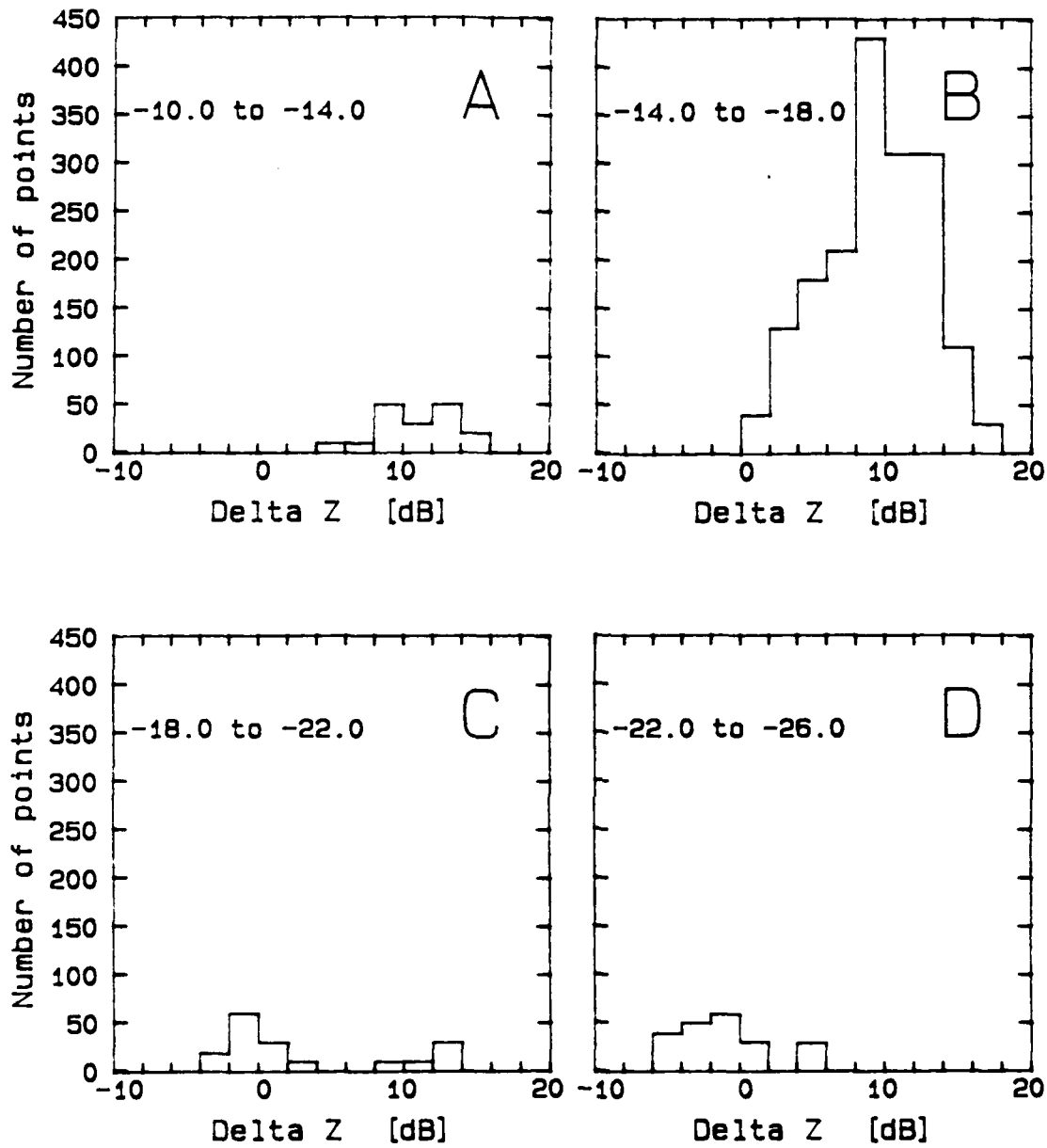


Figure 8. Histograms of the enhancement of the reflectivity in the bright band (ΔZ) as a function of LDR in the bright band.

measurements for a one degree beamwidth radar which is only partially filled by the bright band.

5. TECHNICAL ASPECTS OF IMPLEMENTATION

The Chilbolton radar is a narrow beam research radar which can make measurements of unrivalled polarization purity. Several factors need to be considered if the techniques are to be implemented on conventional C-band radars.

The LDR measurement has the advantage that no fast switching of the transmitted signal is needed. However, the cross-polar signal power is very low, and a signal to noise ratio of more than 20dB is required if an LDR of -20dB is to be detected. We also note that the low power cross-polar signal is much more sensitive than Z and ZDR to ground clutter contamination. Finally, and most importantly, the LDR signal is affected by propagation and attenuation problems at shorter wavelengths. Correction algorithms may be possible at C-band.

If the co-polar cross correlation is to be measured then rapid pulse-to-pulse switching of the polarization of the transmitted signal is required. However, the correlation is unaffected by attenuation and propagation, provided there is sufficient signal level. A signal to noise ratio of 20dB is needed if the correlation is to be measured to 1%. At shorter wavelengths the correlation measurement will be degraded as the time between transmitted pulses approaches the decorrelation time of the return signal. ZDR measurements generally need long dwell times, but it is possible to estimate the correlation from shorter time series and so scan more rapidly.

6. CONCLUSION

These observations suggest that the linear depolarization ratio and/or the co-polar cross correlation can be used to identify the bright band. These parameters may also be of use in identifying anomalous propagation and ground clutter, both of which should have high values of LDR and low correlations.

ACKNOWLEDGEMENTS

This work was supported by AFOSR 89-0121, NERC GR3/5896 and the Meteorological Office.

REFERENCES

- (1) Smith C J (1986) J Atmos Ocean Tech, 3, 129-141.
- (2) Collier C G (1986) J Hydrol, 83, 207-223.
- (3) Cherry S M and Goddard J W F (1982) URSI Symposium on Multiple Parameter Radar Measurement of Precipitation, Bournemouth, UK.
- (4) Hall M P M, Goddard J W F, and Cherry S M (1984) Radio Sci, 29, 132-140.
- (5) Illingworth A J, Goddard J W F and Cherry S M (1987) Q J Roy Meteorol Soc, 113, 469-489.
- (6) Illingworth A J and Caylor I J (1989) Preprints 24th Radar Meteorol Conf, Amer Meteor Soc, Boston, 323-327.
- (7) Caylor I J and Illingworth A J (1989) Preprints 24th Radar Meteorol Conf, Amer Meteor Soc, Boston, 9-12.
- (8) Herzegh P H and Jameson A R (1989) Preprints 24th Radar Meteorol Conf, Amer Meteor Soc, Boston, 315-317.

Part 10

I Frost, A J Illingworth and I J Caylor

'Aircraft and polarization radar measurements of a triggered
lightning event'

1989 Int Conf on Lightning and Static Electricity, Bath, UK.

AIRCRAFT AND POLARIZATION RADAR MEASUREMENTS OF A TRIGGERED LIGHTNING EVENT

Ian R Frost, Anthony J Illingworth and I Jeff Caylor
Department of Physics, UMIST, Manchester M60 1QD, UK

ABSTRACT

The passage of aircraft through clouds can trigger lightning which would not occur naturally. We describe such a triggered event which occurred while the cloud was simultaneously being scanned by the Chilbolton polarization radar. This radar measures new radar parameters: the differential reflectivity (ZDR) which provides an estimate of the mean shape of the precipitation particles, and the linear depolarization ratio (LDR) which reflects their fall mode. Using this information it is possible to distinguish between clouds which contain snowflakes and those where graupel or small hail pellets are present. Measurements of particle type made with the aircraft confirm the radar inferences that the triggered lightning occurred when the aircraft was traversing a region of hail pellets. This conforms with our knowledge of charge generation mechanisms within convective clouds, which predict that appreciable electric fields should be restricted to those regions of clouds containing graupel. It appears that these radar parameters provide a means of remotely locating clouds which pose a threat of triggered lightning to aircraft.

1. INTRODUCTION

There is evidence that many lightning strikes to aircraft are triggered by the presence of the aircraft itself. The existing field in the cloud is insufficient to initiate lightning naturally but the presence of a large conductor raises the field above the critical level (1). Once lightning occurs, many techniques are available to locate its precise position and to study its evolution in time and space. However, detection of electric fields within clouds which are high, but insufficient to initiate natural lightning, is much more problematic. The electrostatic field of the electric dipole structure of the cloud falls off with the inverse cube of the distance from the cloud, so that, apart from very restricted areas, it is impractical to install a network of ground based field sensors.

In Section 2 of this paper we describe a new polarization radar technique which is able to identify the different types of precipitation particle present within clouds. Examples of radar observations of different clouds, including one which triggered a lightning flash to the aircraft, are presented in Section 3. The aircraft measurements of particle type during the penetration when the triggering occurred are compared with aircraft inferences in Section 4, and the implications of these observations are discussed in Section 5.

2. THE CHILBOLTON POLARIZATION RADAR

The Chilbolton radar (2), situated in Hampshire, operates at S-band (10cm) and, with a 25m dish, is the largest steerable radar in the world, having a beamwidth of only a quarter of a degree. It can make measurements of the conventional radar reflectivity factor, Z , with unrivalled resolution, but is also able to make additional polarization measurements which help identification of the precipitation particles.

The conventional radar reflectivity, Z , is proportional to ND^6 , where N is the concentration of particles of diameter D , summed over all sizes. Z is usually expressed in units of dB relative to the signal from a 1mm raindrop per cubic meter. The reflectivity of a raindrop is 7dB higher than the equivalent mass of ice, but from Z alone it is not possible to distinguish rain from ice. Neither can Z be used to differentiate between the various forms of frozen hydrometeors (snow, hail, hailstones etc), or to measure the sizes and concentrations of raindrops.

2.1 Differential Reflectivity

The differential reflectivity (ZDR) provides an estimate of mean hydrometeor shape. It is defined as:

$$ZDR = 10 \log(ZH/ZV) \quad (1)$$

where ZH and ZV are the radar reflectivities measured at horizontal and vertical polarizations respectively. For small raindrops or tumbling ice particles, ZH and ZV are equal and ZDR is zero. The theoretical values of ZDR for oblate particles with their minor axes aligned in the vertical are plotted in Figure 1; ZDR increases with greater oblateness and higher dielectric constant. In heavier rain ZDR is positive and reflects the mean shape (and hence the size) of the raindrops. The ZDR of ice is more complex (3). Because of the low dielectric constant, dry snowflakes have a ZDR close to zero, but wet snowflakes can have high positive values. Graupel tends to tumble and so be associated with a zero ZDR value.

2.2 Linear Depolarization Ratio

The linear depolarization ratio, LDR, is a measure of the hydrometeor fall mode and appears to be an excellent indicator of wet ice. LDR is defined as:

$$LDR = 10 \log(ZVH/ZH) \quad (2)$$

where ZVH is the (horizontal) cross-polar return from a vertically polarized transmitted pulse, and ZH (as in equation

1) is the co-polar (horizontal) return for horizontally polarized transmission.

A cross polar return occurs only when oblate hydrometeors fall with their major or minor axis at an angle to the vertical. If particles fall with their axes aligned in the vertical or horizontal then there is no cross-polar return and LDR is minus infinity. Computations for randomly tumbling oblate spheroids are plotted in Figure 2 and are found to be consistent with Chilbolton observations (4). The values of LDR rise as the particles become either more oblate or of higher dielectric constant. Snowflakes have such a low dielectric constant that even if they are very oblate their LDR is below the antenna limit of -32dB. Oblate dry hail or graupel could have a value of up to -20dB if the axial ratio were as low as 0.5, but LDR values above -20dB can only realistically occur for wet tumbling ice particles. Such high values are restricted to the melting layer. Raindrops give rise to a very low cross-polar return.

The basis of our method for distinguishing between different forms of ice is the value of LDR when the particles start to melt and become coated with water. In stratiform clouds and some showers this melting layer is associated with peak LDR values of about -15dB, consistent (Figure 2) with snowflakes having a rocking or spinning motion and an axial ratio of about 0.5. In contrast, in some vigorous showers which we believe contain graupel, the LDR in the melting layer reaches a maximum value of only -25dB, which we interpret as tumbling water coated graupel pellets with an axial ratio of about 0.8.

2.3 Possible Effect of Static Electric Fields on Radar Parameters.

Computations suggest that the fields required to trigger lightning discharges (300kV/m) are also sufficient to change the shape of large raindrops (5) and to alter the orientation of ice crystals (6). This implies that the electric field might be sensed by its effect on the ZDR of raindrops and the ZDR or LDR of ice crystals. However, although it might be possible to detect sudden changes in these parameters coincident with a lightning flash, it appears impossible to separate the component of ZDR due to the steady electric field. For example, if a high ZDR is associated with raindrops, then, unless we have an independent measurement of drop size, we cannot quantify the distorting effect of the electric field. Similarly with ice crystals, in the upper regions of clouds where Z is low, the values of ZDR are often positive and highly spatially variable, presumably due to the habit of the crystals; but again, unless we have a means of knowing the ZDR of these crystals in the absence of a field, we cannot determine the component due to the electric field.

Large horizontal components of the electric field could cause ice crystals to tilt, and in theory this should lead to an anomalous value of LDR. Unfortunately, the radar return from ice crystals is usually restricted to low Z regions, otherwise it is masked by larger ice particles. For low Z regions, the cross-polar return from dry ice particles will generally fall below the level of radar sensitivity.

3. RADAR OBSERVATIONS OF CLOUDS AND TRIGGERED LIGHTNING

A vertical section (RHI) of the three radar parameters through a shower believed to contain only snowflakes and aggregates is shown in Figure 3. In this case a pronounced 'bright band' of enhanced reflectivity in Z at an altitude of 1.5km is caused by snowflakes becoming wet and reflecting microwaves as if they were giant raindrops. This bright band is clearly visible in the RHI with this narrow beamwidth research radar, but most radars scan in azimuth (PPI) to obtain greater areal coverage, and in such a case the bright band in Z is much more difficult to identify. In Figure 3 the oblate melting snowflakes are associated with a bright band in ZDR with values reaching 2dB, but these values of ZDR cannot be taken as automatic indication of the presence of melting snowflakes. In this example the value of ZDR in the rain is over 0.5dB, and in heavier rain values up to 5 or 6dB are possible. We also note in Figure 3 the slightly positive values of ZDR above 3km altitude; this low Z region presumably containing aligned high density ice crystals.

The presence of the melting snowflakes is much easier to identify from the LDR data in Figure 3, where peak values of LDR reach about -15dB. In contrast, LDR values in the rain are near the antenna limit of -32dB, and reach about -27dB in the low Z ice region above 3km where the ZDR indicated the presence of high density crystals. The high values of LDR very close to the ground in Figure 3 are caused by ground clutter which can easily corrupt the low power cross-polar return.

A vigorous shower is depicted in Figure 4 and it is clear that the polarization parameters have a quite different character: the LDR values in the bright band are much lower than in Figure 3. We believe that this cloud contains graupel. The dry tumbling graupel high in the cloud gives negligible LDR, but melting occurs at about 2km and LDR rises to about -25dB; this weak "LDR graupel bright band" is consistent with tumbling wet ice with an axial ratio of 0.8. In heavy rain the LDR is just detectable and is explicable in terms of a raindrop canting angle of about 5 degrees. Values of ZDR are low for the tumbling dry ice, but rise monotonically as the graupel melts and assumes the equilibrium shape of the large raindrops. The Z in Figure 4 is greater than 50dBZ, but the absolute magnitude of Z cannot be taken as an indication of the presence of graupel; values of Z in the bright band in Figure 3 exceed 40dBZ but some graupel showers have Z values lower than 40dBZ.

The cloud which caused the triggered lightning event is displayed in Figure 5. The values of Z are lower than in Figure 4 and both types of LDR bright band are present. Between 65 and 73km range the peak values of LDR are about -25dB and suggest the presence of melting graupel, but outside these ranges the higher values of LDR in the melting layer are indicative of snowflakes or aggregates. At these ranges, if LDR is low, the cross-polar power is below the level of detectability by the radar.

The Meteorological Office C-130 aircraft was penetrating the cloud in Figure 5 at a height where the temperature was just below zero, and was flying on a radial towards the radar on the same azimuth as the radar scan. As the aircraft penetrated the region where we infer graupel was present, it was struck by lightning, even though the value of Z was only about 40dBZ. A value of 50dBZ is often assumed to be required for lightning. Data from the UK Electricity Supply Industry Lightning Flash Locator (Personal Communication, L J Scott) shows that the first cloud to ground lightning over Southern England was detected from this cloud six minutes after the strike to the aircraft. We conclude that the aircraft triggered the lightning flash and that it did not discharge to ground. In the next Section we analyze the aircraft measurements of particle type.

4. AIRCRAFT OBSERVATIONS OF ICE PARTICLE TYPE

The Meteorological Office C-130 aircraft was equipped with a PMS 2D precipitation probe; an optoelectronic device consisting of a laser light source, focusing optics, a linear 32 element photodiode array and high speed electronics to record the images of the precipitation particles. The photodiode separation is 0.2mm, and the resolution in the direction of the aircraft flight is dependent on aircraft speed but was also about 0.2mm. Manual recognition of the many images is tedious, error prone and subjective, so an automatic system of classifying the shapes following Duroure (7) was implemented.

There are several stages in this analysis system. First, the centre of mass of each image was found, and then the radius of the image a function of angle was calculated. The mean radius, the axial ratio and orientation could then be deduced. Using a fast Fourier transform the power spectra of the radials was calculated and normalised with respect to the mean radius of the image; this spectra is a size independent measure of the periodicities in the edge of the particle image. Classification involves a comparison of the normalised power in the second, sixth, and all the higher harmonics. Aggregates have more power in the higher harmonics, but graupel particles are recognised by their smoother profile.

As a check on the reliability of the image analysis programs, the value of Z was calculated from the aircraft images, assuming the particles to be dry ice, and compared with the Z observed by the radar. The comparison is plotted in Figure 6, where the solid squares are the values computed from the images and the solid line is a polynomial fit through these points. Because the values of Z were changing rapidly with height, and the scan was separated by two minutes from the aircraft lightning strike, there is some uncertainty in the precise values of Z at the aircraft position. Accordingly, the vertical lines in the Figure represent the range of values of Z for the data point at the aircraft flight level and the radar observation 300m above and below this height. Good agreement is obtained. Confirmation of the aircraft position was obtained by a direct 'hit' on the previous RHI radar scan.

Figures 7 and 8 show images during this penetration which the analysis program has classified as graupel and aggregates. The shape of the images has been adjusted in the computations to account for any changes in aircraft speed. These Figures confirm that the classification algorithm is operating satisfactorily. Figure 9 compares the predicted values of LDR when these ice particles become wet with the actual values of LDR observed by the radar at the melting layer. The axial ratio of each particle was determined, and then assuming that they were randomly tumbling and wet, a reflectivity weighted value of LDR was computed. These values are plotted as the open squares; the bold line is a fit through these squares. The observed values of LDR in the melting layer are represented by the solid squares in the Figure; we note that the overall observed variation of LDR with distance agrees well with the values predicted from the images. The oblate aggregates predominate where LDR is high, whereas the more spherical graupel particles are more common where LDR is lower. The actual observed values of LDR are consistently lower than the computations, but this is consistent (Figure 2) with the ice particles becoming slightly less oblate as they acquire a water coating.

5. DISCUSSION AND CONCLUSION

Aircraft and radar comparisons confirm that the LDR value in the melting layer can be used to differentiate regions containing graupel from those where snowflakes are found. The triggered lightning occurred in a region where graupel was predominant. It is widely believed (8) that charge separation in clouds occurs when small ice crystals collide with and separate from graupel particles; where snowflakes are present the ice crystals will be collected. Accordingly, we would expect appreciable electric fields to be limited to regions of graupel.

There are two possible reasons why the presence of the aircraft could raise the electric field to a level needed to trigger lightning. Firstly, the presence of the conducting aircraft itself, and secondly, the charge acquired by the aircraft as a result of collisions with ice crystals. The precise mechanism is unclear. Collisions of the aircraft with ice crystals generally charge up the aircraft negatively (9) which would appear to make the initiation of streamers and subsequent triggering of lightning more difficult (10).

The use of the linear depolarization ratio (LDR) for detecting clouds where there is a danger of lightning appears to have great potential. The results reported here have been made at S-band with a very narrow beamwidth radar; further research is needed before implementing the technique for C-band radars with smaller antennas.

ACKNOWLEDGEMENTS

This work was supported by NERC GR3/5896, AFOSR 89-0121 and the Meteorological Office. John Goddard of RAL implemented the LDR parameter on the Chilbolton radar. We also thank the personnel of the Meteorological Office Research Flight for the aircraft data.

REFERENCES

1 Perala A P and Rudolph T H (1988) Proc 8th Int Conf on Atmos Electricity, Inst of High voltage Research, Uppsala, Sweden 363-370.
 2 Cherry S M and Goddard J W F (1982) URSI Symposium on Multiple Parameter Radar Measurement of Precipitation, Bournemouth, UK.
 3 Illingworth A J, Goddard J W F and Cherry S M (1984) Q J Roy Meteorol Soc, 113, 469-489.
 4 Illingworth A J and Caylor I J (1989) Preprints 24th Radar Meteorol Conf, Amer Meteor Soc, Boston, 323-327.

5 Rasmussen R, Walcek C, Pruppacher H R, Mitra S K, Lew J, Levizzani, Wang P K and Barth U (1985) J Atmos Sci, 42, 1647-1652
 6 Weinheimer A J and Few A A (1980) Vith International Conference on Atmospheric electricity, Manchester, UK, Session I.
 7 Duroure C (1982) J Rech Atmos, 6, 71-84.
 8 Illingworth A J (1985) J Geophys Res, 90, 6041-6046.
 9 Illingworth A J and Marsh S J (1986) Revue Phys Appl, 21, 803-808
 10 Phelps C T (1971) J Geophys Res, 76, 5799-5806.

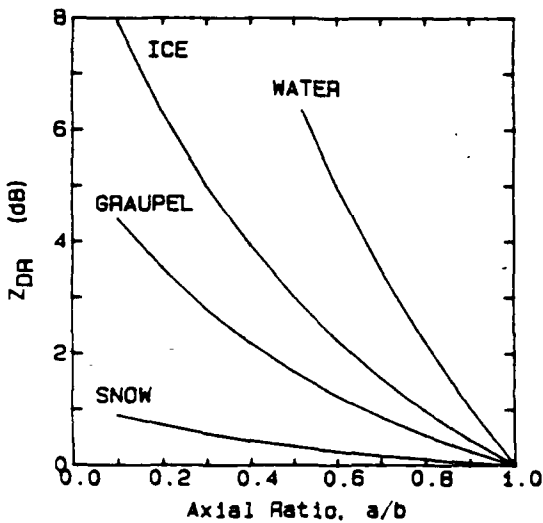


Figure 1. ZDR values as a function of axial ratio for various precipitation particles, assuming the major axis is horizontal.

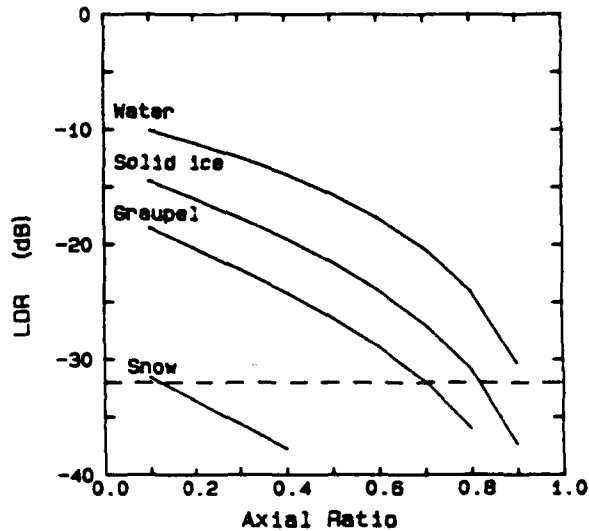


Figure 2. LDR values for randomly tumbling particles as a function of axial ratio. Raindrops do not tumble, but the 'water' curve is applicable to wet ice particles.

RHI SCAN ON 29/05/88 AT 155541 UT
 TAPE 7150 RASTER 52 SCAN 2 AZ 255.00deg

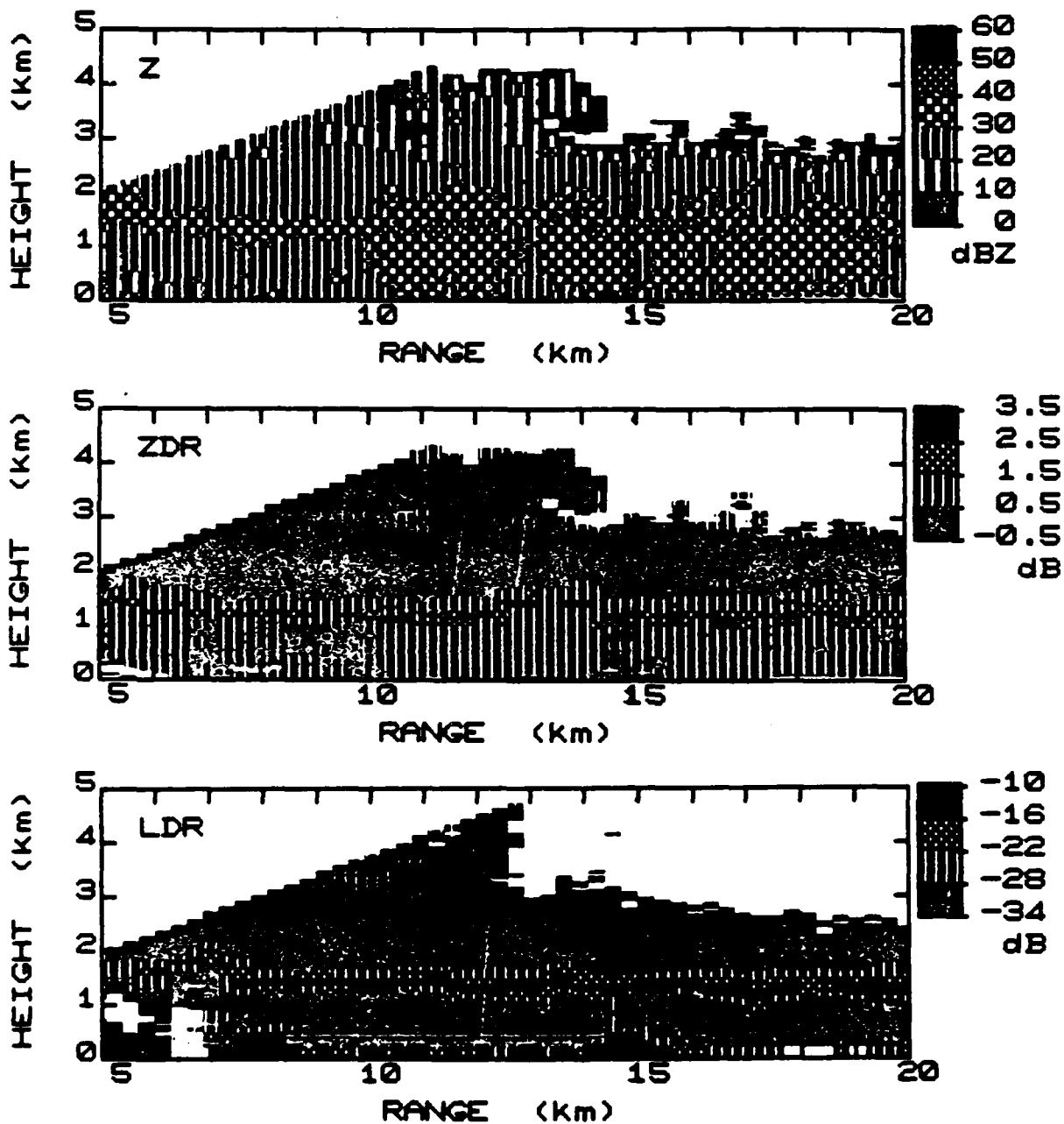


Figure 3. An RHI scan of the radar reflectivity (Z), the differential reflectivity (ZDR) and Linear Depolarization Ratio (LDR) through a shower. The high values of LDR at 1.5km altitude are interpreted as due to melting snowflakes.

RHI SCAN ON 13/07/88 AT 155423 UT
TAPE 5131 RASTER 22 SCAN 1 AZ 253.00deg

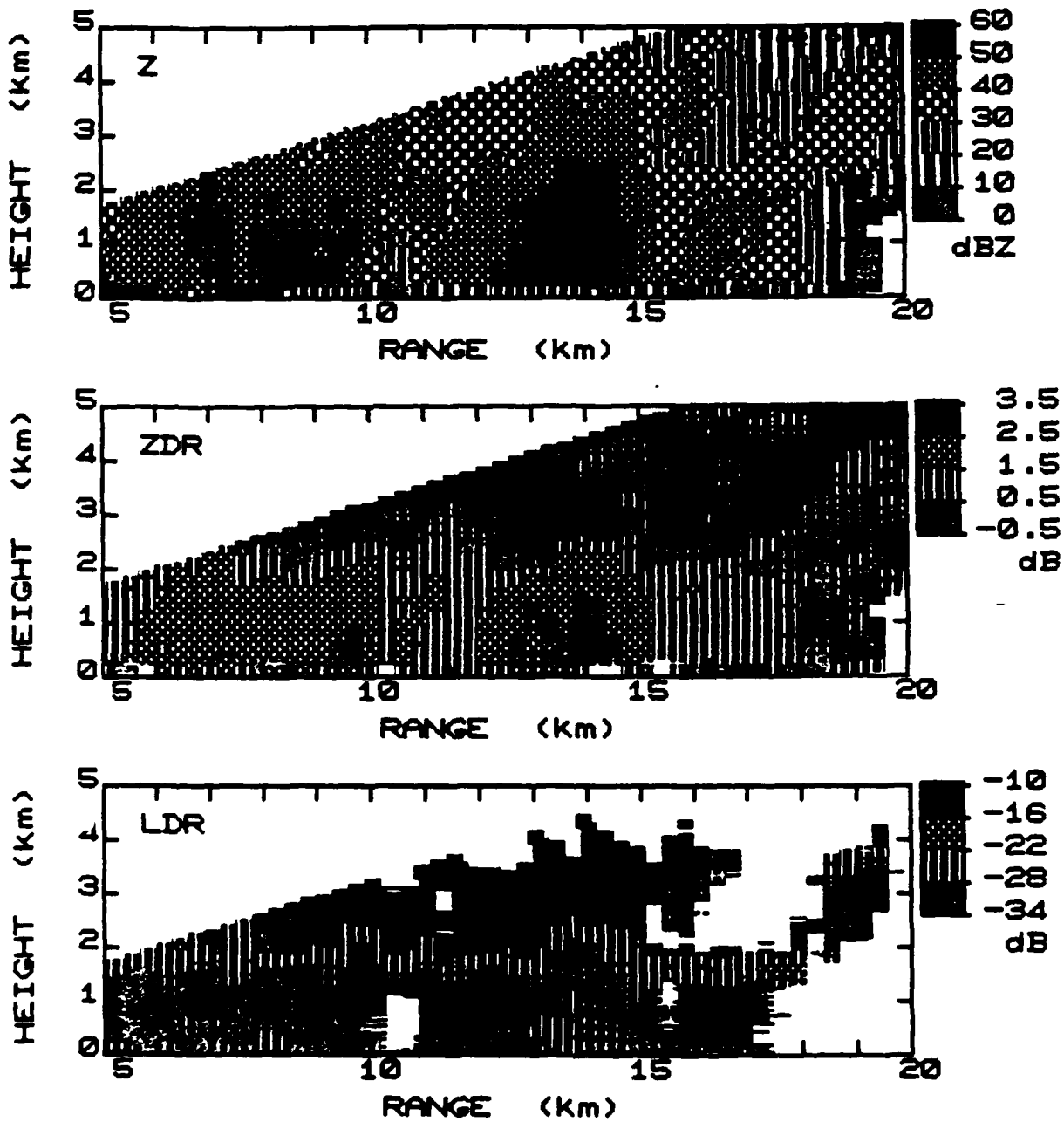


Figure 4. An RHI scan of Z, ZDR and LDR through a shower believed to contain graupel or soft hail pellets. Values of LDR peak at about -25dB at 1.5km altitude as the graupel starts to melt.

RHI SCAN ON 13/07/88 AT 130435 UT
 TAPE 5130 RASTER 28 SCAN 1 AZ 269.50deg

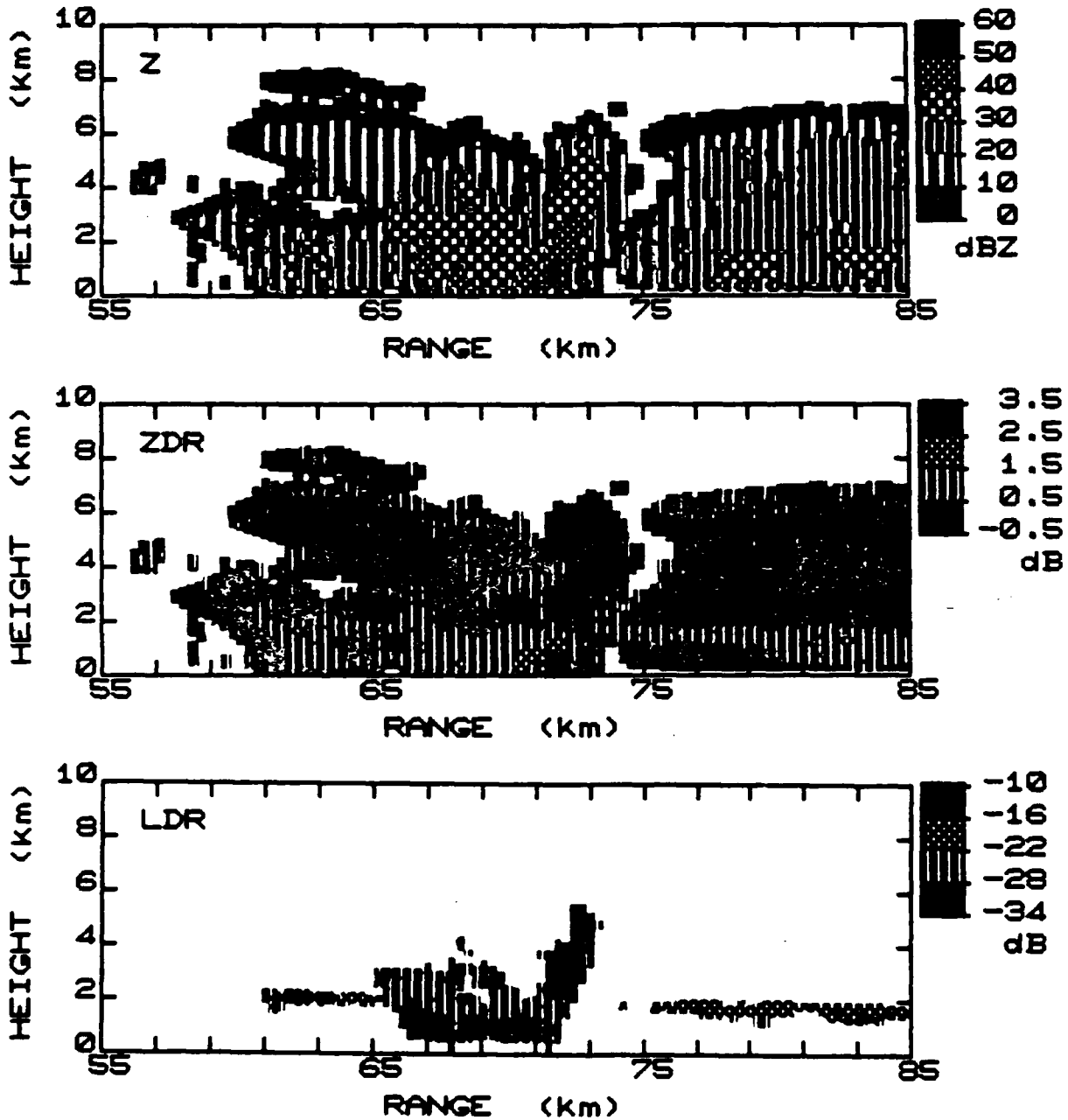


Figure 5. An RHI scan through the cloud which triggered the lightning flash to the aircraft. The lightning occurred at 70km range where the LDR indicates the presence of graupel.

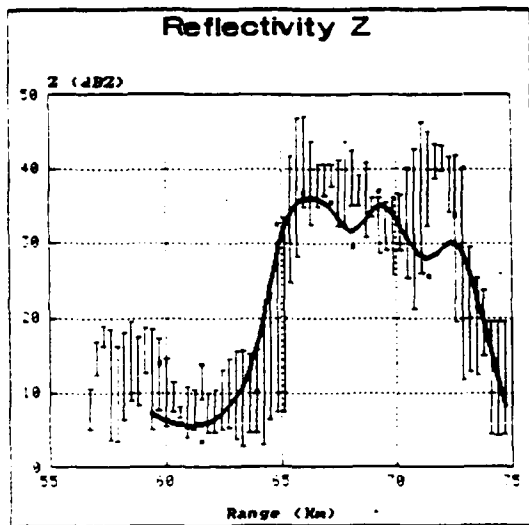


Figure 6. A comparison of the Z values measured by the radar and those inferred from the aircraft probe measurements. For details see text.

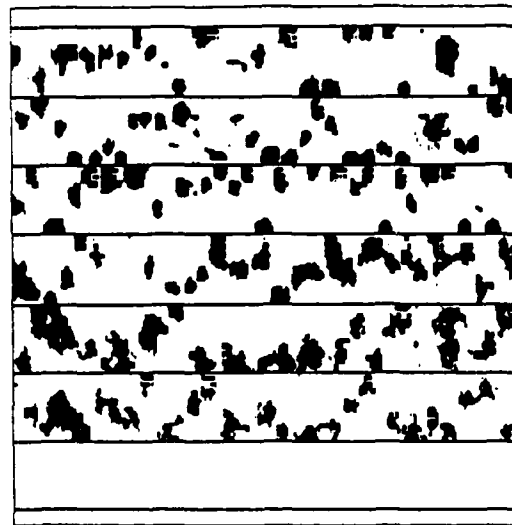


Figure 8. Particles identified as aggregates by the analysis package.



Figure 7. Particles identified as graupel by the analysis package (shape uncorrected for airspeed).

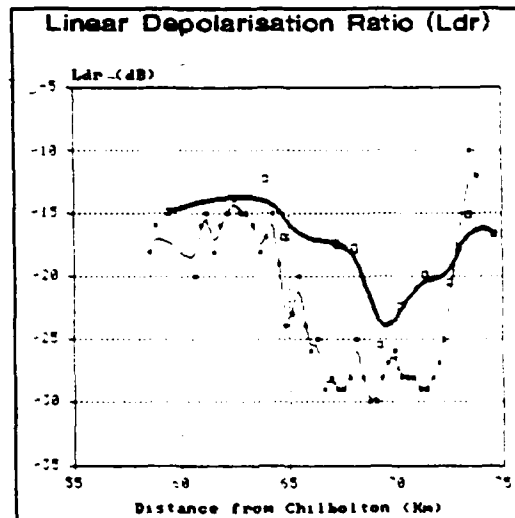


Figure 9. A comparison of the LDR values observed by the radar in the melting layer, with those computed from the aircraft probe images.

